Alternate Cry toxin targets in a lepidopteran insect pest, *Achaea janata*

A thesis submitted to University of Hyderabad for the degree of

DOCTOR OF PHILOSOPHY

by

Thuirei Ningshen Jacob

Department of Animal Sciences
School of Life Sciences
University of Hyderabad
Hyderabad-500 046, INDIA

March, 2012 **Reg. No. 06LAPH05**

Dedicated to my (late) father

Ngahanphung Mathew Ningshen

University of Hyderabad

Hyderabad-500 046, INDIA

Declaration

I hereby declare that this thesis entitled "**Alternate Cry toxin targets in a lepidopteran insect pest, *Achaea janata***" is an original and independent research work carried out by me under the supervision of Prof. Aparna Dutta Gupta. I also declare that it has not been submitted previously in part or in full to this Univeristy or any other University or Institute for the award of any degree or diploma.

Date: Name:

Signature:

University of Hyderabad

Hyderabad-500 046, INDIA

Certificate

This is to certify that **Mr. Thuirei Ningshen Jacob** has carried out research work embodied in this thesis under my supervision and guidance for a full period prescribed under the PhD ordinance of this University. I recommend his thesis entitled "**Alternate Cry toxin targets in a lepidopteran insect pest, *Achaea janata***" for submission for the degree of Doctor of Philosophy of this University.

Research Supervisor

Head,
Department of Animal Sciences

Dean,
School of Life Sciences

Acknowledgements

First and foremost, I would like to express my deep sense of gratitude to Prof. Aparna Dutta Gupta under whose supervison and guidance, my research work was carried out. I am deeply indebted to her for all the help, encouragement and support she had given me.

I thank Prof. M. Ramanadham, Dean, School of Life Sciences and former Dean, Prof. A. S. Raghavendra, for all the School facilities.

I am thankful to Prof. Manjula Sritharan, Head, Department of Animal Sciences, and former Heads, Prof. S. Dayananda and Prof. Aparna Dutta-Gupta, for all the research facilities of the department.

I wish to thank my doctoral committee members, Prof. S. Dayananda and Prof. Ch. Venkataramana for their constructive criticisms and suggestions.

I am deeply grateful to Dr. P.S. Vimala Devi, Directorate of Oilseeds Research, Hyderabad, for gifting DOR5 Bt isolate and supplying the insect cultures.

I thank Prof. B. Senthilkumaran for his help and encouragements.

I convey my acknowledgement to Dr. Prashanth P. Hari, Directorate of Oilseeds Research, Hyderabad, for his assistance in bioassays and maintainance of insect cultures.

My sincere thanks to Dr. P. Aparoy for his valuable assistance in homology modelling studies.

I also acknowledge Dr. Joby Joseph for providing the Injection needles and Dr. Madhusudhan Budatha, for the APN antibody.

Thankful to BGSC, USA, for providing the recombinant BGSC clones.

Let me also thank the non-teaching staff of School of Life Sciences especially Mr. Mallesh, Mr. Lallan, Mr. Ankinaidu, Mrs. Jyoti and Mr. Jagan. Acknowledgements also go to technicians of Scanning Electron Microscope and Confocal Laser Scanning Microscope of Central Instruments Laboratory, University of Hyderabad.

I thank DBT for the award of junior and senior research fellowships. I also acknowledge the financial support from CSIR, UGC-SAP, UGC-CAS, DST, COSIST, CREBB and UPE.

I also take this opportunity to thank all my labmates (past and present) – Dr. Vijay Prasad Rao, Dr. D. Manohar, Dr. G. Damodara Rao, Dr. R.K. Chaitanya, (Late) Mr. Naresh Kumar Reddy, Mr. Venkat Rao and Ms. Pavani, for their help and friendship.

I extend my thanks to all my colleagues from the School of Life Sciences.

Thanks to all my friends from University campus, for their friendship and making my stay in the campus, a nice one.

I am indeed grateful to my uncle Rev. Fr. L.M. Mario Ningshen for supporting me all these years.

My special thanks to Ms. Chanchan Jajo for her unconditional love and support.

Last but not the least, I am ever indebted to my mother and my (late) father for their love, prayers and blessings. I extent my heartfelt thanks and warm regards to my brothers, sisters and relatives.

Thuirei Ningshen Jacob

Contents

Abbreviations

ºC	degree centigrade/celcius
20E	20-Hydroxyecdysone
3D	Three Dimensional
ACP	Acid phosphatase
ALP	Alkaline phosphatase
BCIP	5-Bromo-4-chloro-3-indolyl phosphate
BLAST	Basic Local Alignment Search Tool
BSA	Bovine serum albumin
cDNA	Complementary DNA
CHARMM	Chemistry at HARvard Macromolecular Mechanics
DNA	Deoxyribonucleic acid
DEPC	Diethyl pyrocarbonate
dNTPs	Deoxyribonucleoside triphosphates
DTT	1,4-Dithiothreitol
EDTA	Ethylenediaminetetraacetic acid
EGTA	Ethylene glycol-bis (2-aminoethylether)- N,N,N`,N`-tetraacetic acid
HEPES	N-(2-hydroxyethyl) piperazine-N`-(2-ethanesulfonic acid)
IgG	γ Immunoglobulin
JH	Juvenile hormone
kDa	Kilodalton
LB	Luria-Bertani medium

LD	Light:Dark
mg	Milligram
mM	Millimolar
mRNA	Messenger ribonucleic acid
MTT	3-(4,5-dimethylthiazol-2-yl)-2,5-diphenyltetrazolium bromide
NaCl	Sodium Chloride
NBT	Nitrotetrazolium blue
ng	Nanogram
nM	Nanomolar
PAGE	Polyacrylamide gel electrophoresis
PBS	Phosphate buffered saline
PCR	Polymerase chain reaction
PDB	Protein Data Bank
pH	Negative logarithm (base 10) of the molar concentration of dissolved hydrogen ions (H^+)
PMSF	Phenylmethylsulfonyl fluoride
PNP	Para-nitrophenol
PP	Prepupa
PTTH	Prothoracicotropic hormone
RNA	Ribonucleic acid
SDS	Sodium dodecyl sulfate
SDS-PAGE	Sodium dodecyl sulfate polyacrylamide gel electrophoresis
TAE	Tris-Acetate EDTA

TBS	Tris buffered saline
TBST	Tris buffered saline Tween-20
TE	Tris-EDTA
TEMED	N,N,N`,N`, tetramethylethylenediamine
v/v	volume/volume
w/v	weight/volume
µg	Microgram
µM	Micromolar

General Introduction

The need for biopesticides

For the past many decades, increase in agricultural production had been due to expansion in cultivation area, use of high yielding varieties and hybrids of variety of crops, along with intensive inputs, particularly the chemical fertilizers as well as pesticides, and water. Since early 1970s, agriculturally-dependent developing countries like India have benefitted substantially from these applications in providing and improving self-sufficiency of food and increase in rural income. While the overall gains have been impressive, application of variety of chemical agents has resulted in undesirable effects on environment and human health and thus has generated concerns in the overall sustainability of this farming system. Health hazards including birth defects, impaired nervous function, cancer, reproductive dysfunction, methaemoglobinemia (blue baby syndrome) in humans and other mammals have been reported to be associated with contamination of biotic components of the environment (Kegley and Wise, 1998). With the increasing awareness about the harmful effects of chemical fertilizer and pesticide-based crop protection practices, the demand for technologies as well as products which are produced biologically and are environment friendly has been increasing steadily worldwide.

Biopesticides, a group of control agents based on living organisms as well as plant products, have been proven for their potential in insect pest control and are being currently used across the world. Biopesticides are exemplified by plants (eg. neem *Azadirachta*), macrobials (eg. *Trichogramma* parasitoid), microscopic animals (eg. Nematodes), mico-organisms including bacteria (eg. *Bacillus thuringiensis*), viruses (eg. Nucleopolyhedrosis virus), fungi (eg. *Beauveria* sp.) and the transgenic plants containing the pest combating Cry toxin genes (eg. *Bt* cotton). Use of biopesticides is known to be fairly safe for mammals and other non-target organisms including beneficial insects. They are target-specific and require lower doses to be effective against pests and thus enabling their use in integrated pest management (IPM). The efficacy of many of these biopesticides can equal that of the conventional chemical pesticides.

Bt-based biopesticides

Bt-based biopesticides are the leading biological insecticides which exploit the crystal (Cry) proteins produced by a common soil bacterium *Bacillus thuringiensis* (*Bt*) during sporulation. To date, *Bt*-based control strategies utilize sprayable formulations

(mixture of spores and crystals) as well as *Bt* crops (transgenic plants expressing *cry* genes). *Bt* formulations have been successfully used for almost 60 years in areas such as forestry management, agriculture and many vector-borne disease control (Federici, 2005). Cry proteins display a narrow spectrum of insecticidal activity against one or more genera in the orders of Coleoptera (beetles and weevils), Diptera (flies and mosquitoes), Hymenoptera (wasps and bees), and most importantly Lepidoptera (butterflies and moths), including most of the insect pests of agricultural importance. The use of Cry proteins has further increased tremendously following the success in introduction of *cry* genes into economically important crops. Since 1996, *Bt*-transgenic plants have been commercialized and increasingly incorporated into the pest management programs (Van Rie, 2000; Shelton *et al*. 2002). *Bt*-crops like *Bt*-maize and *Bt*-cotton have thus far proved to be effective against resistant lepidopteran pests.

Cry toxin receptors

Cry toxins bind to the specific receptor proteins located on the apical brush border membrane of the columnar epithelial cells of the insect larval gut, thereby inducing toxicity through a defined mechanism. Binding of Cry toxins to receptor proteins is established to be an important determinant of specificity. In lepidopteran insects, Cry toxins have been shown to bind to four different protein receptors: a glycosylphosphatidyl-inositol (GPI)-anchored aminopeptidase-N (APN) (Knight *et al*. 1994), transmembrane cadherin-like protein (CADR) (Nagamatsu *et al*. 1999), a GPI-anchored alkaline phosphatase (ALP) (Jurat-Fuentes and Adang, 2004) and a 270 kDa glycoconjugate (Valaitis *et al*. 2001).

Aminopeptidases N (APNs): The APN is a class of enzymes that cleaves neutral amino acid residues from the N-terminus of polypeptides. They perform a variety of functions in a wide range of insect species, but in the lepidopteran larval midgut, they work in cooperation with endopeptidases and carboxypeptidases to digest proteins derived from insect's diet (Wang *et al*. 2005). These proteins belong to the Zn^{++} binding metalloproteases family of peptidases called gluzincins (Hooper, 1994). Members of this family are characterized by the presence of highly conserved aminopeptidase activity motif "GAMENWG" and Zn^{++} binding motif "$HEXXHX_{18}H$" (Pigott and Ellar, 2007). The ectoenzyme form of APN is normally attached to the apical brush border membrane of the gut epithelial columnar cells through a GPI-anchor (Fig. 1). Based on the amino

acid sequence identity, the APNs have been divided into five different classes (Herrero *et al*. 2005). The average sequence identity within a class varies from 56% (Class 5) to 67% (Class 4). Among the different classes, class 2 is the least like the others, with an average sequence identity of around 25% relative to the other classes, whereas class 1 and class 3 are the most similar, with an average sequence identity of 38% between them. To date, all known APNs within a particular species have been found to cluster into different classes. The different isoforms of APN in an insect have differential specificities to the N-terminal residues of the protein substrates (Wang *et al*. 2005).

Besides their role in dietary protein digestion, midgut APNs has been identified as Cry toxin receptors that mediate Cry toxicity in a number of lepidopteran insects (Soberón *et al*. 2009). Double-stranded RNA-mediated gene silencing demonstrated that APN is a receptor to Cry1C in *Spodoptera litura* (Rajagopal *et al*. 2002). Heterologous expression of *Manduca sexta* APN in midgut and mesodermal tissues of transgenic *Drosophila melanogaster* caused sensitivity to Cry1Ac toxins suggesting its role as Cry1Ac receptor (Gill and Ellar, 2002). Resistance of *Spodoptera exiqua* to Cry1C was also reported to be due to lack of APN expression (Herrero *et al*. 2005). The 170 kDa APN from *Heliothis virescens* was demonstrated to be responsible in pore formation in midgut membrane vesicles (Luo *et al*. 1997). Different Cry1 toxins including Cry1Aa, Cry1Ab, Cry1Ac, Cry1Ba, Cry1Ca and Cry1Fa have been shown to bind to APNs. Some APNs bind to multiple Cry toxins while some Cry toxins bind to multiple APNs and in other cases, unique toxin-APN pairs have been reported.

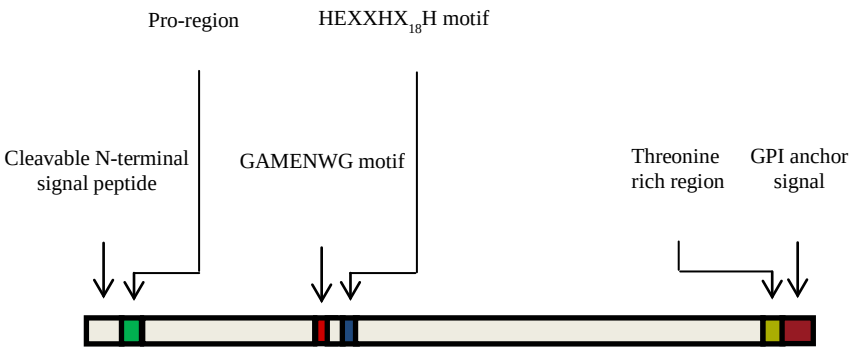

Fig. 1. Schematic representation of a typical lepidopteran APN protein (The pro-region and the threonine-rich region are not present in all the APNs).

Cadherins: The cadherin family of proteins are highly diverse in nature and perform a variety of functions, including cell adhesion, migration, cytoskeletal organization, and morphogenesis (Angst *et al*. 2001). They are transmembrane proteins with a cytoplasmic domain and an extracellular ectodomain with several cadherin repeats (Nagamatsu *et al*. 1999). In insects like *M. sexta* and *Anopheles gambiae*, the cadherins are located in the microvilli of larval midgut epithelial cells, and act as the binding site for Cry toxins (Chen *et al*. 2005). Lepidopteran cadherin-like proteins have been extensively studied as Cry1A receptors and various evidences of their role in mediating Cry toxin susceptibility have been provided. BT-R_1 is a 210 kDa glycoprotein identified in *M. sexta* and is the first cadherin-like protein shown to interact with Cry toxins (Vadlamudi *et al*. 1993). Expression of cadherin-like protein from *Bombyx mori* on the surface of Sf9 cells made resistant cells sensitive to Cry1Aa (Nagamatsu *et al*. 1999). Various studies have indicated that although cadherins confer toxin binding and susceptibility in many insects, seems unlikely that they are universal Cry toxin receptors.

Alkaline phosphatases (ALPs): They are abundant enzymes that are mainly involved in removing phosphate groups from organic molecules. In insects, ALPs have been reported to be involved in many biological processes (Eguchi, 1995; Funk, 2001). Compared to APNs and cadherins, very limited information is available on ALPs as Cry toxin receptors. In *M. sexta* (McNall and Adang, 2003) and *H. virescens* (Jurat-Fuentes and Adang, 2004), membrane-bound ALPs have been shown to bind to Cry1Ac. The down-regulation of HvALP in larval midgut from Cry1Ac resistant *H. virescens* larvae (Jurat-Fuentes and Adang, 2004, 2007) clearly suggests its role in Cry1Ac toxicity. However the role of ALPs in Cry toxin susceptibility and hence in toxicity has not been really established properly till date.

Glycolipids: The recent addition of the molecules which could act as putative Cry toxin receptors are the glycolipids. Cry5B and Cry14 were found to bind to the purified glycolipids of *Caenorhabditis elegans* (Griffitts *et al*. 2005). The alteration in glycolipids levels in *Plutella xylostella* was believed to be involved in the evolution of resistance to Cry1Ac (Kumaraswami *et al*. 2001). It has been hypothesized that both glycolipids and Cry toxin receptors may play a role, sequentially or simultaneously, in positioning Cry toxins appropriately at the bilayer or in inserting toxins into the bilayer. However, the

functional role of glycolipids as Cry toxin receptors has not been established in any organism including insects.

Models of the mode of action of Cry toxins

Two contrasting models have been reported to describe the mode of action of Cry toxin (Soberón *et al*. 2008).

Pore formation model: Upon ingestion by the larval forms of the susceptible insects, crystalline inclusions of ~130 kDa protoxins are solubilized in the alkaline medium and reducing condition of the gut lumen. The solubilized protoxins are cleaved by midgut proteases at the N- and C- terminal ends to yield activated monomeric ~ 60 kDa toxins with a three domain structure (Schnepf *et al*. 1998). The activated toxins bind to primary receptors that are present in the larval midgut cells. The cadherin-like proteins have been described to function as primary receptors for the lepidoptera-specific Cry1A toxins (Vadlamudi *et al*. 1993; Gómez *et al*. 2001, 2003; Xie *et al*. 2005). Binding with the cadherin-like proteins in midgut facilitates additional protease cleavage of the N-terminal end of the toxins, eliminating helix α-1 of domain I (Gómez *et al*. 2002; Jiménez-Juárez *et al*. 2007). This then induces assembly of oligomeric forms of the toxin. The binding affinity of the oligomers is known to be higher and these oligomers bind the secondary receptors which are usually a GPI-anchored APN (eg. *M. sexta*) and/or GPI-anchored ALP (eg. *Heliothis virescens*) (Bravo *et al*. 2004; Jurat-Fuentes and Adang 2004; Fernandez *et al*. 2006). Binding of the oligomers to secondary receptors is followed by its insertion into the membrane microdomains, where GPI-anchored receptors are localized and create pores in the apical membrane of midgut cells. This causes cellular osmosis, eruption or breakdown of the midgut cells and eventually leads to the death of the larvae (Schnepf *et al*. 1998; de Maagd *et al*. 2003; Bravo *et al*. 2004). Thus, this model of mode of action is a multistep process (Bravo *et al*. 2004).

Signal transduction model: The more recent model proposed that the toxicity of Cry toxin is through the activation of Mg^{++}-dependent signal cascade pathway that is triggered by the interaction of the activated ~ 60 kDa toxin with the primary receptor, the cadherin-like protein. This interaction will activate a guanine nucleotide-binding protein (G-protein), which in turn activates an adenylyl cyclase promoting the production of intracellular cAMP. The increased cAMP levels facilitate protein kinase A activation

which promotes an intracellular pathway leading to cell death (Zhang *et al*. 2006). This model states that insect cell death occurs without the participation of oligomeric structures that form lytic pores of Cry toxin or the participation of other receptors as GPI-anchored proteins (Zhang *et al*. 2006).

Cry toxin binding directly to the GPI-anchored receptors and mediating Cry protein toxicity through pore formation or cellular signalling without involvement of the cadherin-like proteins is also suggested as an alternative mechanism of action. At present, the pore formation model is the most widely accepted mode of action of Cry toxins in lepidopteran insects.

Insect resistance to Cry toxins

In agriculture, *Bt*-based biopesticides have been used as a valuable alternative to chemical insecticides for the management of many economically important pests including those belonging to the order Lepidoptera. However, uncontrolled widespread use of *Bt* sprays and *Bt* crops in the last two decades has led to concerns about the effects they may have on environment and human health (Shelton *et al*. 2002). The important issues including the effect of Bt use on non-target organisms (Romeis *et al*. 2006), food safety (Shelton *et al*. 2002) and development of resistant insect population (Bates *et al*. 2005; Ferré and Van Rie, 2002) have been raised. To date, Bt resistant populations of two agriculturally important insect pests, diamondback moth, *Plutella xylostella*, and the cabbage looper, *Trichoplusia ni*, have been reported from the field where sprayable Bt formulations were applied (Tabashnik *et al*. 1990; Shelton *et al*. 1993, Janmaat *et al*. 2003). A number of laboratory-selected lepidopteran insects have developed high levels of resistance to *Bt*, and this is increasing in an alarming pace. Laboratory-selected resistance experiments have indicated the high potential of many species to still evolve resistance against Cry toxins. One of the mechanisms of resistance development was shown to be due to an alteration in the binding ability and/or a decrease in the population of midgut receptor molecules, which bind Cry toxin (Gould, 1998). Some reports suggest that the alteration in protoxin activation property of midgut proteases is also responsible for the development of resistance in insects, as exemplified in a selected strain of *Plodia interpunctella* (Oppert *et al.* 1994). It has been shown that the molecular basis of resistance in laboratory-selected strains of *P. interpunctella* as well as *Helicoverpa virescens* and in a field-selected strain of *P. xylostella* involves an alteration in receptor-

binding properties (Van Rie *et al.* 1990; Ferre *et al.* 1991; Maclntosh *et al.* 1991). The mechanism of insect resistance to *Bt*-based biopesticides could be located at each of the various steps in the mode of action of Cry toxins i.e., solubilization, proteolytic processing, passage through the peritrophic membrane, receptor binding, membrane insertion, pore formation, and osmotic lysis of midgut cells.

Important organs of *A. janata* larvae

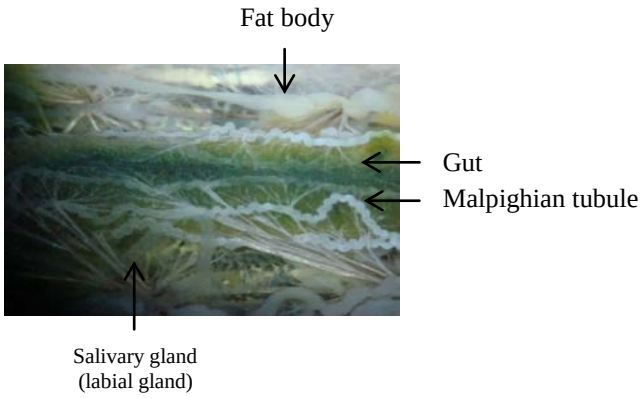

Fig. 2. Abdominal cavity of fifth instar larvae of *A. janata* showing gut, fat body, Malpighian tubule and salivary gland (labial gland)

Gut: In insects, digestion of food takes place in the alimentary canal which runs lengthwise through the body which is divided into different regions based on the specific role of the region in the digestion process. The midgut of lepidopteran larvae is composed of two major cell types (i) columnar epithelial cells with apical brush border microvilli and (ii) the Goblet cells containing a large cavity which is joined to the apical surface by the complex inter-digitated valve. The microvilli increase surface area of the midgut wall and allow maximum absorption of nutrients.

Fat body: Insect fat body tissue is organized in multiple lobes of highly tracheated tissue that bath freely in the hemolymph and have easy access to variety of molecules including nutrients, metabolites, proteins and hormones that are transported through the hemolymph (Fig. 2). The tissue is mainly composed of adipocytes or fat cells. The insect fat body is an organ analogue to vertebrate adipose tissue and liver, and functions as a major organ for nutrient storage and metabolism. Further, they also perform developmentally specific metabolic activities that produce, store and release components central to the prevailing

nutritional requirements or metamorphic events of the insects. Larval fat body synthesize storage proteins like hexamerins and arylphorins during active feeding phase and releases them into hemolymph, while the same tissue selectively sequester and accumulates the hexamerins and store them as storage granules which serve as energy and amino acid pool during metamorphosis (Kiran kumar *et al*. 1997; Burmester and Scheller, 1999). In insects, fat body is the central organ to integrate and co-ordinate different hormonal and nutritional signals for regulating insect development, metamorphosis as well as reproduction (Colombani *et al*. 2005; King Jones and Thummel, 2005).

Malpighian tubules: The term "Malpighian tubules" was named after Marcello Malpighi, an anatomist who first discovered the organ in insects. Malpighian tubules are the excretory and osmoregulatory organ of insects. The system comprises of numerous branching tubules extending from the alimentary canal present at the junction of midgut and hindgut that absorb solutes, water and wastes from the surrounding hemolymph. Finally, the wastes are released from the organism in the form of concentrated solid nitrogenous compounds. These slender tubules or tubes are dominantly found in the posterior regions of the abdominal cavity (Fig. 2). Each tube is composed of a single layer of epithelial cells that is closed off at the distal end with the proximal end joining the alimentary canal.

Salivary glands: Salivary glands are glands associated with the mouth or oral cavity and produce secretions (saliva) that are mixed with the food during feeding and are ingested along with the food. Four types of glands are known to be present in insects- mandibular, maxillary, hypopharyngeal, and labial glands. In Lepidoptera, the labial glands are the silk-producing organs throughout the larval stages, especially just before pupation. The glands occur in pairs and are constantly bathed in hemolymph.

Hemolymph: Hemolymph is a watery dilute to viscous fluid that fills the hemocoel or body cavity of insects which contains plasma and cells. The plasma, which is the main constituent of hemolymph, is characterized by the presence of high concentrations of variety of macromolecules including variety of proteins, carbohydrates, lipids as well as amino acids, free fatty acids, organic phosphates etc. Lipophorins (Kanost *et al*. 1995; Rimoldi *et al*. 1996; Pennington and Wells, 2002), storage proteins (Telfer and Kunkel, 1991), hormone and ion binding proteins (Maya-monteiro *et al*. 2000; Gudderra *et al*.

2002), carrier proteins (Goodman, 1983), regulatory proteins (Arif *et al*. 2004) and immune response proteins (John *et al*. 2001) are the various types of proteins present in the larval hemolymph. Among the storage proteins, hexamerins are the major serum proteins present in the larval hemolymph of lepidopterans. During the active feeding phase, they are synthesized and secreted into the hemolymph, where they circulate freely. However, their concentration in the hemolymph declines significantly during the non-feeding prepupal and early pupal stage due to selective receptor mediated sequestration into the fat body (Kirankumar *et al*. 1997; Manohar *et al*. 2010).

Insect metamorphosis

Metamorphosis in insects is characterized by relatively abrupt changes in the form and/or structure through cell growth and differentiation. Insects that exhibit incomplete metamorphosis, hemimetabolous insects, are polyphyletic while insects exhibiting complete metamorphosis, holometabolous insects, are monophyletic. Complete metamorphosis of a lepidopteran insect consists of an egg and the larvae emerges from the egg and usually molts five times, loses the cytoskeleton that it has out grown and produces a new one, and spins a cocoon and enters the cocoon as a pupa and emerges as an adult. The larvae are voracious feeders and have a habitat and niche that is different from the adult. The pupae are non-feeding and usually hidden in the cocoon.

In insects, molt and metamorphosis are orchestrated by juvenile hormone (JH) and 20-hydroxyecdysone (20E) through the regulation of gene/protein expression. In holometabolous insects, JH level is high throughout the larval instars, declines in the last instar but rises again before the pupal molt and is absent during the pupal stage. 20E initiates molting while JH determines the nature of the molt. So in the presence of JH, pulses of 20E trigger larval-larval molt, and in the absence of JH, 20E directs larval-pupal and pupal-adult metamorphosis (Riddiford, 1994, 2008). The 20E peak in the last instar occurs in the absence of JH, which signal larval-pupal molt (Riddiford, 1996; Davey, 2000). 20E and JH circulate in the hemolymph throughout the insect's body, so all the tissues are exposed to the same concentrations of hormones at any given time.

In insects, 20E triggers degeneration of all the larval specific tissues including gut, fat body, Malpighian tubule and salivary gland through programmed cell death. In holometabolous insects, the tissues are partly or entirely eliminated during larval-pupal transformation (Terashima *et al*. 2000; Mané-Padrós *et al*. 2008). During the period of

insect metamorphosis, these tissues undergo developmental remodelling process where the massive destruction of larval tissues is accompanied by simultaneous growth and differentiation of adult tissues from small clusters of progenitor cells. Besides, lysosomal enzymes are also known to play important role in the histolysis of larval organs and cellular destruction during metamorphic development. Acid phosphatase (ACP) is one of the most commonly used marker enzyme to study the lysosomal activity in insects (Verkuil, 1979, 1980). In dipteran and lepidopteran insects, ACP activity is known to increase at the beginning of the wandering or prepupal stage, preceding the actual metamorphosis (Verkuil *et al*. 1979; Ashok and Dutta-Gupta, 1988).

Lepidopteran insect model: *Achaea janata*

Lepidopteran larvae are the most destructive group of insect pests for the world's economically important crops. A lepidopteran pest, *Achaea janata*, commonly known as castor semilooper is widespread throughout the tropical and subtropical regions of the world. Castor plant (*Ricinus communis*) is the preferred host for the larval forms of *A. janata*, but occasional hosts include cabbage, mustard, sugar cane, rose, tomato, *ficus*, banana, crowns of thorns and tea, as well as some legumes. Castor is an important non-edible oilseed crop which is predominantly grown in India, China and Brazil (Lakshminarayana and Raoof, 2005). In India, outbreaks of this pest are common during July to September (Gaikwad and Bilapate, 1992). The entire life cycle of *A. janata* from egg to adult takes place in 48-50 days (French, 1950). There are five caterpillar stages or instars before pupation. When fully grown, the caterpillars are about 2½ inches in length. Each larval stage lasts about 2 days, except for the last instar which lasts for about 4 days.

Relevance of the study

A major threat to the success of *Bt*-based biopesticide industry is the development of resistance in insect pests against Cry toxins. Considering the numerous advantages *Bt*-based biopesticides hold against synthetic or chemical pesticides, if *Bt*-based biopesticide products become ineffective due to resistance, the loss to the organic farmers would be irreplaceable (McGaughey *et al*. 1998). Till date, three basic approaches are used in the resistance management programs. The ultimate aims of these management approaches have been to avoid resistance where and if possible, delaying resistance as long as possible and making resistant insect populations revert to susceptibility (Croft, 1990). The

first approach involves minimizing the exposure to toxins and/or maintaining the susceptible traits in the gene pool of the insects by allowing mating between the resistant insects and a large population of the susceptible insects. The second approach is based on the assumption that insects are likely to develop resistance more easily when a single control technique is used rather than the combination of two or more control techniques used simultaneously. Finally, the third approach employs strategy that involves s "trap plants" to lure pests away from the agricultural crops.

At the moment, none of the strategies provide considerably high chance of success in preserving *Bt* as a safe and effective insect pest control agent. With the increasing world population, the need to control insect pests from destroying food crops has become even more urgent. Besides trying to improve the existing strategies, we need to also look for alternate strategies and identify target molecules in various vital tissues and organs of Cry toxin sensitive insects, to manage the problem of pest outbreak and damage on agricultural crops. Identification and characterization of Cry toxin interacting proteins in vital larval tissues, and understanding the biochemical and physiological implications of such interaction would be critical in designing and validation of novel eco-friendly pest management strategies. RNAi technique could provide insights into the functional properties of candidate target molecules and this knowledge would help facilitate the efforts in designing efficient pest control strategies. In this line, we have adopted an unconventional mode of Cry toxin delivery i.e., hemocoelic delivery of Cry toxins to the voraciously feeding larvae of a lepidopteran model insect, *A. janata*, and tested if this putative mode of Cry toxin delivery could be an alternative pest management strategy. Our study was carried out with the following objectives :– (1) Toxicity effects of Cry toxins upon hemocoelic delivery to *A. janata* larvae. 2) Identification and characterization of Cry toxin targets in *A. janata*. 3) Developmental and hormonal regulation of APN expression in *A. janata*. 4) Functional elucidation of *AjAPN*1 expression in non-gut visceral tissues of *A. janata*.

Part 1

Toxicity effects of Cry toxins upon hemocoelic delivery to *A. janata* larvae

1. Introduction

Insect pest management by chemical pesticides comes at the cost of health of humans and environment including eradication of beneficial insects and development of pesticide-resistant pests (Roush *et al*. 1990). Biopesticides based on *Bacillus thuringiensis* (*Bt*), a gram-positive bacterium, and *Bt* transgenic crops provide a valuable alternative to chemical insecticides as they are more insect species-specific and least harmful to the natural enemies. Crystal inclusions produced by *Bt* are toxic to a wide range of insects including those belonging to the order Lepidoptera (Crickmore *et al*. 1998). These inclusions are composed of insecticidal proteins called crystal proteins or Cry proteins or δ-endotoxins. When susceptible insects ingest the Cry toxins, they are solubilized in the alkaline medium of the gut and processed by the gut proteases to yield the active toxins (Hofte and Whiteley, 1989; Gill *et al*. 1992). The activated toxins then bind to the specific receptors located on the brush-border membranes of the midgut epithelial cells, resulting in cell lysis and eventual death of the insects (Ferre and Van Rie, 2002). Midgut receptors that have been identified in lepidopteran insects include glycosylphosphatidylinositol (GPI)-anchored aminopeptidases N (APNs), cadherins, membrane-bound alkaline phosphatases (ALPs) and glycolipids (Knight *et al*. 1995; Vadlamudi *et al*. 1995; Banks *et al*. 2003; Jurat-Feuntes and Adang, 2004; Fabrick and Tabashnik, 2007; Krishnamoorthy *et al.* 2007). However, in the face of enormous selective pressure generated by widespread use of *Bt*-based biopesticides in crops and organic farming, a number of insects have developed resistance to *Bt* Cry toxins (McGaughey, 1985; Shelton *et al*. 1993; Luo *et al*. 1997; Ferre and Van Rie, 2002; Tabashnik *et al*. 2005). Alteration in the binding ability and/or a decrease in the population of receptor molecules in the insect midgut have been cited as the reason for the development of resistance to Cry toxins (Gould, 1998). Resistance in laboratory-selected strains of *Plodia interpunctella* (Van Rie *et al.* 1990) and *Heliothis virescens* (Maclntosh *et al.* 1991), as well as in field-selected strains of *Plutella xylostella* (Tabashnik *et al*. 1990; Ferre *et al.* 1991; Shelton *et al*. 1993) and the cabbage looper, *Trichoplusia ni* (Janmaat *et al*. 2003) was shown to be associated with an alteration in receptor-binding properties. In addition, altered protoxin activation by midgut proteases is also reported to be involved in resistance (Oppert *et al.* 1994).

In order to tackle the problem of insect resistance, there has been continuous move to improve the toxicity of the available *Bt* strains, find new potent isolates as well as

management of insect resistance against these agents. Delta-endotoxin engineering approach could be effectively used to increase the toxicity potency and widen the spectra of the target pests. Use of alternate bioinsecticides like baculoviruses against many insect pests mainly lepidopterans have been reported (Moscardi, 1999). Baculovirus-induced apoptosis of hemocytes and fat body was reported in the infected *Spodoptera litura* and *Spodoptera exiqua* larvae (Feng *et al.* 2007). Apoptosis is hypothesized to play an important role in insect immunity to baculovirus infection (Clarke and Clem, 2003). During insect metamorphosis, the tissues and organs are partly or entirely eliminated through programmed cell death at larval-pupal transformation (Chinzei, 1975; Schwartz, 1992; Terashima *et al.* 2000). The role of lysosomal enzymes including acid phosphatase in the histolysis of larval organs, cellular destruction, tissue remodeling and reorganization during metamorphosis is also well established (von Gaudecker and Schmale, 1974; Lee and Baehriecke, 2001; Thummel, 2001).

Intrahemocoelic injection of Cry1 toxins was shown to elicit toxic response in terms of larval food intake, growth and survival in *Lymantria dispar* (Lepidoptera) and *Neobellieria bullata* (Diptera) (Cerstiaens *et al*. 2001). However, role of apoptosis as a limiting factor for Cry toxin induced toxicity, either by oral ingestion or hemocoelic delivery has not been reported. In the present study, we investigated the toxicity effects of hemocoelic delivery of various Cry toxins (Cry1Aa, Cry1Ab, Cry1Ac and DOR5) individually to third instar larvae of an economically important lepidopteran pest, *A. janata*. We also studied the morphological and phenotypic responses of *A. janata* to the presence of Cry toxins in the larval hemocoel. This investigation was aimed to identify new molecular targets in the insect body, which could be exploited for the management of pests using alternate modes of delivery of *Bt*-based biopesticide. Here we show that hemocoelic delivery of Cry toxins by injection induced larval mortality, inhibited food intake, blocked larval growth and gave rise to smaller pupae in a dose-dependent manner. For the first time, we report apoptotic cell death in fat body tissue upon hemocoelic Cry toxin delivery. The involvement of lysosomal enzymes in Cry toxin-induced cell death in fat body is also highlighted. We also observed various morphological changes in gut, Malpighian tubule and salivary gland of the Cry toxin injected larvae. The results obtained in our present study suggest hemocoelic Cry toxin delivery to be an effective approach to pest control, which however, still require in-depth investigation.

2. Materials and methods

2.1. Insect rearing

Egg masses of *A. janata* were collected from castor fields of Directorate of Oilseeds Research, Hyderabad. Immediately after hatching, the neonates were transferred to a growth chamber and reared on fresh castor leaves (*Ricinus communis*) as diet under a photoperiod of 14:10 h (light:dark), 60-70% relative humidity at 27±2°C till pupation. The pupae were transferred onto moist sand in a container and allowed to develop into adults. The adults were then transferred to an aerated chamber and fed with 10% honey solution supplemented with vitamin E as diet. The female adults deposited their eggs onto the surface of castor leaves in rearing chamber, which were then allowed to hatch into neonate larvae for maintenance of regular cultures. Under our rearing condition, a majority of *A. janata* larvae reached late third instar on sixth day post-hatching and the larva weighs around 0.2±0.03g. For Cry toxin hemocoelic injection studies, we used the 5 days old larvae and hereafter, we refer the 5 days old larvae as “third instar”. Similarly, we will refer the 8 days, 10 days and 12 days old larvae as “fourth instar”, “fifth instar” and “late fifth instar” larvae respectively. Majority of the larvae entered pre-pupal or wandering stage on the fourteenth day.

2.2. Bacterial strains and growth conditions

The *Bt* isolate DOR5 was kindly provided by Dr. P. S. Vimala Devi, Principal Scienstist, Directorate of Oilseeds Research, Hyderabad. It was isolated from the soil of a region in Andhra Pradesh with no history of *Bt* use. For the preparation of crystal δ-endotoxin, the isolate was grown in G-Tris medium containing yeast extract at a concentration of 0.5g/100 ml media for 4 days with agitation at the speed of 200 rpm/min at 30°C until sporulation and cell lysis was complete (Aronson *et al*. 1971). For isolation of plasmid DNA, DOR5 isolate culture was grown in Luria-Bertani (LB) broth for overnight at 30°C.

E. coli JM103 strains expressing recombinant Cry1Aa, Cry1Ab and Cry1Ac (where the cDNA of specific toxin was cloned in expression vector pKK223-3) were grown in LB broth with ampicillin (50µg/ml) for 48 h at 37°C and were used for the purification of Cry1Aa, Cry1Ab and Cry1Ac toxins (Lee *et al*. 1992).

2.3. Isolation of plasmid and *cry* gene profiling

The plasmids were isolated according to the method of Kado and Liu (1981) with some modifications and additional steps. The culture was grown overnight in 30 ml of LB broth at 30ºC to an optical density of 0.8 at 600 nm. Cells were pelleted by centrifugation (6000 rpm, 4°C, 10 min) and resuspended the cells in 10 ml of E-buffer (40mM Tris-acetate and 2mM sodium EDTA) by pipeting up and down several times. The cells were lysed by adding 20 ml of lysis solution (3% SDS and 50mM Tris, pH 12.6). The lysate was then incubated at 60°C for 30 min in water bath. To this, two volumes of unbuffered phenol: chloroform solution (1:1 v/v) was added. The solution was emulsified by shaking briefly and centrifuged at 6000 rpm for 15 min at 4°C. The aqueous layer was collected and two volumes of cold absolute ethanol were added to it. After incubating it for overnight at -20°C, the solution was centrifuged at 14,000 rpm at 10°C for 30 min. The DNA pellet thus collected was dissolved in TE buffer (10mM Tris- HCl, pH 8.0 with 1mM EDTA) and stored until use.

Analysis of the *cry*1 and *cry*2 gene content of DOR5 isolate was performed following triplex PCR technique and using the primers published by these workers (Ceron *et al.* 1995; Juarez-Perez *et al*. 1997; Masson *et al*. 1998). Presence of novel *cry*-type genes in DOR5 isolate was analyzed based on the procedure described by Beron *et al*. (2005).

2.4. Preparation and purification of activated Cry toxins

The DOR5 spores and crystals were harvested by centrifugation at 7000 rpm for 10 min at 4°C. Sporangial debris was removed by washing with ice-cold deionized water and the pellet was resuspended in 50mM Tris-HCl (pH 7.5). Spores and crystals were separated using differential ultracentrifugation using a discontinuous sucrose density gradient (Thomas and Ellar, 1983). Ultracentrifugation was carried out in a Beckman L8-80M ultracentrifuge in a SW 50.1 rotor operating at 42,000 rpm for 4 h at 4°C. Crystal proteins was collected and washed three times with ice-cold 50mM Tris-HCl (pH 7.5) to remove the sucrose by centrifugation at 15,000 rpm for 5 min at 4°C. The final crystal pellet was solubilized in 50mM sodium carbonate buffer (pH 10.5) containing 0.1% 2-mercaptoethanol by incubating at 37°C for 2 h and then centrifuged at 10,000 rpm for 15 min to remove the insoluble debris.

For preparation of recombinant toxins, JM103 cells were harvested (10000 X g, 10 min) and the pellet resuspended in a buffer (50mM Tris-HCl, 50mM EDTA, 15%

sucrose, pH 8.0). Cell suspension was sonicated on ice (10 min, 30 s) and centrifuged at 15000 X g for 15 min. The pellet obtained was washed three times with ice-cold 0.5M NaCl containing 2% Triton X-100, five times with 0.5M NaCl and finally two times with distilled water. The crystal protein was solubilized in 50mM sodium carbonate buffer (pH 10.5) containing 10mM DTT at 37°C for 2 h (Lee *et al*. 1992).

The solubilized crystal proteins were digested with trypsin in a trypsin/protoxin ratio of 1:50 (by mass) at 37°C for 2 h. 1mM PMSF was added to stop the proteolytic reaction and the profile of the digested toxin was assessed by SDS-PAGE. Activated toxins were individually purified by gel filtration on Sephadex G-100 column.

2.5. Hemocoelic injection assay

Third instar larvae were narcotized by placing them on ice for 15 min. The insects were then injected with activated Cry1Aa, Cry1Ab, Cry1Ac and DOR5 Cry toxins at doses of 0.1, 0.5, 1, 5 and 10 µg/0.2 g body weight of the larvae through the dorsal side using a Hamilton microsyringe. The control larvae received the same volume of the carrier solvent. Care was taken to incur minimum injury. After injection, the wound was sealed with bees wax and the larvae were placed on ice for 15 min before transferring them back to the rearing chamber provided with fresh castor leaves. They were then allowed to grow normally. A minimum of 20 larvae were used for each dose and the experiment was repeated three times independently. The body weight of each larva was examined at every 24 h for 5 days. Larval mortality for each dose was calculated 2 day post-injection. The weights of the pupae were also recorded.

2.6. Collection, preparation and estimation of hemolymph protein

The larvae of the appropriate stage were narcotized on ice for 15 min. The prolegs were cut with a fine sharp scissor and the oozing hemolymph was collected with the help of a capillary tube into centrifuge tubes precoated with 0.025% phenylthiourea in order to prevent tyrosinase activity and melanization. The hemolymph samples were centrifuged at 1000 X g for 3 min at 4°C to sediment the hemocytes. The supernatant i.e., the clear plasma sample was either stored at -80°C or diluted with 10mM Tris-HCl (pH 7.8) and used immediately. Total protein content was estimated by Bradford's method (1976) using BSA as standard.

2.7. Western blotting

The hemolymph proteins were resolved by 10% SDS-PAGE and electro-blotted onto a nitrocellulose membrane using trans-blot apparatus (Bio-Rad) according to the procedure of Towbin *et al*. (1979). The blots were blocked using 5% skimmed-milk powder (w/v) in Tris-buffered saline (10mM Tris-HCl, pH 7.4, 150mM NaCl) supplemented with 0.1% Tween-20 (TBST) for 1 h at room temperature to block the non-specific binding sites. The blots were then incubated with *A. janata* hexamerin polyclonal antibody (1:5000 dilutions) (Budatha *et al*. 2011). Subsequently, the blots were incubated with alkaline phosphatase (ALP)-conjugated goat anti-rabbit IgG and visualized by developing with ALP substrate, NBT-BCIP substrate (Sigma Aldrich, USA).

2.8. Fixation of larvae for histological study

2 day post-injection, the larvae were briefly narcotized on ice and dissected in Ringer solution (130mM NaCl, 0.5mM KCl and 0.1mM $CaCl_2$). An incision was made in the abdominal region and was extended through the complete length of the larvae. Further, the gut contents were removed carefully and the insects were properly rinsed in Ringer solution. The larvae were then fixed overnight in 4% paraformaldehyde. After washing with 0.1M phosphate buffered-saline (PBS, pH 7.4) for 10 min, the larvae were dehydrated in ethanol series and were then placed in xylene for 5 min for proper clearance. The samples were then impregnated with molten paraffin at 60°C for 3 h followed by final embedding in paraffin. Sections of 5 µm thickness were prepared using Leica microtome (Leica, Germany) and spread onto glass slides.

2.9. Hematoxylin-eosin staining

The sections on slides were de-parafinized in xylene, re-hydrated in ethanol series, followed by staining in hematoxylin (nuclear stain) and eosin (cytoplasmic stain). The sections were de-hydrated in ethanol series, cleared in xylene and mounted on slides using DPX mountant.

2.10. TUNEL staining

ApoAlert DNA Fragmentation assay kit (ClonTech, USA) was used to detect nuclear DNA fragmentation in the tissues of control and toxin injected whole-larva sections. TUNEL staining (terminal deoxynucleotidyltransferase-mediated fluorescein-dUTP nick-end labeling) was performed according to manufacturers' protocol and instructions.

2.11. MTT staining of fat body tissue

The 3-(4, 5-dimethylthiazol-2-yl) -2, 5-diphenyl tetrazolium bromide (MTT) (Himedia Chemicals) was used to measure tissue viability. Fat body from larvae were dissected out in sterile insect Ringer solution and placed in 500 µl of TC-100 insect culture medium (Sigma Aldrich, USA) containing traces of streptomycin sulphate. To this, 100 µl of MTT solution (5ng/ml) was added and incubated at 25°C with gentle shaking for 30 min in dark. The tissue was then rinsed in PBS (pH 7.4) for removal of the excess nonspecific stain and culture media. The tissue was mounted on a slide and observed under fluorescence microscope. Positive control used was the fat body tissue from fifth instar larvae, while negative control was the heat-killed fat body tissue from fifth instar larvae.

2.12. Acid phosphatase assay

The assay was carried out according to the method of Henrikson and Clever (1972) with slight modifications. The reaction mixture contained 100mM sodium acetate buffer (pH 5.0) and homogenate containing100 µg protein. The enzyme sample with the buffer was incubated at 37°C for 10 min to exclude glucose-6- phosphatase activity. The reaction was initiated with the addition of 8mM *p*-nitrophenyl bisodium phosphate to the assay mixture followed by incubation for 1 h at 37°C. The reaction was terminated by the addition of 0.5 ml of 0.1N NaOH. The yellow color thus developed was measured at 410 nm against a substrate blank. The *p*-nitrophenol (PNP) was used for the preparation of a standard curve. The activity of the enzyme was expressed as nano moles of PNP released/h/µg protein.

2.13. Phenotypic analysis

Larval-pupal intermediates and adults developed upon Cry toxin injection were photographed with a FinePix S9600 digital camera and their phenotypic features were analyzed. The wings of the normal and defective adults developed from control and toxin injected larvae respectively were placed on an aluminium stub and coated with gold in a FullamEMS-76m evaporator for 15 min and the scale morphology was examined using Geol scanning electron microscope.

2.14. Statistical analysis

Data are expressed as mean ± standard deviation of three independent experiments (n=3). Differences between groups were analyzed for statistical significance by One-Way ANOVA followed by Students-Newman-Keuls (SNK) test using SigmaPlot 11.0 software. A probability of $p > 0.05$ is considered statistically significant.

3. Results

3.1. Effect of hemocoelic Cry toxin injection on larval mortality, larval growth and pupal weight of *A. janata*

Protoxin and the subsequent activated forms of Cry1Aa, Cry1Ab, Cry1Ac and DOR5 toxins were prepared and purified by gel filtration using Sephadex G-100 column (Fig. 1A, 1B, 1C & 1D). Lepidopteran-specific insecticidal gene profiling of DOR5 Bt isolate revealed the presence *cry1*Aa (Fig. 2B; Lane: Aa), *cry1*Ab (Fig. 2B; Lane: Ab), *cry1*C (Fig. 2B; Lane: C), *cry1*I (Fig. 2C; Lane: 2), *cry2*A (Fig. 2D; Lane: 2A), *cry2*B (Fig. 2D; Lane: 2B) and vegetative insecticidal proteins (*vip*) genes (Figs. 2E; Lane: 2 & 2F; Lane: 1). DOR5 did not contain *cyt* genes (Fig. 2G; Lane: 2).

Cry toxin	Feeding bioassay LC_{50}(ng/cm^2 of leaf surface)
Cry1Aa	107.56
Cry1Ab	47.83
Cry1Ac	35.87
DOR5	4.908

Table 1. **Evaluation of insecticidal activity of Cry toxins against *A. janata* larvae after oral ingestion**. Feeding bioassay was performed on castor leave discs. Both sides of the leave discs were painted with Cry toxins, shade dried and placed onto moist cotton in petriplates. Seven treatment concentrations i.e., 2, 4, 6, 8, 10, 12 & 14ng/cm^2 and one control (carrier solvent painted) were selected. Triplicates were maintained for each treatment and 20 two days old *A. janata* larvae were released on each leaf disc. Mortality was recorded at every 24 h interval for 5 days and LC_{50} was calculated 2 day post-treatment by using probit analysis with the help of Finney's table (Finney, 1952).

The results of feeding bioassays presented in table 1 clearly show that all the recombinant Cry toxins i.e., Cry1Aa, Cry1Ab and Cry1Ac were insecticidal. Further the LC_{50} doses of Cry1Ab and Cry1Ac were much lower when compared with Cry1Aa for *A. janata* larvae. However, it is interesting to note that DOR5 Cry toxins had high insecticidal activity with fairly low LC_{50} (4.9ng/cm^2 of leaf surface). Unlike the feeding bioassay, where very low doses of the toxins caused significant mortality (Table 1), injection of fairly high doses of toxins were required to induce significant mortality, which was monitored 2 day post-injection. Injection of 10 µg of Cry1Aa (Fig. 3A), 5 µg of Cry1Ab (Fig. 3B), 5 µg of Cry1Ac (Fig. 3C) and 1 µg of DOR5 Cry (Fig. 3D) toxins resulted in 50%-70% mortality. Nearly complete larval mortality was observed when 5 µg of DOR5 toxin was injected to the third instar larvae (Fig. 3D). Injection of activated Cry1Aa, Cry1Ab, Cry1Ac and DOR5 toxins individually to third instar larvae at various concentrations (0.1, 0.5, 1, 5 and 10 µg/0.2g body weight of the larvae) resulted in inhibition of food intake in all of the injected insects. Each of the toxin mentioned above inhibited larval growth rate in a dose-dependent manner. The larvae including the controls begin to feed only after 24 h of injection. Results presented in figure 4 clearly show that Cry1Aa (Fig. 4A), Cry1Ab (Fig. 4B) and Cry1Ac (Fig. 4C) at doses of 1, 5 or 10 µg/0.2g body weight blocked the development and the increase in the body weight of these larvae were significantly lower than that of the controls till wandering stage. Further, the effects of DOR5 toxin was more pronounced than that of recombinant Cry1Aa, Cry1Ab or Cry1Ac toxins and it has significant effect at a much lower dose of 0.5 µg/0.2g body weight of third instar larvae (Fig. 4D). Each of the control larvae reached a maximum body weight of around 0.8g, whereas the weight of the DOR5 toxin injected larvae reached only 0.3g or so. Further, comparable effect was obtained with 5 and 10 µg of Cry1Aa (Fig. 4A), Cry1Ab (Fig. 4B) and Cry1Ac (Fig. 4C). Furthermore, injection of 1 µg of Cry1Aa (Fig. 5A), Cry1Ab (Fig. 5B) and Cry1Ac (Fig. 5C) and 0.5 µg of DOR5 (Fig. 5D) toxins retarded larval growth and reduced the pupal weights significantly. The weight of each pupa of the control group reached to 0.55±0.013g while the pupal weights of the Cry toxin injected insects were as low as 0.38±0.04g (Fig. 5).

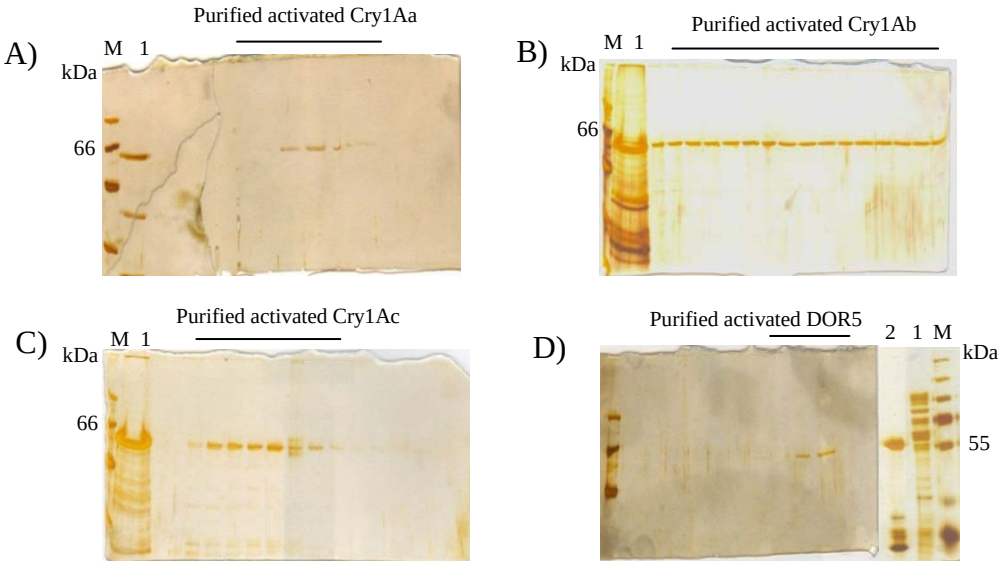

Fig. 1. **Purification of activated Cry toxins for hemocoelic injection**. The activated Cry toxins were purified by gel filtration on Sephadex G-100 column. **A)** Cry1Aa; Lane M: protein ladder, Lane 1: trypsinized Cry1Aa toxin mixture, remaining lanes: purified activated Cry1Aa toxins. **B)** Cry1Ab; Lane M: protein ladder, Lane 1: trypsinized Cry1Ab toxin mixture, remaining lanes: purified Cry1Ab toxins. **C)** Cry1Ac; Lane M: protein ladder; Lane 1: trypsinized Cry1Ac toxin mixture, remaining lanes: purified activated Cry1Ac. **D)** DOR5; Lane M: protein ladder, Lane 1: discontinuous sucrose density ultracentrifugation prepared DOR5 protoxins, Lane 2: trypsinized DOR5 Cry toxin mixture, remaining lanes: purified activated DOR5 Cry toxins.

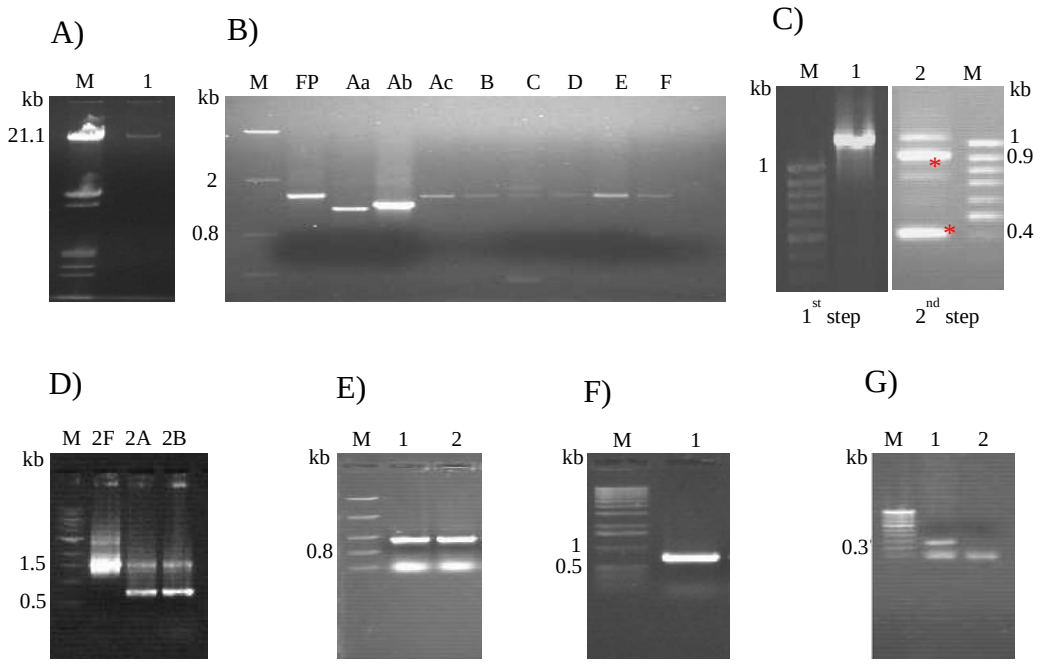

Fig. 2. **Lepidopteran-specific insecticidal gene profiling of DOR5 Bt isolate**. **A)** DOR5 plasmid; Lane M: DNA ladder, Lane 1: Plasmid. **B)** *cry1* profiling; Lane M: DNA ladder, Lane FP: *cry1* family primers l (+) and l (-), Lanes Aa to F contain a type primer along with *cry1* family primers l (+) and l (-), Lane Aa: *cry1*Aa, Lane Ab: *cry1*Ab, Lane Ac: *cry1*Ac, Lane B: *cry1*B, Lane C: *cry1*C, Lane D: *cry1*D, Lane E: *cry1*E and Lane F: *cry1*F. **C)** Detection of known and novel *cry* genes; Lanes M: DNA ladder, Lane 1: 1st step PCR product, Lane 2: 2nd step PCR product, * represents *cry1*I (confirmed upon cloning and sequencing). **D)** *cry2* profiling; Lane M: DNA ladder, Lane 2F: *cry2* family primers II(+) & II (-), Lane 2A: *cry2*A specific primer with II(+) & II(-), Lane 2B: *cry2*B specific primer with II(+) & II(-). **E)** Identification of *vip* genes in plasmid; Lane M: DNA ladder, Lane 1: HD1 *Bt* strain (positive control), Lane 2: DOR5 *Bt* isolate. **F)** Identification of *vip* genes in genome; Lane M: DNA ladder; Lane 1: DOR5 *Bt* isolate. **G)** Identification of *cyt* genes; Lane M: DNA ladder, Lane 1: *Bt* strain G30 (positive control); Lane 2: DOR5 *Bt* isolate.

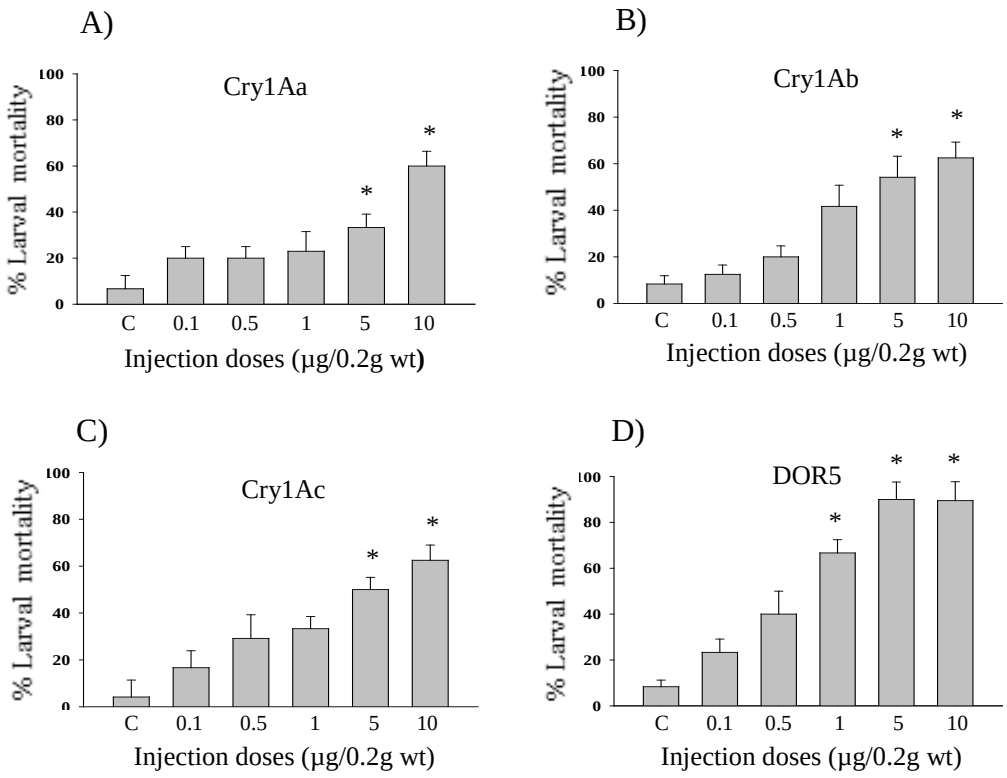

Fig. 3. **Effect of Cry toxin injection on larval mortality**. Third instar larvae were injected with Cry toxin doses of 0.1, 0.5, 1, 5 and 10 µg/0.2g body weight of larvae. Larval mortality for each dose was calculated 2 day post-injection. 20 larvae were used for each dose. **A)** Cry1Aa. **B)** Cry1Ab. **C)** Cry1Ac. **D)** DOR5. Values presented are the mean ± standard deviation of three independent experiments (n=3). * ≥ 50% mortality.

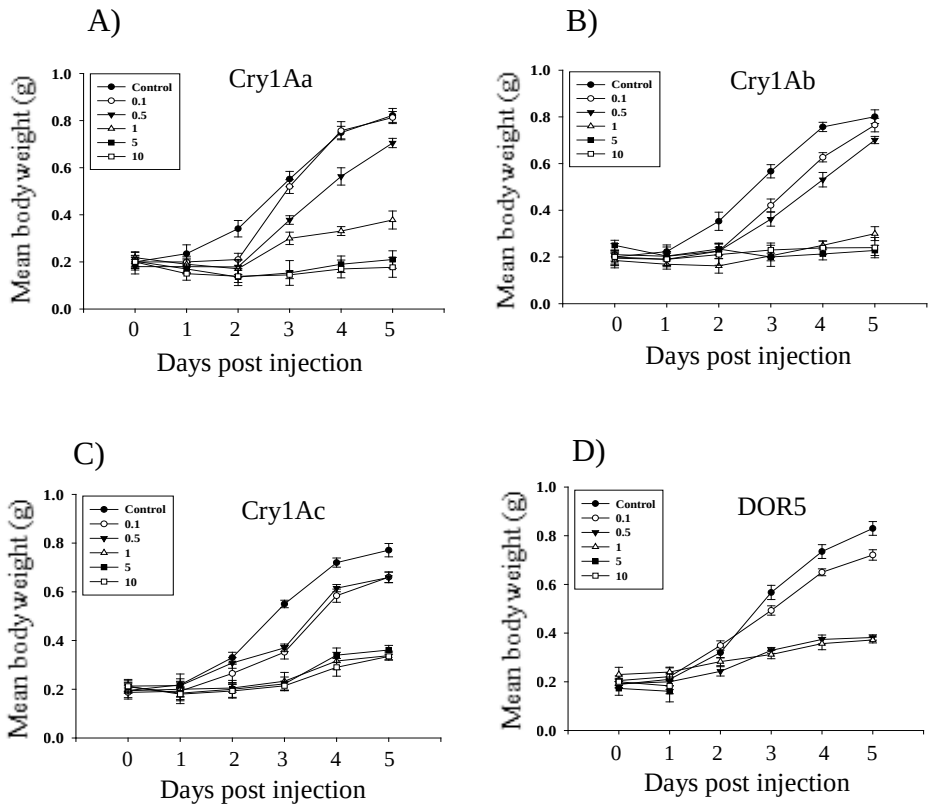

Fig. 4. **Effect of Cry toxin injection on larval growth**. Third instar larvae were injected with Cry toxin doses of 0.1, 0.5, 1, 5 and 10 µg/0.2g body weight of larvae. The weight of each larva was taken at every 24 h interval post-injection for 5 days. 20 larvae were used for each dose. **A)** Cry1Aa. **B)** Cry1Ab. **C)** Cry1Ac. **D)** DOR5. Values presented are the mean ± standard deviation of three independent experiments (n=3).

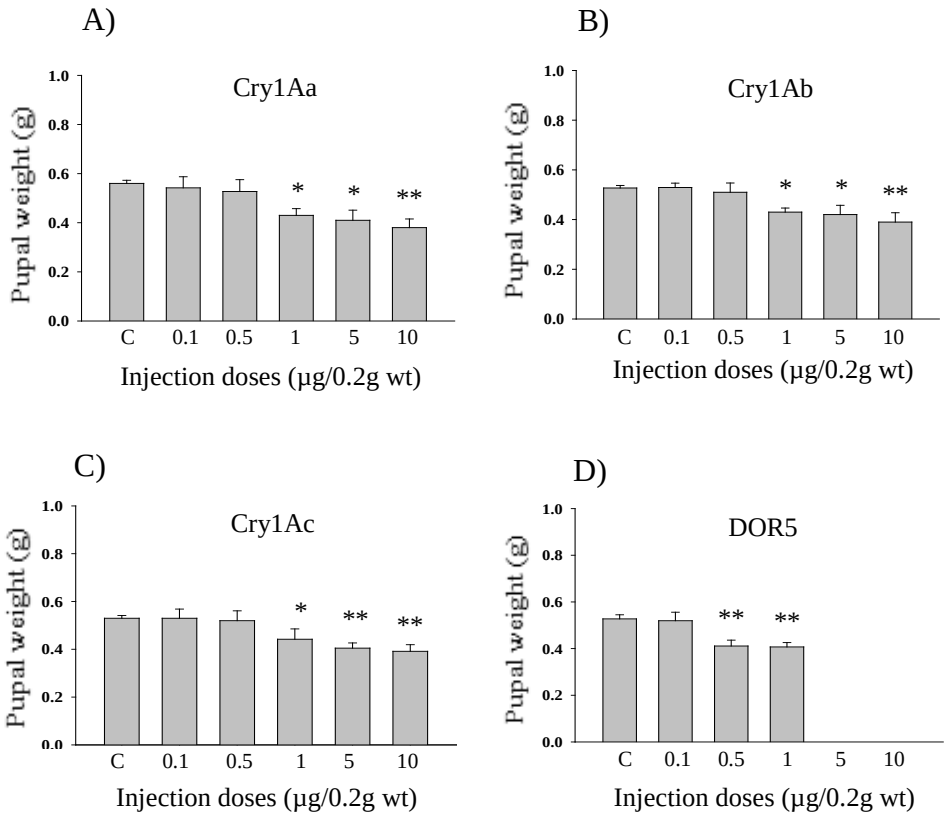

Fig. 5. **Effect of Cry toxin injection on pupal weight**. Third instar larvae were injected with Cry toxin doses of 0.1, 0.5, 1, 5 and 10 µg/0.2g body weight of larvae. 20 larvae were used for each dose. **A)** Cry1Aa. **B)** Cry1Ab. **C)** Cry1Ac. **D)** DOR5. Values presented are the mean ± standard deviation of three independent experiments (n=3). Significance between groups was tested by One-Way ANOVA followed by SNK test using SigmaPlot 11.0 software. Means marked with * $p < 0.05$, ** $p < 0.001$ indicate statistical significance.

3.2. Effect on total protein and hexamerin profile of hemolymph

Upon injection of 1 µg of DOR5 Cry toxins to the third instar larvae, the increase in total protein content of hemolymph (normally seen during larval development) was drastically reduced (Fig. 6A). It is interesting to note that the protein content of the 2 day post-injected and the four days post-injected larvae was not only lower than that of the control insects but was even lower to that of the larvae used for injection. Further, the total protein content of the hemolymph of fourth instar larvae increased nearly 2.8-fold from the third instar larvae, the stage at which the toxins were injected and remained more or less at same level in fifth instar (Fig. 6A). The protein content of the control larvae (fifth instar) reached 2.1±0.07mg/mL of hemolymph, whereas the toxin injected larvae of same chronological age showed only 0.34±0.04 mg/mL of the hemolymph. SDS-PAGE (Fig. 6B) and western blot analysis (Fig. 6C) of the hemolymph hexamerin protein profile revealed that DOR5 Cry toxins caused a significant reduction in 80-85kDa hexamerins in 2 day post-injected (Figs. 6B & 6C, Lane: 4i) as well as in 4 day post-injected (Figs. 6B & 6C, Lane: 5i) larvae. However, the hemolymph of both the control groups (i.e., 2 day and 4 day post-injected) showed the presence of fairly high amount of hexamerins (Figs. 6B & 6C, Lanes: 4c & 5c). Similar hexamerin protein profile was observed when third instar larvae were orally fed with toxin painted castor leaves (0.1ng/cm^2) and analyzed (Figs. 6D & 6E). Further this inhibition of hexamerin protein release from the fat body into the hemolymph was found to continue during the period of experimentation.

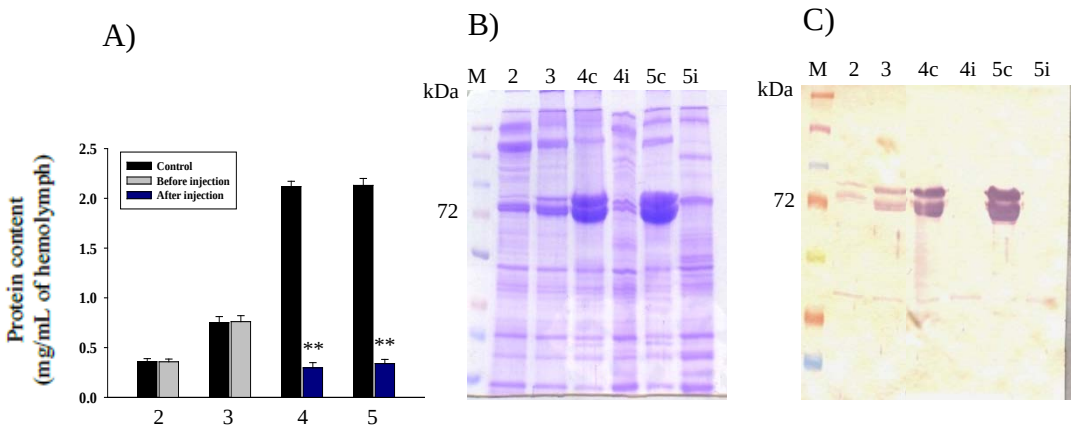

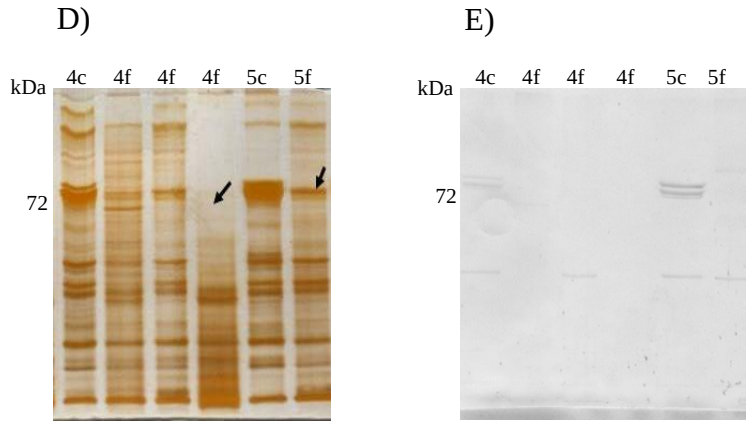

Fig. 6. **Effects of Cry toxin injection and feeding on hemolymph total protein content and hemolymph hexamerin profile**. Third instar larvae were injected with DOR5 Cry toxin dose of 1 µg/0.2g body weight of larvae. Another set of third instar larvae were also fed with DOR5 Cry toxin painted castor leaves (0.1ng/cm^2). Hemolymph total protein content and hexamerin protein profile were analysed 2 and 4 day post-injection/post-feeding. **A)** Larval hemolymph protein content. **B)** 10% SDS-PAGE analysis of larval hemolymph protein profile. **C)** Western blot analysis of hexamerin profile. **D)** 10% SDS-PAGE analysis of larval hemolymph protein profile after oral ingestion of DOR5 Cry toxins. **E)** Western blot analysis of hexamerin profile after oral ingestion of DOR5 Cry toxins. Note the disappearance of 80-85 kDa hexamerin protein from the hemolymph of 2 day and 4 day Cry toxin post-injected and post-fed larvae. Values represent the mean ± the standard deviation of three independent experiments (n=3). ** $p < 0.001$ (ANOVA and SNK test); Lane 2 – second instar, Lane 3 – third instar, Lane 4 – fourth instar, Lane 5 – fifth instar, Lane 4c – fourth instar control, Lane 4i – 2 day Cry toxin post- injected, Lane 4f – 2 day post-fed, Lane 5c – fifth instar control, Lane 5i – 4 day Cry toxin post-injected and Lane 5f – 4 day post-fed.

3.3. Pathological effects of Cry toxin injection

Detailed microscopic studies of vital larval tissues and organs from 2 day post-injected insects (1 µg of DOR5 Cry toxins) revealed the presence of thin and loosely developed fat body tissues, and it appeared as flattened sheet of fat body cells (adipocytes) which were fairly scarce in cytoplasmic granules (Fig. 7C). The gut of the toxin injected larvae revealed a comparatively narrow lumen, which was fairly empty of any food contents (Fig. 7C). The Malpighian tubules also appeared thin and opaque in appearance (Fig. 7D) while in controls it was transparent (Fig. 7A).

Hematoxylin and eosin (H&E) staining was used to investigate the alteration in the structure of various internal organs upon Cry toxin injection. The slides prepared

using whole-larva sections revealed extensive nuclear fragmentation and presence of large vacuolar regions in fat body, indicating fat body tissue degeneration/histolysis (Fig. 8B; b). Histological sections from gut of the Cry toxin treated larvae revealed the presence of cellular debris in the lumen and irregular arrangement of Goblet as well as columnar cells in the gut epithelium (Fig. 8A; b). We observed many large vacuoles in the cytoplasmic regions of the single-layered cell epithelium of Malpighian tubule. However, the nucleus of the cells appeared slightly elongated but not fragmented (Fig. 8C; b). The salivary gland of the Cry toxin injected larvae did not show any structural difference from the control glands. However, the glandular epithelium was much thinner in Cry toxin treated insects (Fig. 8D; b) compared to that of control insects (Fig. 8D; a). TUNEL staining of the whole-larval sections identified nuclear DNA fragmentation in numerous TUNEL-positive cells in fat body tissue confirming apoptotic cell death upon DOR5 Cry toxin injection (Fig. 9B; b). However, TUNEL positive signals were not detected in gut, Malpighian tubule and salivary gland of the Cry toxin injected larvae (Figs. 9A; b, 9C; b & 9D; b). Both histological as well as TUNEL studies revealed fat body tissue to be most affected by Cry toxin injection. MTT staining was performed with fat body tissue to check the viability of the cells of the tissue. Cell death in fat body tissue via apoptosis upon Cry toxin injection was further supported by a weak MTT staining of the tissue as compared to the dark purple staining of the control tissue (Fig. 10B; b). The fat body tissue from fifth instar larvae stained immediately after dissection (Fig. 10A; a) or after heat-killing (Fig. 10A; b) was used as the positive and negative controls respectively. Heat-killed fat body tissue did not show the deposit of any dark purple crystal indicating the non-viablility of the tissue cells (Fig. 10A; b).

3.4. Participation of lysosomal acid phosphatase activity

Estimation of acid phosphatase activity in gut, fat body, Malpighian tubule and salivary gland of the 1 µg DOR5 Cry toxin injected larvae showed an elevated level of enzyme activity only in the fat body tissue. Gut, Malpighian tubule and salivary gland did not show significant alteration in enzyme activity (Fig. 11). The assay was performed using 2 day post-injected larvae.

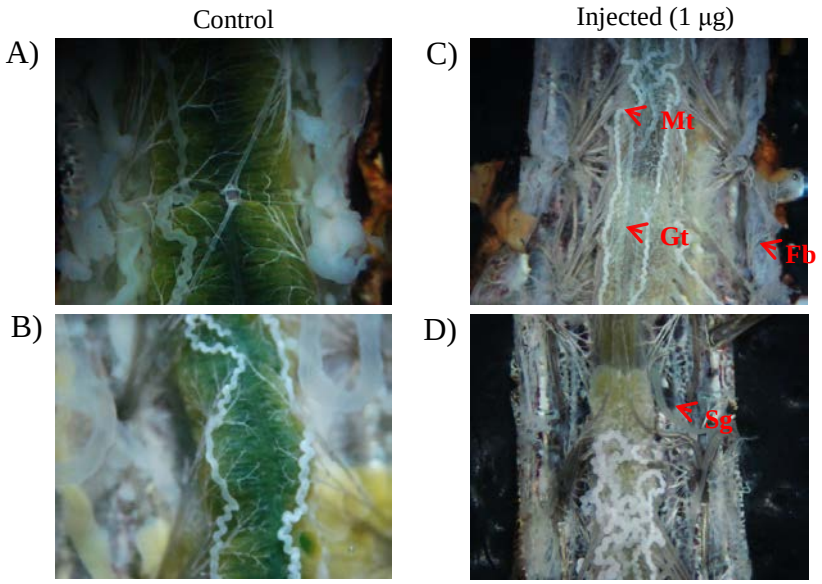

Fig. 7. **Effect of Cry toxin injection on larval tissue morphology**. Third instar larvae were injected with DOR5 Cry toxin dose of 1 µg/0.2g body weight of larvae. Morphology of tissues and organs of control (Control) and Cry toxin injected (Injected) larvae were observed 2 day post-injection. Arrows indicate the changes induced by the Cry toxin injection. Gt – gut, Fb – fat body, Mt – Malpighian tubule and Sg – salivary gland.

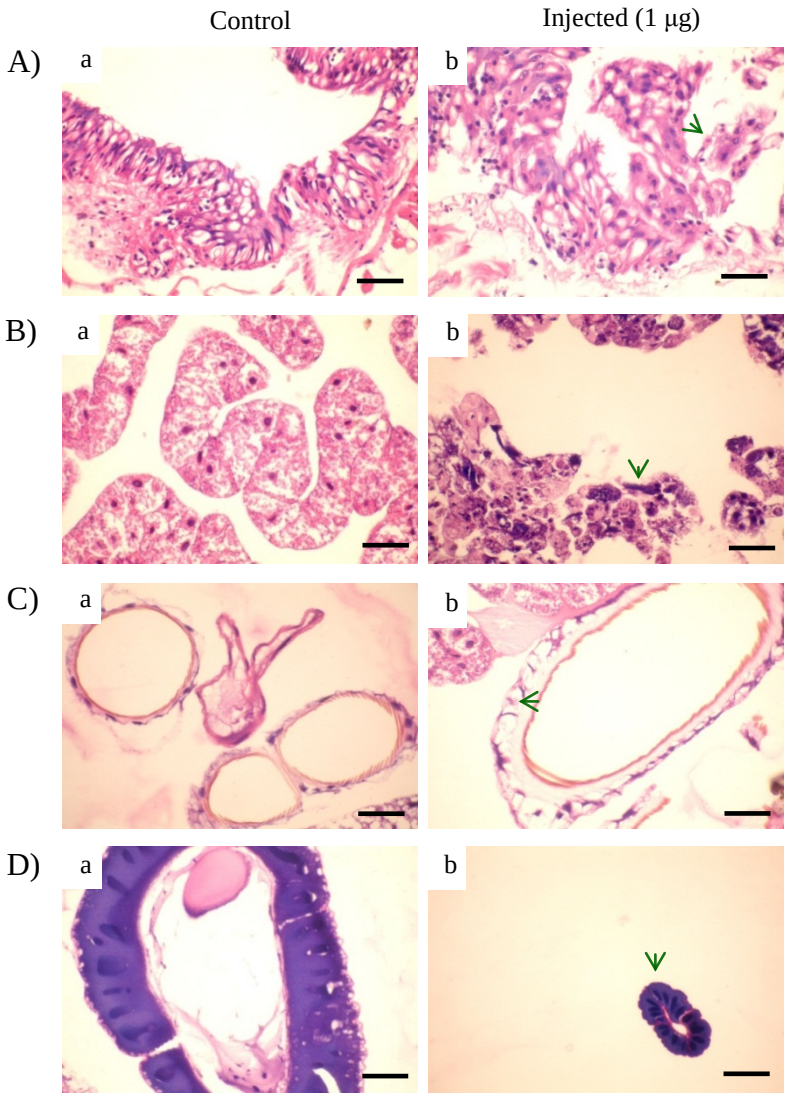

Fig. 8. **Histopathology of Cry toxin induced larval tissues**. Third instar larvae were injected with DOR5 Cry toxin dose of 1 µg/0.2g body weight of larvae. Tissue sections of control (Control) and toxin injected (Injected) were prepared from 2 day post-injected larvae and stained with H&E. **A)** Gut. **B)** Fat body. **C)** Malpighian tubule. **D)** Salivary gland. Arrows indicate the changes induced by Cry toxin injection. Scale bars of all the images represent 5 µm.

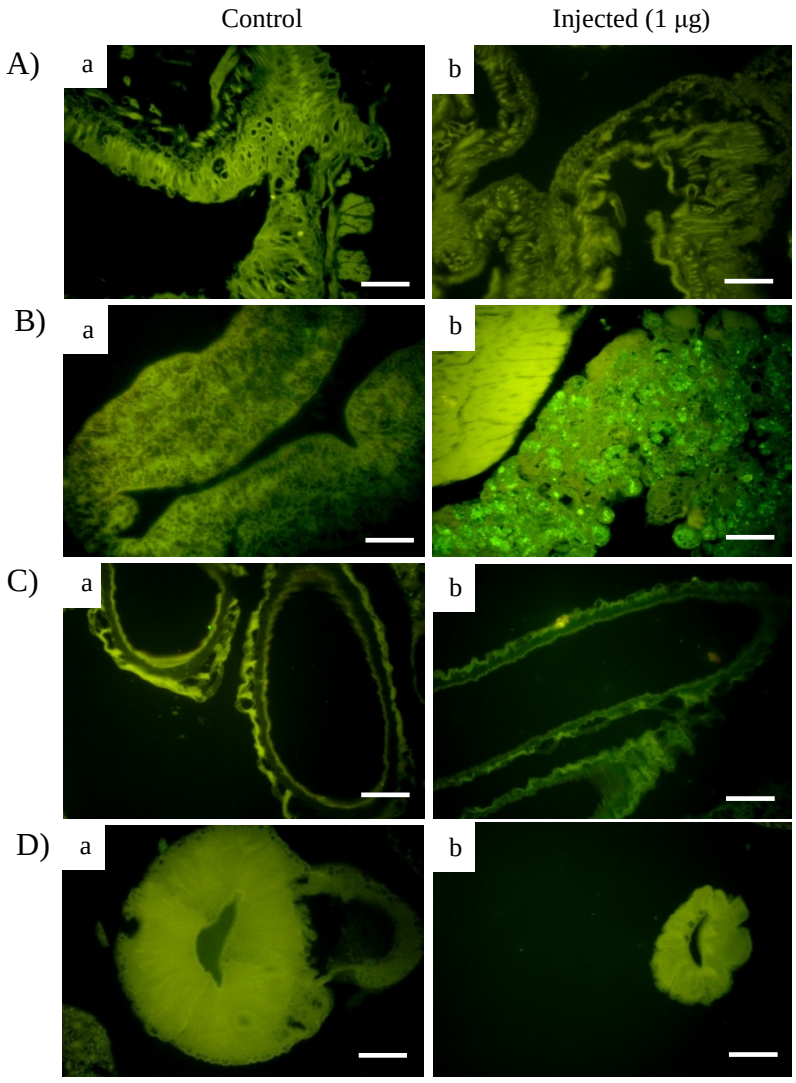

Fig. 9. **TUNEL detection of cell death**. Third instar larvae were injected with DOR5 Cry toxin dose of 1 µg/0.2g body weight of larvae. Tissues were processed for TUNEL staining from 2 day post-injected larvae. **A)** Gut. **B)** Fat body. **C)** Malpighian tubule. **D)** Salivary gland. Note the presence of extensive number of TUNEL-positive cells in fat body tissue of Cry toxin injected larvae (Injected). Scale bars of all the images represent 5 µm.

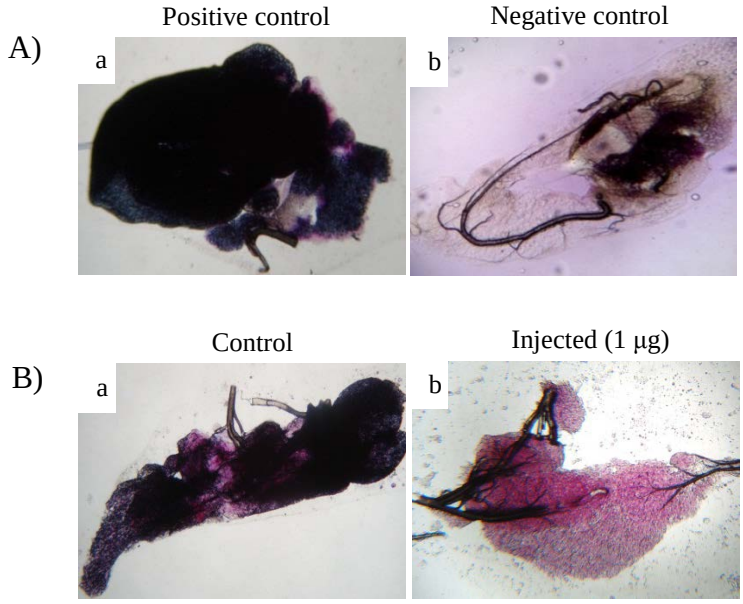

Fig. 10. **MTT staining of fat body tissue**. Third instar larvae were injected with DOR5 Cry toxin dose of 1 µg/0.2g body weight of larvae. Observations were made from 2 day post-injected larvae. **A)** Positive (a) and negative (b) controls. Positive control is the fifth instar larva fat body stained immediately after dissection. Negative control is the heat-killed fifth instar larva fat body tissue. **B)** Fat body tissues of control (a) and toxin injected (b) larvae.

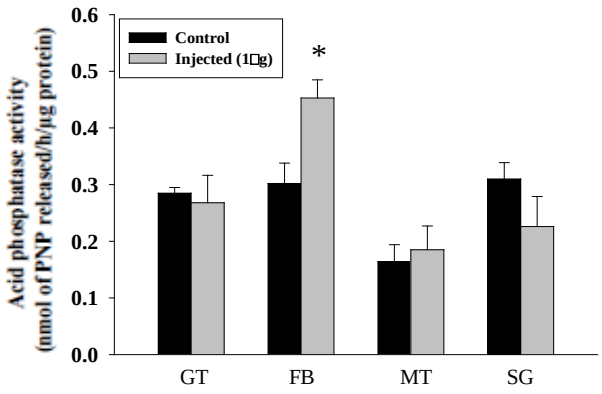

Fig. 11. **Analysis of acid phosphatase activity in the larval tissues upon Cry toxin injection**. Third instar larvae were injected with DOR5 Cry toxin dose of 1 µg/0.2g body weight of larvae. Tissues were collected 2 day post-injection and assay was performed. The enzyme activity is expressed as nmol of PNP released/hour/mg of proteins. Values are the mean ± standard deviation of three independent experiments (n=3). * $p < 0.050$ (ANOVA and SNK test); GT- gut, FB- fat body, MT- Malpighian tubule and SG- salivary gland.

3.5. Induction of lethal larval-pupal phenotypes and alteration in development

DOR5 Cry toxin injection at the concentration of 1 µg/0.2g body weight to third instar larvae resulted in 66% larval mortality (Fig. 3D), development of 20% lethal larval-pupal intermediates (Figs. 12C & 12E), 9% deformed but viable adults (Figs. 12D & 12F) and 5% phenotypically normal viable adults (Figs. 12A & 12G). Injection of different Cry toxins concentrations ranging from 0.1 to 10 µg/larva inhibited larval feeding and resulted in decreased larval growth in a dose-dependent manner. In our study using 1 µg as the injection dose, 20% of the larvae that developed into lethal larval-pupal intermediates exhibited an obvious “incomplete-ecdysis” phenotype, which usually could form only a portion of a pupal structure but failed to complete the ecdysis and died within 2-3 days (Figs. 12E; 3, 12E; 4, 12E; 5 & 12E; 6). The mortality noticed in larval-pupal intermediates developed from Cry toxin injected larvae was predominantly either in the larval-early pupal transformation (Figs. 12E; 1 & 12E; 2) or larval-mid pupal transformation stages (Figs. 12E; 3, 12E; 4, 12E; 5 & 12E; 6). No specific lethal phenotype appeared during the larval stages of the Cry toxin treated insects. Few defective adults emerged from the pupae of the treated insects, which had fairly developed but improperly folded and crumbled wings and as a result, the adults could not fly (Fig. 12F; 1). On the contrary, only 5% of the control larvae died due to injury during the larval stages and 95% of the control larvae developed and molted normally throughout the larval stages, metamorphosed into pupae and emerged as normal adults. We did not observe any phenotype of incomplete ecdysis, abnormal pupae and defective adults in the control group.

Scanning electron microscopic analysis of the wing scale morphology of the deformed adult revealed the presence of numerous piliform (hair-like) minute scales in addition to the lamellar (blade-like or flattened) form of wing scales. Most of the lamellar form of scales of the treated insect also showed irregular transverse and longitudinal ridges (Fig. 12F). On the other hand, the control insects showed the presence of only lamellar scales. The lamellar scales of the control insects showed a smooth inferior lamella and proper transverse and longitudinal ridges (Fig. 12G).

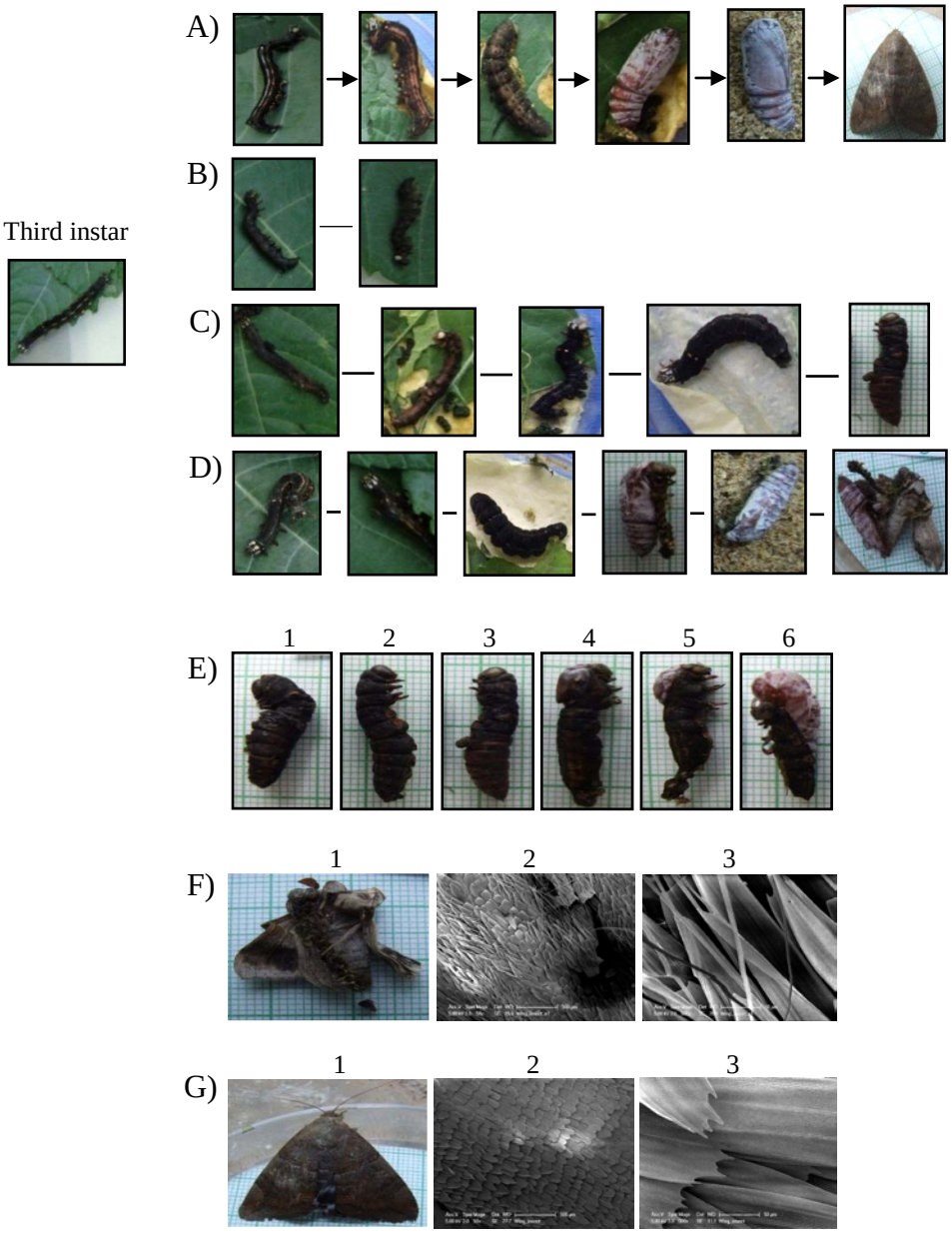

Fig. 12. **Effect of Cry toxin injection on larval-pupal and pupal-adult metamorphosis**. Third instar larvae were injected with DOR5 Cry toxin dose of 1 µg/0.2g body weight and their development was analyzed. **A)** Normal larval growth and metamorphosis. **B)** Larval death (mostly 2 day post-injection). **C)** Retarded larval growth and development of non-viable larval-pupal intermediates. **D)** Development of viable but defective adults. **E)** Different phenotypes of non-viable larval-pupal intermediates. **F)** Defective adult and SEM micrographs of its wing scale morphology. **G)** Normal adult and SEM micrographs of normal wing morphology.

4. Discussion

The major tissues and organs present in the insect larval hemocoel include the fat body, Malpighian tubule, salivary gland and testis which play important functions in insect development and reproduction. Hussein *et al*. (2006) demonstrated a nearly 74% reduction of the reproductive potential in the females of a moth *Spodoptera litoralis* feeding on the transgenic potato cultivar expressing beetle-specific Cry3Aa toxin. The insects were found to assimilate Cry3Aa present in the potato leaves and accumulate in the female pupae. The suppression of fertility by Cry toxins was also demonstrated in Colorado potato beetle, fed on transgenic potatoes expressing Cry3B endotoxin (Arpaia *et al*. 2000). The likely explanation for this mechanism was that the toxins penetrated into the hemolymph and altered the functions of the body organs involved in vitellogenin production. Cerstiaens *et al*. (2001) observed inhibition of food intake, growth arrest and death of *Lymantria dispar* (Lepidoptera) and *Neobellieria bullata* (Diptera) larvae upon hemocoelic injection of Cry1 toxins. However till date, no organs or cells other than the midgut epithelial cells have been established as targets for Cry toxins in insect pests. In the present study, we analyzed the morphological and physiological effects of hemocoelic Cry toxin delivery to a lepidopteran pest, *A. janata*. Hemocoelic injection of Cry1Aa, Cry1Ab, Cry1Ac and DOR5 Cry toxins individually to third instar larvae of *A. janata* induced larval mortality, reduced larval growth and gave rise to smaller pupae in a dose-dependent manner. Budatha *et al*. (2007) had previously demonstrated a relatively low percentage of larval mortality when injected to the fifth instar larvae of *A. janata*. However, our study in the same insect species demonstrated that third instar larvae were more susceptible to hemocoelic Cry toxin injection. Larvae younger than third instar were however not considered for the injection studies as they are too small and delicate to handle. We were able to observe a significantly high percentage of larval mortality to toxin dose as low as 0.1 µg/0.2 g body weight of the third instar larvae. Dose-dependent increase in larval mortality rate of the Cry toxin in injected larvae, as compared to the carrier solvent-injected control larvae clearly suggests that the mortality was the result of toxicity effect induced by Cry toxins and not due to injury. Since larval mortality was analyzed just 2 day post-injection, we are also convinced that the larvae did not die due to starvation, as larvae of this age can survive for upto 4-5 days without feeding. DOR5 isolate, whose gene profile showed to contain *cry1*Aa, *cry1*Ab, *cry1*C, *cry1*I, *cry2*A,

*cry2*B and vegetative insecticidal proteins (*vip*) genes obviously proved to be more potent than Cry1Aa, Cry1Ab and Cry1Ac toxins injected individually.

In holometabolous insect development, hexamerins are mainly synthesized by the fat body of the actively feeding larval stages, released into the hemolymph where they circulate. Later at the non-feeding stage, hexamerins are sequestered back into the fat body again and stored as protein granules, which serve as the main source of nitrogen and amino acids during pupal-adult metamorphosis and reproduction (Kanost *et al*. 1990; Bitondi *et al*. 2006). Contrary to the hemolymph hyperproteinemia reported in the Cry toxin ingested larvae of *Plodia maculipennis* (Narayan and Jayaraj, 1974) and *S. litura* (Tripathi and Singh, 2002), a significant hypoproteinemia was observed when Cry toxins were injected into the hemocoel of *A. janata*. Accumulation of storage proteins in large quantities in the hemolymph of last larval instar is essential for the fat body cells to sequester and maintain a reservoir for the subsequent development (Tojo and Yoshiga, 1994; Burmester, 2001). In the present study, a 6-fold decrease in the hemolymph total protein content of the 4 day post-injected larvae was observed. Further the decline in protein content was associated with a significant reduction in hexamerins, which are the main hemolymph storage proteins, and this could be responsible for the impaired development and metamorphosis with other associated factors.

The cytotoxic activity of Cry toxins against some vertebrate cells including human cancer cells have been reported (Mizuki *et al*. 1999, 2000; Lee *et al*. 2000; Ito *et al*. 2004). Cry toxin was reported to induce cell death of Jurkat cells by apoptosis-like cellular events (Amano *et al*. 2005). Induction of apoptosis in insects upon oral inoculation with baculovirus is also well reported (Feng *et al*. 2007). For the first time, we report the induction of cell death via apoptosis in the fat body tissue of *A. janata* larvae as a result of hemocoelic Cry toxin delivery. Histological analyses of the Cry toxin injected larvae revealed morphological and structural changes in gut, fat body, Malpighian tubule and salivary gland. Extensive degeneration and disintegration of fat body tissue was evident from the appearance of numerous fragmented nuclei and large cytoplasmic cavities. Almost negative MTT staining and detection of a number of TUNEL-positive signals in the damaged tissue further confirmed apoptotic cell death in fat body induced by hemocoelic Cry toxin delivery. During post-embryonic development, programmed cell death (PCD) of the fat body tissue follow two major pathways viz. apoptotic and autophagic cell death during pupal-adult metamorphosis (Sumithra *et al*. 2009). During

metamorphosis, acidic autophagic vacuoles are known to accumulate in the fat body cells and the activity of several lysosomal enzymes including acid phosphatase (ACP) increase and cause the lysis of larval tissues (Thummel, 2001; Lee and Baehriecke, 2001). The role of lysosomal enzymes in the histolysis of larval organs, cellular destruction, tissue remodeling, and reorganization are well known (Ashok and Dutta-Gupta, 1988, 1991). Further, the fat body which occupies the major portion of hemocoelic cavity shows high level of lysosomal enzymes when compared with other tissues (Hansen *et al*. 2002). Present study showed significantly elevated level of ACP activity primarily in fat body tissue and not in other tissues; indicating the involvement of lysosomes in Cry toxin-induced cell death in fat body. In holometabolous insects, degeneration as well as remodeling in the larval tissues through programmed cell death occur during the larval-pupal transformation which is triggered by 20-hydroxyecdysone (20E), an insect steroid hormone (von Gaudecker and Schmale, 1974; Ashok and Dutta-Gupta, 1988, 1991; Terashima *et al*. 2000; Mané-Padrós *et al*. 2008).

TUNEL-negative signals and the absence of significant changes in the ACP activity levels in gut, Malpighian tubule and salivary gland clearly ruled out the involvement of apoptotic and/or autophagic modes of cell death in these tissues upon Cry toxin injection. However, presence of cell debris in the gut lumen and the disorganization of the columnar epithelial cells and Goblet cells indicate loss of gut tissue structure and damage induced by Cry toxin injection. This would affect the food storage and digestive roles of the gut and hence disturb the overall supply of nutrients. The large pores and cavities seen in the epithelium of Malpighian tubule and significant reduction in the size of salivary gland of the Cry toxin injected larvae are evidences that these tissues are far from being normal. Malpighian tubules are primarily involved in excretion of nitrogenous wastes from the insect hemolymph and osmoregulation of various ions like sodium and potassium, while the function of salivary glands in actively feeding larvae is to produce secretions that are mixed with the food during feeding. In a lepidopteran insect like *A. janata*, salivary glands attain maximum size during the last larval instar and pre-pupal stage, and are involved in silk secretion during these stages, which is an important physiological event that allows puparia formation for successful larval-pupal transformation. The tremendous decrease in the gland size of the Cry toxin injected larvae also suggests that the abnormal development which is seen in the present study might also be related to insufficient silk secretion during larval-pupal transformation. Finally,

different larval tissues appeared to respond to Cry toxin injection differently. The fat body being the principle metabolic organ in the larval forms (Price, 1973; Haunerland and Shirk, 1995; Burmester and Scheller, 1999), any damage to this tissue as a result of Cry toxin injection would derail all the ongoing metabolic activities of the tissue and significantly affect normal development and metamorphosis.

Besides inducing mortality, relatively high percentage of the surviving larvae developed into non-viable larval-pupal intermediates exhibiting "incomplete ecdysis" phenotype. Scanning electron microscopic analysis of the wing scale morphology of the defective adults further revealed numerous piliform (hair-like) scales and under-developed lamellar scales, as compared to the presence of only well-developed lamellar (blade-like) scales in the control adults, clearly supported abnormal pupal-adult metamorphosis. The pathological symptoms seen in the larval tissues including the fat body, induced by Cry toxin injection might have caused the failure in the larval-pupal transformation and pupal-adult metamorphosis. The mode of action of Cry toxins in the larval hemocoel is not known, but believed to be different from the one that occurs after oral ingestion. However, the identification of APN in fat body (Budatha *et al*. 2007), Malpighian tubule and salivary gland (data not published) of *A. janata*, which is an authenticated Cry toxin receptor in midgut of the larval forms of many lepidopteran insects, suggest this putative molecule as a potential target site for Cry toxin binding in these tissues. Cry toxin binding and pore forming ability on *in vitro* cultured fat body cells strongly suggest the possibility of binding to these membrane molecules (APNs) and hence affecting the tissue function (Cheon *et al*. 1997).

In conclusion, the effects of hemocoelic Cry toxin delivery which were demonstrated to be dependent on the type and dose of the Cry toxins suggest a specific but unknown mode of action that possibly target the tissues and cells present in the insect hemocoel of *A. janata*. Based on the results of this study, we can infer that the larval mortality and the inability of the surviving insects to complete the larval-pupal and pupal-adult metamorphosis are the results of morphological changes followed by tissue degeneration of the vital larval organs/tissues/cells induced by the toxicity of Cry toxins in the larval hemocoel. This putative mode of Cry toxin delivery could be an effective approach to control many economically important agricultural pests like *A. janata*. However, understanding this mechanism of action would require more fundamental research.

Part 2

Identification and characterization of Cry toxin targets in *A. janata*

1. Introduction

Insect midgut has always been the primary target site for *Bt*-based biopesticides and *Bt* transgenic crops. Crystal inclusions produced by this gram-positive bacterium are toxic to a wide range of insects including those belonging to the order Lepidoptera (Crickmore *et al*. 1998). Upon ingestion by the larval forms of the susceptible insects, the insecticidal crystal protein (ICP)-containing inclusions are proteolytically activated in the alkaline environment of the gut. These activated toxins then bind to the specific receptors located on the brush border membrane of the midgut epithelial cells, induce pore formation and ultimately cause death (Ferre and Van Rie, 2002; Pigott and Ellar, 2007). The toxin-receptor interaction in the gut is critical in determining toxicity to target insects (Hofmann *et al*. 1988; Van Rie *et al*. 1990; Lee *et al*. 1992; Zhang *et al*. 2009). In lepidopteran midgut, receptors that mediate Cry toxin toxicity include GPI-anchored APNs (Knight *et al*. 1994; Valaitis *et al*. 1995; Luo *et al*. 1997; Yaoi *et al*. 1997; Rajagopal *et al*. 2002; Banks *et al*. 2003), cadherins (Nagamatsu *et al*. 1999; Fabrick and Tabashnik, 2007), GPI-anchored ALPs (Jurat-Feuntes and Adang, 2004) and glycoconjugates (Valaitis *et al*. 2001).

APNs (EC 3.4.11.2) by far are the most widely explored and well characterized Cry toxin receptors. They are a class of peptidases belonging to a Zn^{++} dependent gluzincin family of metalloproteases M1 type (Hooper, 1994; Albiston *et al*. 2004) that cleave single amino acid residue from the N-terminus of oligopeptides, preferentially the neutral amino acids. Thus, larval midgut APNs play a dual role in dietary protein digestion (Terra and Ferreira, 1994) and in Cry toxin induced toxicity (Bravo *et al*. 2007). APN has been isolated and cloned from the midgut of a number of lepidopteran larvae including *Manduca sexta* (Knight *et al*. 1994), *Heliothis virescens* (Gill *et al*. 1995), *Lymantria dispar* (Garner *et al*. 1999), *Bombyx mori* (Yaoi *et al*. 1999), *Plutella xylostella* (Chang *et al*. 1999), *Plodia interpunctella* (Zhu *et al*. 2000), *Spodoptera exigua* (Herrero *et al*. 2005), *Trichoplusia ni* (Wang *et al*. 2005), *A. janata* (Budatha *et al*. 2007a), *Epiphyas postvittana* (Simpson *et al*. 2008), *Chilo suppressalis* (Yu *et al*. 2010), *Ostrinia nubilalis* (Crava *et al*. 2010) and *Helicoverpa armigera* (Angelucci *et al.* 2008, Lomate and Hivrale, 2010). Besides midgut, APN expression has also been detected in fat body (Budatha *et al*. 2007a, 2007b; Simpson *et al.* 2008) and Malpighian tubule (Wang *et al*. 2005; Simpson *et al*. 2008; Crava *et al*. 2010) of lepidopteran insects but complete cDNA sequence has only been cloned from the fat body of *A. janata* (Budatha *et al*. 2007a) and *S. litura* (Budatha *et al*. 2007b).

Sequences are commonly identified as APNs due to the presence of aminopeptidase motif "GAMENWG", Zn^{++} binding motif "$HEXXHX_{18}E$", N-terminal signal peptide, several glycosylation sites and C-terminal GPI-anchor signal. Currently, over 100 isoforms of APN are reported from the midgut of various species of Lepidoptera. Reported gut APNs of lepidopteran insects have been classified either into five classes (Piggot and Ellar, 2007) or into seven classes (Angelucci *et al*. 2008). Different isoforms have distinct role in protein digestion and have been shown to interact with different types of Cry toxins (Piggot and Ellar, 2007). Feeding on transgenic potato cultivar expressing beetle-specific Cry3Aa toxin did not result to mortality but caused significant reduction in fertility and fecundity of *S. litoralis*, prompting the authors to suggest the possibility of toxins crossing the gut membrane to hemolymph where they could interact with various tissues and interfere with their normal functioning (Hussein *et al*. 2006). Cerstiaens *et al*. (2001) demonstrated the toxic effect of Cry1C hemocoelic injection on *L. dispar* (Lepidoptera) and *Neobellieria bullata* (Diptera) larvae. Peyronnet *et al*. (1997) showed that neither Cry1Aa nor Cry1C had any depolarizing effect when applied on the basolateral side of the midgut membrane of *L. dispar*. Transgenic *Drosophila melanogaster* expressing *M. sexta* APN and Sf21 insect cells expressing *H. armigera* APN exhibit sensitivity to lepidopteran-specific Cry1Ac which otherwise were tolerant to the toxin (Gill and Ellar, 2002; Sivakumar *et al*. 2007). Immunolocalization of Cry toxin binding, the subsequent tissue disintegration as well as pore forming ability exhibited by Cry toxins on *in vitro* cultured fat body cells suggest the toxic effects on the cells (Cheon *et al.* 1997). All these studies are indicative of the possibilities of Cry toxin toxicity being induced by interaction with some binding proteins present on the cell membranes of putative target organs that are possibly accessible upon toxin injection.

Where the experimental determination of protein three-dimensional (3D) structure is not possible due to various problems, comparative or homology modeling is the most reliable approach for determining the protein 3D structure. Molecular models of midgut-specific APNs for *M. sexta* (Singh and Sivaprasad, 2009) and *S. litura* (Pazos and Salamanca, 2008) were generated by comparative modeling strategy. Till date, crystal structure of insect APN has not been determined. Since the role of APN expression in insect tissues other than the midgut has not been properly elucidated, construction of a molecular model of AjAPN1, which is expressed in fat body, Malpighian tubule and salivary gland, could provide information of their functional properties.

In the present investigation, our aim was to find out whether the toxicity effects induced by hemocoelic delivery of Cry toxins to the larval forms of *A. janata* was possibly due to interaction with putative proteins expressed in the larval visceral tissues. Interestingly, *in vitro* ligand binding analysis and co-immunoprecipitation experiments revealed specific interaction of different Cry toxins to ~110 kDa protein in fat body, Malpighian tubule and salivary gland protein preparations. Full-length cDNA clones from Malpighian tubule and salivary gland exhibited all the signature motifs of an APN including the aminopeptidase motif "GAMENWG", Zn^{++} binding motif "$HEXXHX_{18}E$", N-terminus signal peptide, several glycosylation sites and C-terminal glycosylphosphatidylinositol anchor signal. APN isoform specifically expressed in fat body, Malpighian tubule and salivary gland belonged to Class 1 and midgut-specific APN isoform belonged to Class 4 of APN classification. The expression of APN in these tissues was demonstrated by immunofluorescence, immunoblot and APN enzyme activity analyses. Analysis of fat body, Malpighian tubule and salivary gland specific APN molecular models strongly suggest its potential role in Cry1A toxin interaction and toxicity.

2. Materials and methods

2.1. Insect rearing

Egg masses of the lepidopteran moth, *A. janata* were collected from the castor fields of Directorate of Oilseeds Research, Hyderabad. Immediately after hatching, neonates were transferred to a growth chamber and reared on fresh castor leaves (*Ricinus communis*) as diet under a photoperiod of 14:10 h (light:dark), 60-70% relative humidity at 27±2ºC till pupation. The pupae were transferred onto moist sand in a container and allowed to develop into adults. The adults were then transferred to an aerated rearing chamber and fed with 10% honey solution supplemented with vitamin E. The female adults deposit their eggs onto the surface of castor leaves in the rearing chamber which then hatched into neonate larvae. Under this rearing condition, majority of the 10 days old larvae are fifth instar and for this part of the study, we used fifth instar larvae.

2.2. Tissue isolation

The larvae were first narcotized by placing them on ice for 15-20 min. The larval cuticle were cut open from the ventral side of abdomen and cut-through the length of the larvae. Midgut, fat body, Malpighian tubule and salivary gland were dissected out in ice-

cold insect Ringer solution. Midgut was cleared of food contents and peritrophic membranes. The tissues were used for total RNA isolation, histological studies and preparation of protein samples for *in vitro* ligand binding studies, western blot and APN enzyme activity analyses.

2.3. Preparation of midgut brush border membrane vesicles (BBMVs)

BBMVs were prepared as described by Wolfersberger *et al*. (1987). Dissected gut tissues were transferred to a centrifuged tube containing ice-cold MET buffer (300mM mannitol, 17mM Tris-HCl pH 7.5, 5mM EGTA and 1mM PMSF), vigorously vortexed and briefly centrifuged for 5 min at 1000 X g to obtain clean midguts. Gut tissues were homogenized on ice in a tightly fitting glass homogenizer in ice-cold MET buffer (10% w/v). The homogenate was diluted with an equal volume of ice-cold 24mM $MgCl_2$, blended and held on ice for 15 min before centrifugation at 2500 X g for 15 min at 4ºC. Supernatant was centrifuged at 30,000 X g for 30 min at 4ºC. Pellet was re-suspended in MET buffer and centrifuged at 2500 X g at 4ºC for 15 min. The supernatant was further centrifuged at 30,000 X g for 30 min at 4ºC. The resulting pellet, which corresponds to the BBMV preparation was re-suspended in HBS-N buffer (10mM HEPES, pH 7.4, 150mM NaCl), flash- frozen in liquid nitrogen and stored at -80ºC until use.

2.4. Preparation of fat body membrane fraction

The fat body tissue was homogenized on ice in buffer A (5mM HEPES, pH 8.5 and 0.1mM $CaCl_2$). The fat body membrane fraction was prepared according to the method described by Kirankumar *et al.* (1997). The fat body homogenate was centrifuged at 30,000 X g for 30 min at 4°C and the pellet thus obtained was washed once with buffer A followed by suspension in a small volume of buffer B (5mM HEPES, pH 7.0 and 0.1mM $CaCl_2$). This particular fraction was used as membrane preparation and stored at -80°C until use.

2.5. Preparation of Malpighian tubule and salivary gland protein homogenates

The tissues (100 mg) were homogenized in 200 µl of homogenization buffer (10mM Tris-HCl, pH 7.4, 0.1% Triton X-100, 1mM PMSF, 1mM EDTA and 1mM DTT). The homogenates were centrifuged at 1000 X g for 5 min to remove larger debris and the aliquots of the supernatant were used.

2.6. Purification of activated Cry toxins

The methodology involved in the preparation and purification of activated Cry1Aa, Cry1Ab, Cry1Ac and DOR5 Cry toxins have already been described in "Materials and methods" section of part 1.

2.7. Biotinylation of Cry toxins

Trypsin activated Cry1Aa, Cry1Ab, Cry1Ac and DOR5 Cry toxins, each 500 µg were biotinylated using the biotinylation kit (Bangalore genei, India) and purified using Sephadex G25 columns following manufacturers' protocol and instructions. The biotinylated Cry toxins were detected with ALP-conjugated streptavidin and visualized by developing with NBT-BCIP substrate (Sigma Aldrich, USA).

2.8. *In vitro* Cry toxin binding analysis of larval tissue protein.

The fat body membrane, Malpighian tubule and salivary gland protein preparations (30 µg each) were separated by 7.5% SDS-PAGE and electro-transferred to nitrocellulose membranes (Pall-Life Sciences, USA). The membranes were blocked in a blocking buffer [3% (w/v) BSA in 0.01M Tris-buffered saline (TBS, pH 7.4)] for 1 h, followed by incubation in a blocking buffer containing individual biotinylated Cry1Aa, Cry1Ab, Cry1Ac and DOR5 Cry toxins (200 ng/mL) for 1 h. Following this, the blots were washed with TBS (pH 7.4) supplemented with 0.1% Tween-20 (TBST), and then incubated for 2 h in a blocking buffer containing streptavidin-ALP conjugate (1:1000 dilutions). Cry toxin-bound proteins were detected using the ALP substrate, NBT-BCIP (Sigma Aldrich, USA). The membrane blots incubated with the same concentration of the corresponding unlabeled Cry toxins were used as controls.

2.9. Immunoprecipitation of Cry toxin binding proteins

Triton X-100-solubilized Malpighian tubule and salivary gland protein preparations (200 µg each) were incubated with Cry1Ab toxins (5 µg) in binding buffer (50mM sodium phosphate, pH 7.5, 50mM NaCl and 3mM $MgCl_2$) for 24 h at 4ºC. This was followed by incubation with 5 µl of Cry1Ab antibody (2.5 µg) for another 3 h. Subsequently, 50 µl of Protein A agarose beads was added to the mixture and incubated for another 2 h at 4ºC on a rotary shaker. The agarose beads were pelleted, washed six times with binding buffer, re-suspended in equal volume of 2X of SDS sample buffer containing 2-mercaptoethanol [125mM Tris-HCl, pH 6.8; 4% (w/v) SDS; 20% (v/v) glycerol; 10% (v/v) 2-mercaptoethanol and 0.002% Bromophenol Blue] and heated at 100ºC for 5 min. The pulled-down interacting proteins were separated by 7.5% SDS-

PAGE and electro-blotted onto nitrocellulose membranes (Pall-Life Sciences, USA). The membranes were then incubated with *A. janata* fat body-specific APN polyclonal antibody (1:10000 dilutions) (Budatha *et al*. 2007a) which was followed by incubation with ALP-conjugated goat anti-rabbit IgG and finally visualized using ALP-substrate, NBT-BCIP (Sigma Aldrich, USA).

2.10. Isolation of total RNA from larval tissues and synthesis of cDNAs

Total RNAs from midgut, fat body, Malpighian tubule and salivary gland were isolated using TRI reagent ™ (Sigma Aldrich, USA) following the manufacturer's instructions. The RNA quantity was determined by Nanodrop 1000 (Thermo Scientific, USA). Quality and integrity of RNA were assessed by denaturing electrophoresis on a 1% agarose gel. Total RNA was reverse transcribed to corresponding cDNAs using SuperScript III first strand synthesis kit (Invitrogen). The cDNAs was either stored at -20°C or used immediately for PCR reactions.

2.11. Isolation of full-length APN cDNA clones from Malpighian tubule and salivary gland of *A. janata* by rapid amplification of cDNA ends (RACE) strategy

Degenerate primer pair of F1-5′YTTCYRCATACYTGSTMGCTTTYMW3′ and R1-5′GYWWSGTCARCMSARTSWGTYMMRAAGTA3′ as forward and reverse primer respectively, was designed from the conserved regions of reported insect APN genes including the *A. janata* midgut-specific and fat body-specific APNs. The PCR products obtained from Malpighian tubule and salivary gland were cloned into PTZ57R-T vector (MBI, Fermentas) and sequenced. Based on the nucleotide sequence information of the cloned fragments, gene specific primers were designed to obtain the remaining 5′ and 3′ regions of the sequences using Gene Racer ™ kit (Invitrogen) and following the manufacturers' instructions. The gene specific reverse primers designed for 5′RACE of Malpighian tubule and salivary gland APNs were R2-5'CAG GAA TGG CTG CTT GCT GCA TG3' and R2 nested-5'GCC ACT CGC TCG TAG TGA GAG ACG A3'. For the 3′RACE of Malpighian tubule APN, the gene specific forward primers used were F2-5'GGA GCT ATG GAG AAC TGG GGT CTG T3' and F2 nested-5'GCT TGG TGG GAT AAC CTC TGG CTA A3'. For the 3′RACE of salivary glands APN, the gene specific forward primers used were F2-5'GGA GCT ATG GAG AAC TGG GGT CTG T3'; and F2 nested-5'GCT TGG TGG GAT AAC CTC TGG CTA A3'; F3-5′CCG TGC TCA GAT TGT CGA CGA CG3′ and F3 nested-5′GCACCCTGGGATGCCGCTATC3′. The PCR amplified RACE fragments were cloned in PTZ57R-T vector and sequenced.

The cDNA sequences of all the cloned fragments from Malpighian tubule and salivary gland were then aligned properly to obtain the respective full-length APN cDNA sequences. APN cDNA clones of *A. janata* Malpighian tubule and salivary gland were designated as "AjMtAPN" and "AjSgAPN" respectively.

2.12 Analysis of Malpighian tubule (AjMtAPN) and salivary gland (AjSgAPN) cDNA sequences

Primers were designed using Lasergene 7 and Beacon Designer 7 programs. The amino acid sequences encoded by AjMtAPN and AjSgAPN were deduced from the corresponding cDNA sequences using the translation tool at the ExPASy Proteomics website http://expasy.org/translate/. The nucleotide and deduced amino acid sequences of AjMtAPN and AjSgAPN were verified using the NCBI-BLAST search. The deduced amino acid sequences were aligned with already reported fat body-specific APN (ABE02186) and midgut-specific APN (ABH07377) of *A. janata*. The *A. janata* APN sequences were also aligned with other reported lepidopteran APNs using ClustalW2 program (http://www.ebi.ac.uk/tools/msa/clustalw2/). The result of the computational analysis was then visualized as a colored classification using Jalview software. The phylogenetic tree was constructed with the aligned sequences using PhyML using bootstrapping procedure (500 replicates). The presence and location of signal peptide cleavage sites in the amino acid sequences were determined using SignalP 4.0 Server (http://www.cbs.dtu.dk/services/SignalP/). The presence of glycosylphosphatidylinositol (GPI) anchor in the sequences was predicted using PredGPI software (http://gpcr.biocomp.unibo.it/predgpi/pred.htm). The presence of potential N-, C- and O-linked glycosylation sites in the sequences was analyzed using NetOGlyc2.0 program (http://www.cbs.dtu.dk/services/netOGlyc). The computation of the theoretical pI (isoelectric point) and MW (molecular weight) was carried out with Compute pI/Mw program (http://www.expasy.org/compute_pi/).

2.13. Semi-quantitative and real-time PCR analyses

For semi-quantitative PCR analysis, we used 5′CTTACTACTGCTACTGACTC3′ and 5′GTTAAGAATGGTAGATGTTGAA3′ as forward and reverse primer respectively, designed to specifically amplify a 441 bp fragment of *AjAPN*4. A primer pair of 5′TGGCTGGATATGGTATTACT3′ and 5′GATATTGAATGCTCTGGTGTA3′ as forward and reverse primer respectively was used to amplify a 476 bp fragment of *AjAPN*1. A primer pair of 5′GGTAGTAGACAATGGCTCGGG3′ and

5′CCCAGTTAGTGACGATTCCGTG3′ as forward and reverse primer was used to amplify a 180 bp fragment of lepidopteran insect β- actin as an internal control.

Real-time quantitative PCR was performed in a 20 µl reaction volume using a custom-made TaqMan gene expression assay (Applied Biosystems). The forward primer 5′TGCTCAGTCTAGTCTGTA3′, reverse primer 5′GCCCTGTTCAAATAGTGA3′ and TCCTCTCACGATTGCTGCTCTT as probe were used for *AjAPN*4 expression analysis. Similarly, 5′AGGAATACACAGGCTATCCGTACT3′, 5′GGCTGCTTGCTGCATGAT3′ and CAATGACCGAGAACATC were used as forward, reverse and probe respectively for the expression analysis of *AjAPN*1. Insect 18S RNA was used as an internal reference to normalize the APN transcript expression levels. The real-time expression analysis was performed in triplicates for each sample. Relative expression was then calculated according to the equation $2^{-\Delta Ct}$.

2.14. Preparation of paraffin-embedded tissue sections

The midgut, fat body, Malpighian tubule and salivary gland of fifth instar larvae were fixed in 4% paraformaldehyde (PFA) in phosphate-buffered saline (PBS, pH 7.4) at 4°C for 24 h. The fixed tissues were rinsed in PBS for 10 min to remove the PFA and dehydrated through a graded ethanol series, cleared in xylene for 5 min for proper embedding. The samples were then transferred to 100% paraffin solution and infiltrated at 60°C with three changes at 1 h intervals. The tissues were finally embedded in paraffin blocks, cooled and sectioned with 5 µm thicknesses using a rotary microtome (Leica, Germany).

2.15. Histological and immunolocalization studies

The sections were de-parafinized in xylene, re-hydrated in ethanol series, followed by staining in hematoxylin (nuclear stain) and eosin (cytoplasmic stain). The sections were de-hydrated in ethanol series and mounted on a slide using DPX mountant. For immuno-localization studies, the paraffin sections were de-parafinized with xylene and hydrated in the ethanol series which was followed by washing with double distilled water (DDW) and 0.1M PBS (pH 7.4) with 0.1% Tween-20 (PBST). The sections were processed through 10mM citrate buffer in a micro-oven for 11 min and then permeabilized by treatment with 0.1% Triton X-100 in PBS for 15 min, and washed with DDW and PBST. Endogenous peroxidases were inhibited by treatment with 3% H_2O_2 in methanol for 45 min. After washing with DDW and PBST, the sections were blocked with 10% goat serum for 45 min. Excessive blocking buffer was gently wiped off and the

sections were incubated either with *A. janata* midgut-specific APN polyclonal antibody (1:1000 dilutions) or fat body-specific APN polyclonal antibody (1:1000 dilutions) in 2% rabbit serum at 4°C overnight. Finally the sections were brought to room temperature; unbound antibodies were washed off with PBST, and subsequently incubated with Alexa Flour 594-labeled goat anti-rabbit IgG (1:1000 dilutions) in PBST at room temperature for 1 h. The nuclear staining was carried out using blue with DAPI (ClonTech, USA). After washing with PBST, the sections were mounted using 90% glycerol and observed under scanning laser confocal microscope (Leica, Germany).

2.16. Western blot analysis

The midgut BBMVs, fat body membrane, Malpighian tubule and salivary gland polypeptides were electrophoretically separated by 7.5% SDS-PAGE and electro-blotted onto nitrocellulose membrane (Pall-Life Sciences, USA) using trans-blot apparatus (Bio-Rad) according to the procedure of Towbin *et al*. (1979). For this, the gel was first equilibrated in Towbin buffer (25mM Tris, 192mM glycine and 20% methanol) for 30 min and then transferred to the membrane at 70 V with 250 mA current limit for 3 h. The transfer of protein to membrane was checked by reversible Ponceau S staining (100 mg Ponceau S in 100 ml of 5% acetic acid). The stain was removed by 3-4 washes with TBST [10mM Tris-HCl, pH 7.4 containing 150mM NaCl and 0.1% Tween-20 (v/v)]. For immunostaining, the protein blot was processed with 5% skim milk powder (w/v) in TBST for 1 h at room temperature to block the non-specific binding sites followed by washing with TBST. The blot was then incubated with *A. janata* fat body-specific APN polyclonal antibody (1:10000 dilutions) in TBST containing 5% milk powder (w/v) for overnight. This was again followed by thorough washing in TBST. The antibodies bound to proteins were detected using ALP-conjugated goat anti-rabbit IgG for 1 h at room temperature. Once again the blot was washed in TBST. The visualization of the specific cross-reactivity was carried out with NBT-BCIP (Sigma Aldrich, USA).

2.17. APN enzyme activity assay

APN enzyme activity in various tissue samples was examined as described by Garczynski and Adang (1995). Assay was carried out with 20 µg each of midgut BBMVs, fat body membrane, Malpighian tubule and salivary gland protein preparations at 25°C in assay buffer (250mM Tris-HCl, pH 7.8; 250mM NaCl) using 1mM *L*-leucine-*p*-nitroanilide (Sigma Aldrich, USA) as substrate. Absorbance was measured at 405 nm and the molar absorbance co-efficient of *p*-nitroanilide was taken as $9.9x10^{-3}$ mol/L (Malik

and Riazuddin, 2001). The specific activity was expressed as µmol of *p*-nitroanilide released/min/mg of proteins.

2.18. Construction of 3D molecular models of AjAPN4 and AjAPN1

A computational homology modeling approach was employed to develop the 3D structures of AjAPN4 and AjAPN1. The crystal structures of the tricorn interacting factor F3 from *Thermoplasma acidophilum* (PDB code: 1Z1W) (Kyrieleis *et al*. 2005) and human endoplasmic reticulum aminopeptidase-1 (PDB code: 3QNF) (Kochan *et al*. 2011) were selected as template structures for the construction of the models. The BLAST program (Altschul *et al*. 1990) against Protein Data Bank (PDB) (Berman *et al*. 2000) available at National Centre for Biotechnology Information (NCBI) was selected as template structures for both the query proteins. We used AjMtAPN as the representative sequence for AjAPN1 structure as AjFbAPN (ABE02186), AjMtAPN and AjSgAPN share 99% sequence identity. The *A. janata* midgut-specific APN (AjAPN4) sequence was obtained from NCBI (http://www.ncbi.nih.gov; accession number: ABH07377). Using multiple templates rather than a single template is advantageous if the sequence homology is low (<30%) and when different templates have similar sequence identities to the target. Even if the overall sequence identities of different templates with respect to the target sequence may be similar, the different templates could have varying degrees of sequence similarity in different regions of the sequence alignment which would help in development of a more reliable model (Nayeem *et al*. 2006). Sequence alignment of the templates with the target was done to identify structurally conserved regions (SCRs) common to templates and target. To construct a protein model for the target sequence, we used MODELLER program (Eswar *et al*. 2007) interfaced by EasyModeller (Kuntal *et al*. 2010). Using this program, twenty models were generated and analyzed. The model showing the best DOPE score was saved for further refinement and validation. Layers of water with thickness 10 Å were added to the whole protein using the VMD software (Humphrey *et al*. 1996). A layer of water allows hydrophilic residues to interact with water instead of interacting with each other as they would do if modeled in vacuum. The protein model was energy minimized using CHARMM forcefield of NAMD (Phillips *et al*. 2005). The minimization was carried out using 1000 steps of steepest descent followed by 10000 steps of conjugate gradient to relieve all the bad contacts of the system. The quality of the refined structure obtained was checked with ERRAT program (Colovos *et al*. 1993). The ERRAT program was used to assess the false statistics of bad non-bonded

interactions within the structure of the model. To verify the protein model, the coordinates of the protein model were submitted to PROCHECK (Laskowski *et al*. 1993). The stereochemical quality of the protein structures was examined by Ramachandran plot using the PROCHECK program. The number of residues that are in the allowed or disallowed regions of Ramachandran plot determines the quality of the model. The root mean square deviation of the model with respect to Cα atoms of the template was measured using the Combinatorial Extension (CE) method. The *B. mori* APN (AAC33301) 3D model was constructed using the crystal structure of the soluble domain of human endoplasmic reticulum aminopeptidase-1 (Erap1) (PDB code: 2YD0) as the template and following the same procedure. The structure of Cry1Aa toxin binding region of *B. mori* APN, AjAPN4 and AjAPN1 was analyzed and compared between them.

3. Results

3.1. *In vitro* Cry toxin binding analysis

The interaction of Cry toxins with fat body membrane, Malpighian tubule and salivary gland protein preparations was investigated by ligand blot analysis. The binding assay was performed by blotting 30 µg proteins of fat body membrane fraction, Malpighian tubule and salivary gland protein preparations after separation by 7.5% SD-PAGE. The blots were overlayed with biotinylated Cry toxins and their interactions with the proteins of various tissues were probed with streptavidin-ALP conjugate and detected with the ALP substrate, NBT-BCIP. The results obtained (Fig. 1) clearly show different patterns of interaction with different types of Cry toxins in fat body, Malpighian tubule and salivary gland. However, all the four different Cry toxins i.e., Cry1Aa, Cry1Ab, Cry1Ac and DOR5 toxins strongly bind to ~110 kDa protein in fat body (Fig. 1A), Malpighian tubule (Fig. 1B) and salivary gland (Fig. 1C). Further, the interaction of these toxins to ~110 kDa protein of salivary gland appeared to be comparatively less (Fig. 1C). Cry1Ac toxin showed fairly low interaction with ~110 kDa protein in all the tissues (Figs. 1A, 1B & 1C; Lanes: 5). Control blots which were incubated with unlabeled corresponding Cry toxins (Figs. 1A, 1B & 1C; Lanes: 2) did not show any binding. Further, the interaction was found to be highest with DOR5 toxins (Figs. 1A, 1B & 1C; Lanes: 6) where more than one protein (~110 kDa) cross-reacted with biotinylated Cry toxins. We further notice interaction of few low molecular weight proteins with various Cry toxins in all tissues. However in the present study, our focus was primarily on the ~

110 kDa protein, as the midgut APNs of lepidopteran insects have their molecular weight ranging between 110-120 kDa.

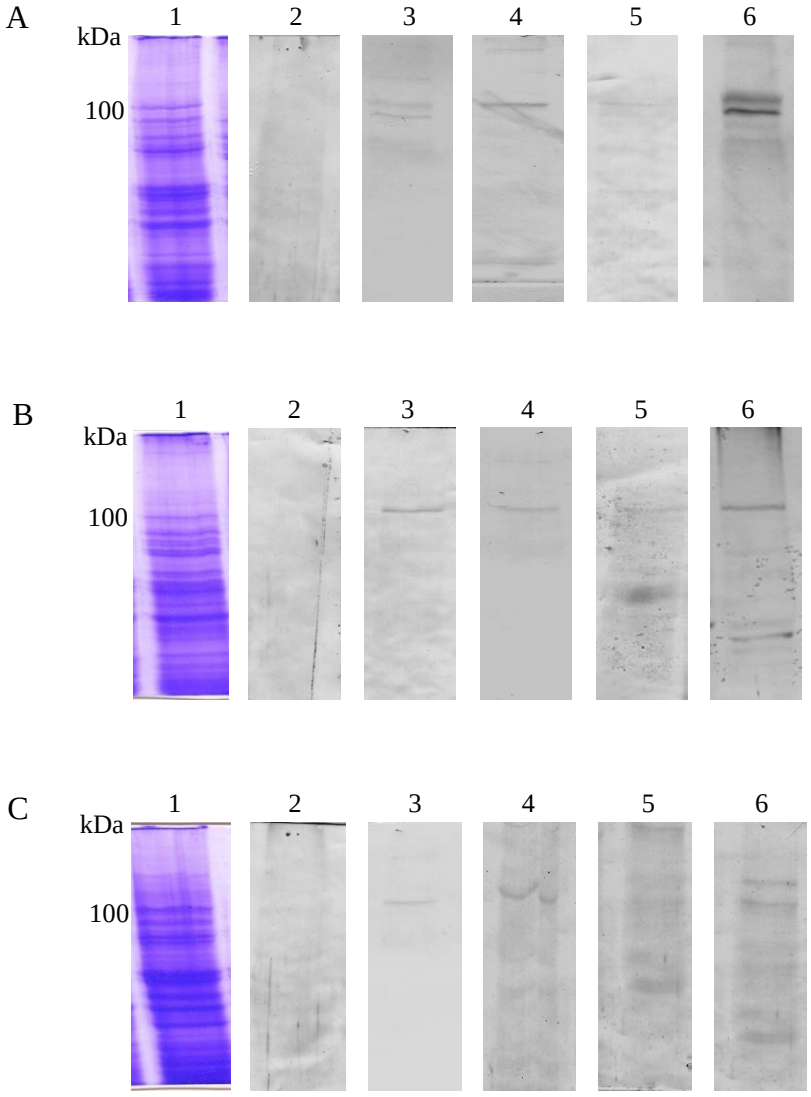

Fig. 1. ***In vitro*** **ligand binding analysis**. **A) Fat body**. **B) Malpighian tubule**. **C) Salivary gland**. 30 µg of fat body membrane protein, Malpighian tubule and salivary gland protein preparations per lane were separated by 7.5% SD-PAGE and transferred onto nitrocellulose membranes. The blots were individually incubated with biotinylated Cry1Aa, Cry1Ab, Cry1Ac and DOR5 Cry toxins (200ng/ml), followed by incubation with streptavidin-ALP conjugate and finally detected with ALP-substrate, NBT-BCIP. The blots which were incubated with the corresponding unlabeled Cry toxins act as controls. Lanes 1: Coomassie brilliant blue stained polyacrylamide gel, Lanes 2: Controls, where the protein blots were incubated with unlabeled corresponding Cry toxins; Lanes 3, 4, 5 & 6: protein blots individually incubated with biotinylated Cry1Aa, Cry1Ab, Cry1Ac and DOR5 Cry toxins respectively.

3.2. Immunoprecipitation of Cry toxin interacting proteins

The specificity of interaction between the ~110 kDa protein and the Cry toxins were further analyzed and confirmed by co-immunoprecipitation. Triton X-100 solubilized Malpighian tubule and salivary gland protein preparations were incubated with 5 µg of purified activated Cry1Ab and the toxin-protein complex was subsequently precipitated with Cry1Ab antibody using Protein A-agarose beads. Analysis of the immunoprecipitated Cry toxin-protein complex by western blot using *A. janata* fat body-specific APN antibody (Budatha *et al*. 2007a) detected the ~110 kDa interacting protein in both Malpighian tubule (Fig. 2A; Lane: + Cry1Ab) and salivary gland (Fig. 2B; Lane: + Cry1Ab). This result further supports that in both the tissues, the ~110 kDa interacting protein is most likely an APN. The control experiments which were performed by incubating the tissue protein samples in the absence of Cry1Ab showed the absence of any interacting proteins in the blots of either Malpighian tubule (Fig. 2A; Lane: -Cry1Ab) or salivary gland (Fig. 2B; Lane: -Cry1Ab).

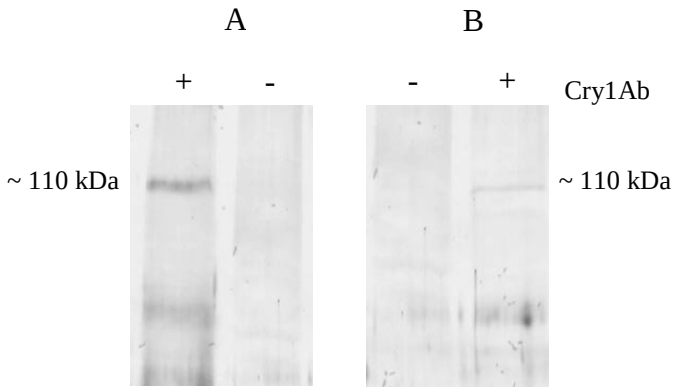

Fig. 2. **Immunoprecipitation of Cry1Ab toxin interacting proteins**. Triton X-100 solubilized Malpighian tubule and salivary gland protein preparations (200 µg each) from *A. janata* fifth instar larvae were separately incubated with purified activated Cry1Ab toxin (5 µg) followed by Cry1Ab antibody (2.5 µg). The ligand-interacting protein complex was pulled-down with Protein A-agarose beads, resolved by 7.5% SDS-PAGE, transferred onto a nitrocellulose membrane, incubated with *A. janata* fat body-specific APN antibody and ALP-conjugated secondary antibody and finally detected with ALP substrate, NBT-BCIP. **A)** Malpighian tubule protein preparation incubation without Cry1Ab (-) and with Cry1Ab (+). **B)** Salivary gland protein preparation incubation without Cry1Ab (-) and with Cry1Ab (+). Note the presence of ~110 kDa interacting protein in both the tissues.

3.3. Identification of APN expression in different tissues of *A. janata*

Semi-quantitative PCR analysis revealed APN transcript expression in midgut, fat body, Malpighian tubule and salivary gland (Fig. 3). The APN transcript expression was found to be most abundant in gut. Among the visceral tissues, Malpighian tubule showed maximum expression. The transcript expression could not be detected in testis, ovary and body carcass. The 451bp fragment was amplified using a degenerate primer pair designed based on the consensus sequence region of reported lepidopteran APNs containing the highly conserved aminopeptidase motif "GAMENWG" and Zn^{++} binding motif "$HEXXHX_{18}E$". Gut, fat body, Malpighian tubule, salivary gland, testis and carcass were isolated from last instar larvae while ovary was from freshly emerged adults.

3.4. Cloning and characterization of APN cDNAs from larval Malpighian tubule and salivary gland of *A. janata*

Using degenerate primer pair of F1 and R1 as forward and reverse primers, partial cDNA fragment of 451 bp from Malpighian tubule as well as salivary gland were cloned and sequenced. Upon sequencing, both the fragments from Malpighian tubule and salivary gland were found to have 99% nucleotide sequence identity. As the identity was very high, the experiments were repeated several times but gave similar confirmatory results. The 5′-RACE and 3′-RACE analysis of Malpighian tubule APN cDNA yielded a 0.78kb and a 1.87kb fragment respectively. Alignment of the three nucleotide fragments revealed that the Malpighian tubule cDNA is 3095 bp long containing an open reading frame (ORF) of 2982 bp, which would encode a 994 amino acid putative protein with a theoretical molecular mass of 111 kDa and pI of 4.83 (Fig. 4).

For salivary gland, the 5′-RACE analysis also yielded a 0.78kb fragment but the 3′-RACE first resulted in amplification of a 1.1kb fragment and using forward primers designed based on this sequence, we further amplified a 0.8kb fragment, which was then cloned and sequenced. Full-length cDNA cloning of APN from salivary gland proved to be fairly tricky probably due to the low level of expression in this tissue. Proper alignment yielded a complete cDNA sequence of 3125 bp containing an ORF of 2994 bp, which encodes a putative protein of 998 amino acids with a theoretical molecular mass of 112 kDa and pI of 4.83.

The complete cDNA sequences of Malpighian tubule and salivary gland were designated as "AjMtAPN" and "AjSgAPN" respectively. Computational analysis revealed the presence of consensus aminopeptidase activity motif "GAMENWG" and

Zn^{++} binding motif "$HEXXHX_{18}E$" in both the sequences (Figs. 4 & 5). The presence of a cleavable signal peptide, with the most likely cleavage site between amino acid position 20 (alanine) and 21 (phenylalanine) of N-terminal region was detected in both the cDNA sequences (Figs. 4 & 5). A GPI anchor signal sequence was also detected at the C-terminus of the deduced amino acid sequences of both Malpighian tubule and salivary gland APNs (Figs. 4 & 5). Further, 66 O-glycosylation and 1 N-glycosylation sites were also identified in both deduced amino acid sequences. However, no C-glycosylation site was predicted to be present. Multiple sequence alignment of AjMtAPN and AjSgAPN amino acid sequences with the reported lepidopteran APNs revealed that the consensus "GAMENWG" and "$HEXXHX_8E$" motifs were conserved in all the APNs (Fig. 7A, Red boxes). In addition, the amino acid residues adjacent to "GAMENWG" and "$HEXXHX_{18}E$" sequences were fairly conserved in all the APN sequences. All the APN sequences depicted high variability in the N and C-terminal regions. Based on the presence of these signature motifs and other related features, we classify AjMtAPN and AjSgAPN under gluzincin family of aminopeptidases. Comparison between the amino acid sequences of APNs of *A. janata* revealed that gut-specific APN (AjMgAPN) (ABH07377) shared only 32% sequence identity with AjMtAPN, AjSgAPN and fat body-specific (AjFbAPN) (ABE02186), while AjMtAPN, AjSgAPN and AjFbAPN shared 99% sequence identity between them. Phylogenetic tree constructed based on the amino acid sequence homology among the reported lepidopteran insect APNs revealed that AjMtAPN and AjSgAPN along with AjFbAPN belong to Class 1 of APNs and on the other hand, midgut specific AjMgAPN was found to belong to Class 4 (Fig. 7B). We followed the classification nomenclature proposed by Herrero *et al*. (2005). According to this classification, lepidopteran APNs are grouped into five sub-families. We categorized and named AjMgAPN as "AjAPN4" and AjFbAPN, AjMtAPN and AjSgAPN as "AjAPN1" as they belonged to these classes. Bootstrapping analysis was performed in order to test the robustness of the generated tree. Thus in the present study, we isolated two isoforms of APN from *A. janata* which were significantly different from each other.

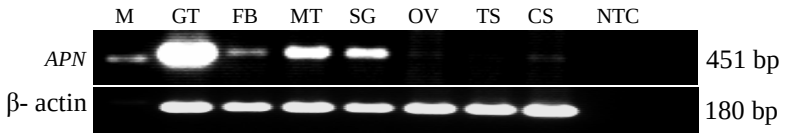

Fig. 3. **PCR analysis of APN transcript distribution in various tissues of *A. janata* fifth instar larvae**. A highly consensus 451bp fragment containing the conserved aminopeptidase activity motif "GAMENWG" and Zn^{++} binding motif "$HEXXHX_{18}E$" was amplified using a degenerate primer pair (upper panel). Lepidopteran insect β-actin was used as an endogenous internal control (lower panel). M- DNA ladder; GT- gut; FB- fat body; MT- Malpighian tubule; SG- salivary gland; OV- ovary; TS- testis; CS- carcass and NTC- non template control.

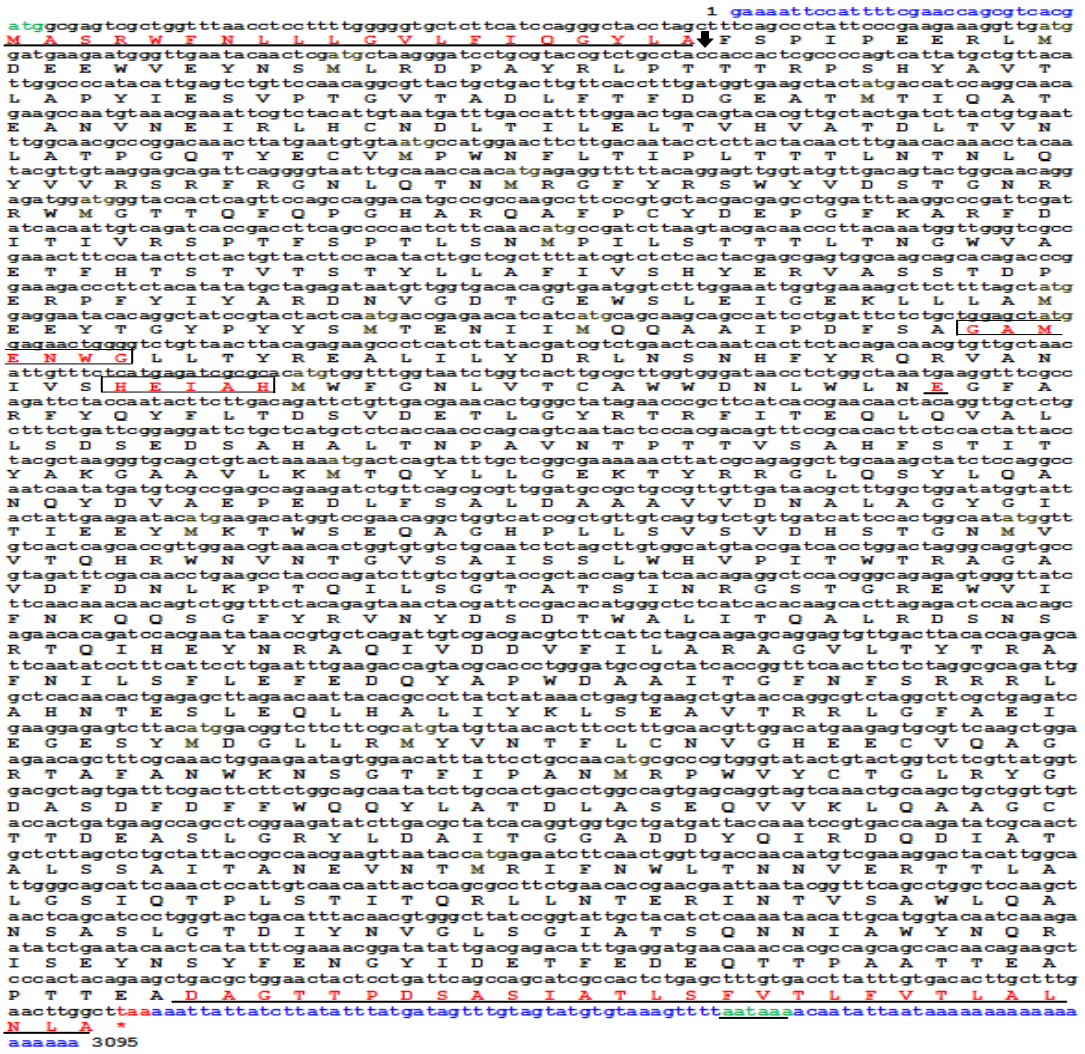

Fig. 4. **Full-length cDNA sequence and deduced amino acid sequence of *A. janata* Malpighian tubule APN**. Green color nucleotides indicate the start codon while red color nucleotides (with *) indicate stop codon. The termination signal is shown in green and underlined. 5′ and 3′ UTR nucleotides are shown in blue color. Aminopeptidase activity motif "GAMENWG" and Zn^{++} binding motif "HEXXHX$_{18}$E" are labeled in red colored boxes. Underlined amino acid residues (1-20) and the arrow head, at the N-terminus represent signal peptide and putative cleavage site respectively. Underlined amino acid residues (966-993) at the C-terminus represent GPI anchor sequence.

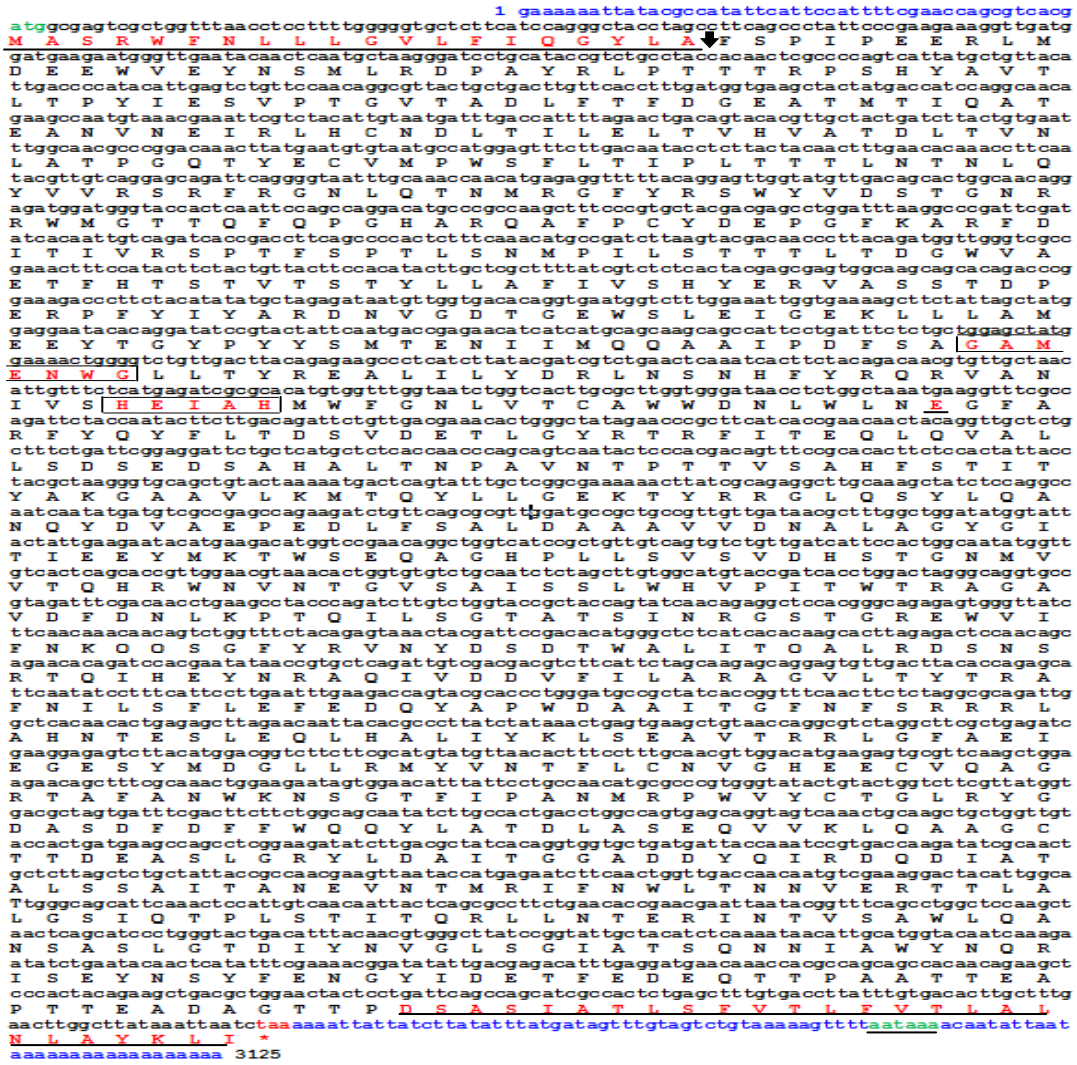

Fig. 5. **Full-length cDNA sequence and deduced amino acid sequence of *A. janata* salivary gland APN**. Green color nucleotides indicate the start codon while red color nucleotides (with *) indicate stop codon. The termination signal is shown in green and underlined. 5′ and 3′ UTRs nucleotides are shown in blue color. Aminopeptidase activity motif "GAMENWG" and Zn^{++} binding motif "$HEXXHX_{18}E$" are labeled in red colored boxes. Underlined amino acid residues (1-20) and the arrow head at the N-terminus represent signal peptide and putative cleavage site respectively. Underlined amino acid residues (972-997) at the C-terminus represent GPI anchor sequence.

Fig. 6. **Comparison of amino acid sequences of *A. janata* larval APNs using ClustalW software**. Red boxes indicate the consensus aminopeptidase activity motif "GAMENWG" and Zn^{++} binding motif "$HEXXHX_{18}E$" in all the sequences. AjMgAPN showed 32% amino acid sequence identity with AjFbAPN, AjMtAPN and AjSgAPN. AjFbAPN, AjMtAPN and AjSgAPN shared 99% amino acid sequence identity between them.

A

Fig. 7. **A) Comparison of amino acid sequences of *A. janata* larval APNs with reported lepidopteran insect APNs using ClustalW**. Red boxes indicate the consensus aminopeptidase activity motif "GAMENWG" and Zn^{++} binding motif "$HEXXHX_{18}E$" in all the sequences. **B)** Phylogenetic tree describing the amino acid sequence similarity with known lepidopteran insect APNs. Full-length amino acid sequences were aligned using ClustalW to generate a phylogenetic tree. Bootstrap analysis with 500 replicates was used to assess the strength of nodes in the tree.

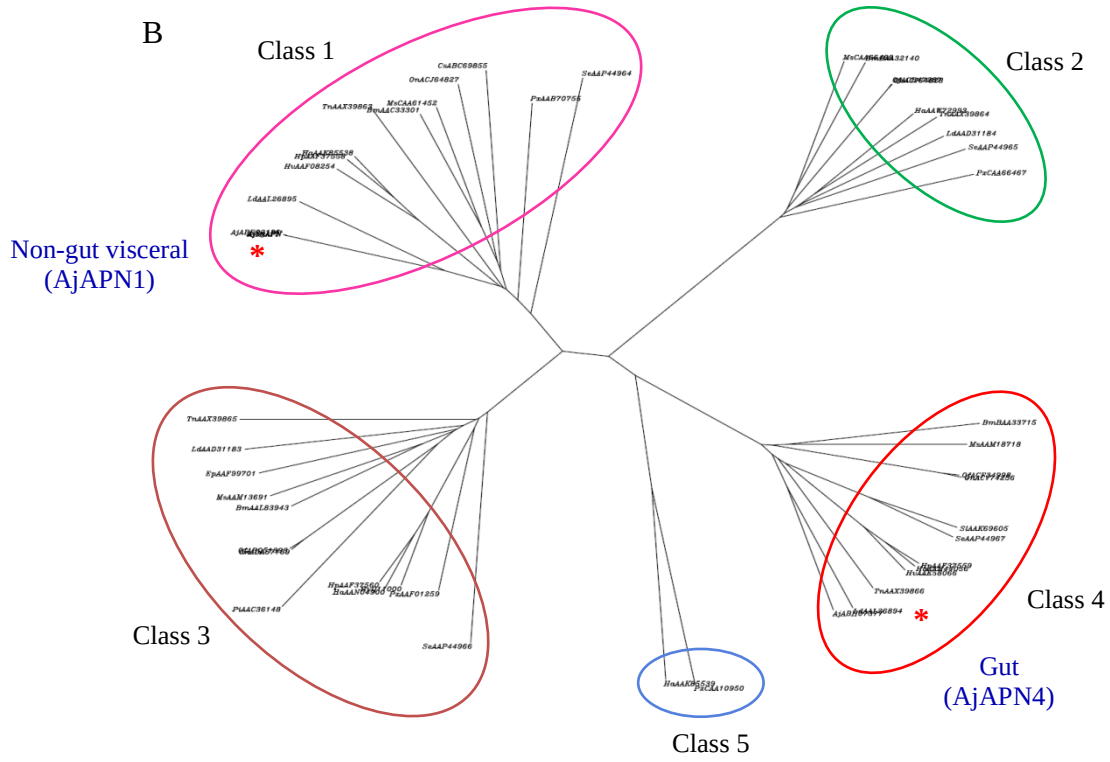

APNs were from *Achaea janata* (AjABH07377; AjABE02186; AjMtAPN-*A. janata* Malpighian tubule-specific APN and AjSgAPN-*A. janata* salivary gland-specific APN), *Plutella xylostella* (PxAAB70755; PxAAF01259; PxCAA66467; PxCAA10950), *Manduca sexta* (MsCAA61452; MsCAA66466; MsAAM13691; MsAAM18718), *Lymantria dispar* (LdAAL26895; LdAAD31184; LdAAD31183; LdAAL26894), *Heliothis virescens* (HvAAF08254; HvQ11000; HvAAK58066), *Trichoplusia ni* (TnAAX39865; TnAAX39866; TnAAX39864, TnAAX39863), *Helicoverpa armigera* (HaAAK85539; HaAAM44056; HaAAN04900; HaAAW72993; HaAAK85538), *Bombyx mori* (BmBAA33715; BmAAL83943; BmBAA32140; BmAAC33301), *Helicoverpa punctigera* (HpAAF37558; HpAAF37560; HpAAF37559), *Spodoptera litura* (SlAAK69605), *Spodoptera exigua* (SeAAP44967; SeAAP44966; SeAAP44965; SeAAP44964), *Ostrinia nubilalis* (OnACV74256; OnADA57169; OnACJ64828; OnACJ64827), *Ostrinia furnacalis* (OfACF34998; OfABQ51393; OfACB47287), *Epiphyas postvittana* (EpAAF99701), *Plodia interpunctella* (PiAAC36148) and *Chilo suppressalis* (CsABC69855).

3.5. Tissue-specific expression of *AjAPN*4 and *AjAPN*1

Semi-quantitative PCR analysis using gene specific primers showed the expression of *AjAPN*4 transcripts only in the gut and not in other tissues (Fig. 8A). On the other hand, *AjAPN*1transcripts were dominantly expressed in fat body, Malpighian tubule and salivary gland (Fig. 8C). Quantitative real-time analysis using Taqman probe further revealed high expression levels of *AjAPN*4 only in the gut tissue (Fig. 8B). *AjAPN*1 was found to be expressed dominantly in fat body, Malpighian tubule and salivary gland (Fig. 8D). Among the non-gut visceral tissues, *AjAPN*1 expression was most dominant in Malpighian tubule. It is interesting to note that *AjAPN*1 transcript expression was also seen in the gut tissue, but at a much lower level when compared with other non-gut visceral tissues (Fig. 8D).

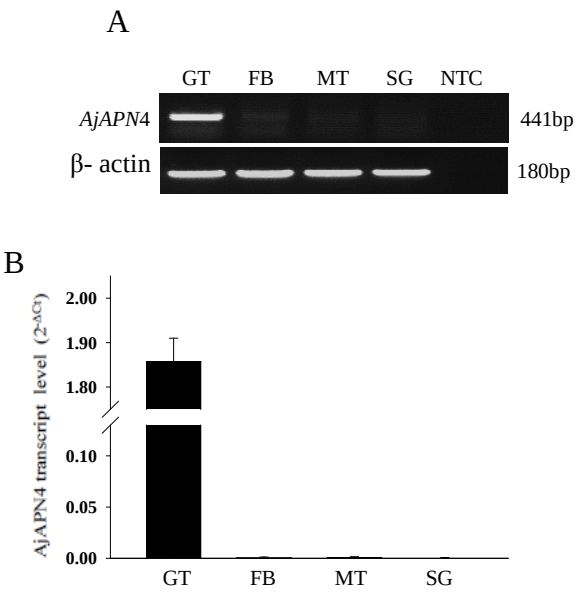

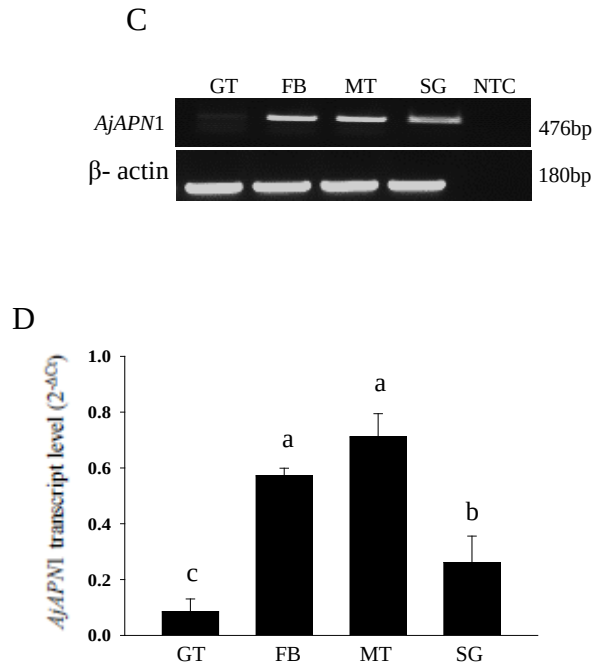

Fig. 8. **Quantitative PCR analyses of *AjAPN*4 & *AjAPN*1 expression in different larval tissues of *A. janata***. **A)** Semi-quantitative PCR analysis of *AjAPN*4 expression in different tissues. **B)** Quantitative real-time PCR analysis of *AjAPN*4 expression in different tissues. **C)** Semi-quantitative PCR analysis of *AjAPN*1 expression in different tissues. β-actin was used as an internal endogenous control. **D)** Quantitative real-time PCR analysis of *AjAPN*1 expression. Data for real-time PCR are expressed as mean ± standard deviation of three independent experiments (n=3). The real-time expression of *AjAPN*4 & *AjAPN*1 transcripts was normalized with 18sRNA. Significance between groups was tested by One-Way ANOVA followed by SNK test using SigmaPlot 11.0 software. Means denoted with different letters showed statistical significance ($P<0.05$).

3.6. Localization of APN proteins in different tissues of *A. janata*

Figure 9A shows micrograph of hematoxylin-eosin (H&E) stained sections of midgut (Fig. 9A; a), fat body (Fig. 9A; b), Malpighian tubule (Fig. 9A; c) and salivary gland (Fig. 9A; d). Gut sections showed the presence of well-defined gut epithelium which is mainly comprised of columnar cells (C) bearing a border of tightly packed apical membrane protrusions called microvilli (Fig. 9A; a). The microvilli are present along the entire apical surface of tissue epithelium. Goblet cells (G) are interspersed among the columnar cells of the epithelium. Fat body tissue sections revealed large fat cells or adipocytes (F) with distinct nuclear component (Fig. 9A; b). Malpighian tubule sections showed a distinct single layer of epithelial cells surrounding the tubule lumen and a thin basal

lamella lined the outer surface of the tubule (Fig. 9A; c). The salivary gland sections also showed a single layer of columnar epithelial cells (CE) with stretched or elongated nuclei (N) and a thin cuticular lining (C) towards the apical border of cells surrounding the lumen (L) of the gland (Fig. 9A; d). Immunofluorescence analysis of midgut tissue sections using *A. janata* gut-specific APN antibody showed abundant distribution of APN all along the microvillar brush border membranes of the columnar cells as evident from the intense flourencence of Alexa Flour 594 (Fig. 9B; a).

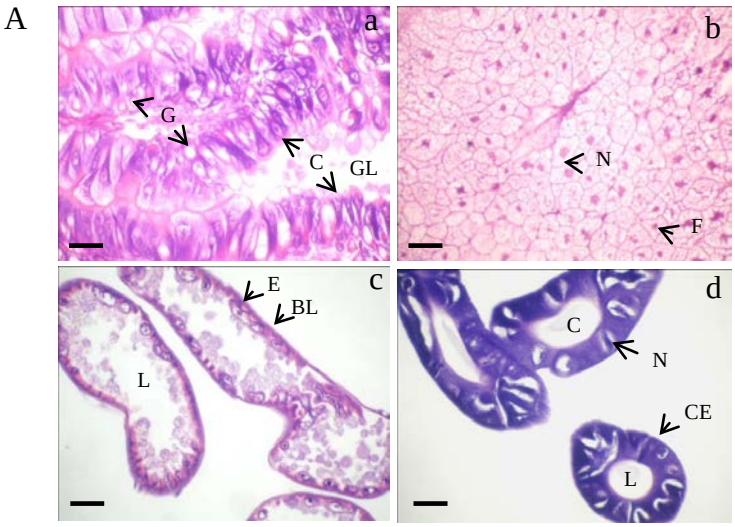

Fig. 9. **A) Histological structure of larval tissues of fifth instar larvae (H&E)**. **a)** Midgut. G: goblet cell, C: columnar cell, GL: gut lumen. **b)** Fat body. N: nucleus, F: fat body cells or adipocytes. **c)** Malpighian tubule. E: epithelial cell (single layer), BL: basal lamella, L: lumen. **d)** Salivary gland. N: stretched nuclei, C: thin cuticular lining the lumen, CE: columnar epithelium and L: lumen.

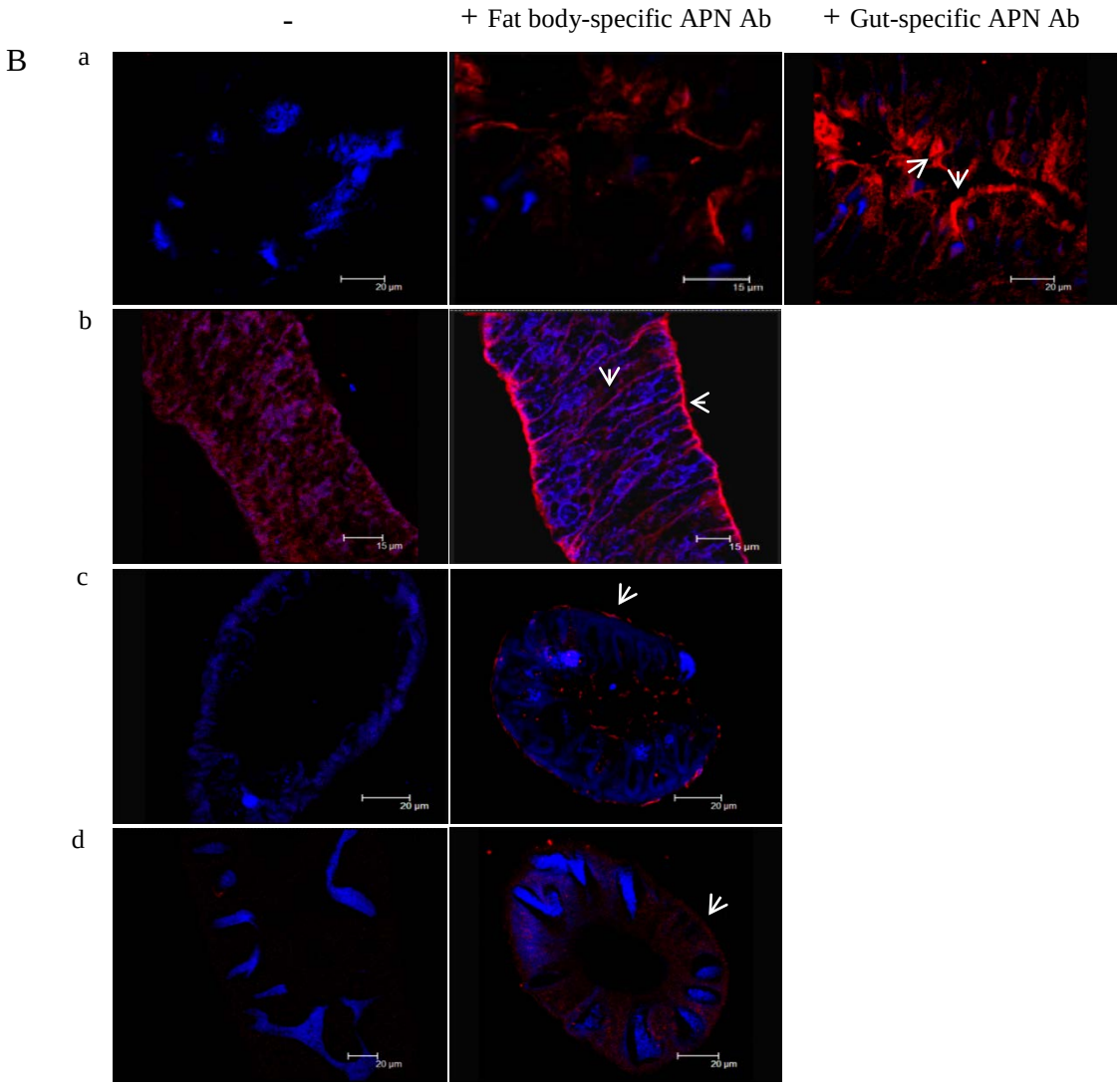

Fig. 9. **B) Immunolocalization of APN protein expression**. Immunolocalization was performed with Alexa Flour 594-conjugated secondary antibody using fluorescence microscopy. Nuclei were stained blue with DAPI. **a)** Midgut tissue. Intense fluorescence observed along the apical microvillar brush border membrane of the gut columnar epithelial cells. **b)** Fat body. APN expression localized on cell membranes of the fat cells or adipocytes, more intensely on the cell membranes forming the tissue surface. **c)** Malpighian tubule. Fluorescence was detected both on the basement membrane and apical brush border membrane of the epithelial cells. **d)** Salivary gland. No fluorescence was detected in salivary gland tissue sections.

Immunolocalization of APN protein expression in fat body, Malpighian tubule and salivary gland tissue sections were performed using *A. janata* fat body-specific APN antibody. Analysis of immuno-stained fat body sections revealed distribution of APN primarily in the plasma membranes of the fat cells or adipocytes, most abundantly on the membranes of the cells forming the surface of the tissue (Fig. 9B; b). In Malpighian tubule, fluorescence corresponding to the APN localization was detected along both the basement membrane and apical brush border membrane of the epithelial cells (Fig. 9B; c). Immunolocalization of APN protein in salivary gland sections did not show any positive results (Fig. 9B; d). Analysis of midgut sections using *A. janata* fat body-specific APN antibody also showed distribution of APN protein on the microvillar brush border membranes of the epithelial columnar cells indicating cross-reactivity of fat body-specific APN antibody with the gut-specific APN protein (Fig. 9B; a). In all the tissues, the nuclei were stained with the blue fluorescent DAPI reagent. For the controls, sections were pre-incubated with pre-immune serum followed by incubation with Alexa Flour 594-conjugated secondary antibody and when analysed, revealed total absence of fluorescence.

3.7. Immunoblot analysis of APN expression in different tissues of *A. janata*

To correlate the APN transcript expression levels with protein levels in gut, fat body, Malpighian tubule and salivary gland, we carried out western blot analysis. The *A. janata* fat body-specific APN antibody recognized the ~110 kDa protein in the fat body (Fig. 10A; Lane: FB), Malpighian tubule (Fig. 10A; Lane: MT) and salivary gland (Fig. 10A; Lane: SG). The antibody also cross-reacted with the ~110 kDa protein as well as two other lower weight proteins of the gut, which could all be isoforms of APN (Fig. 10A; Lane: GT). Densitometric analysis of the ~110 kDa protein from all the tissues showed maximum APN content in gut, followed by Malpighian tubule and then in fat body (Fig. 10B). The immuno-reactivity observed in salivary gland was fairly low or negligible (Fig. 10B). For the above analysis, the *A. janata* fat body-specific APN polyclonal antibody used was generated against a recombinant 46 kDa APN peptide containing the conserved sequences (Budatha *et al*. 2007a).

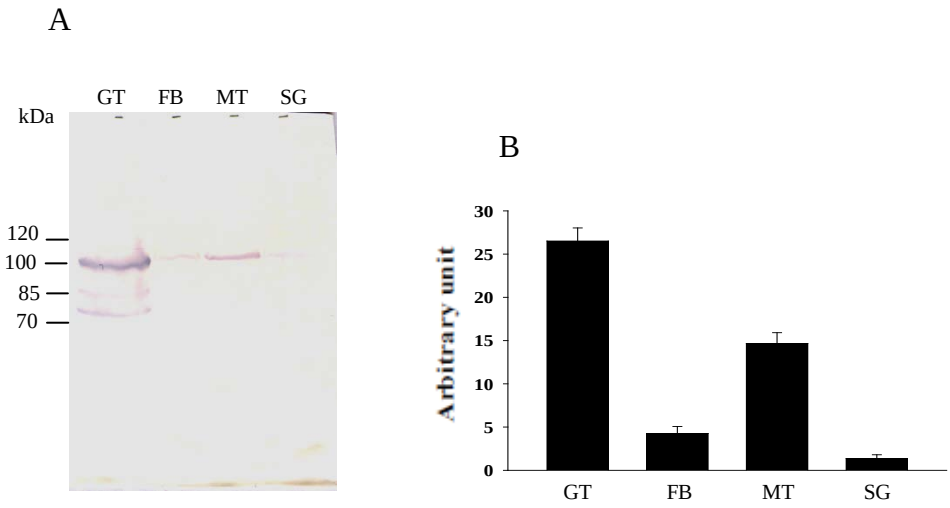

Fig. 10. **A) Western blot analysis of APN protein expression in various tissues**. Midgut BBMV, fat body membrane fraction, Malpighian tubule and salivary gland protein homogenates (all 30 µg each) were separated by 7.5% SDS-PAGE and electro-transferred onto nitrocellulose membrane. The blot was incubated with *A. janata* fat body-specific APN polyclonal antibody followed by incubation with goat anti-rabbit ALP-conjugated secondary antibody and visualized with ALP-substrate, NBT-BCIP. Note the presence of ~110 kDa APN protein band in fat body (FB), Malpighian tubule (MT) and salivary gland (SG). *A. janata* fat body-specific APN antibody cross reacted with three protein bands in the gut BBMV (GT) including the ~110 kDa band. **B)** Densitometric analysis of the western blot.

3.8. Detection of APN enzyme activity in different tissues of *A. janata*

APN enzyme activity in midgut BBMV, fat body membrane, Malpighian tubule and salivary gland was determined as described by Garczynski and Adang (1995) using *L*-leucine *p*-nitroanilide as substrate. The midgut BBMV showed high specific activity of 531.37±32.7 µmol of *p*-nitroanilide released/min/mg of protein (Fig. 11). The Malpighian tubule and salivary gland showed specific activity of 220.63±42 and 135.98±25 µmol of *p*-nitroanilide released/min/mg of protein respectively (Fig. 11). However, the enzyme activity in salivary gland was found to be very low at 13.2±7.57 µmol of *p*-nitroanilide released/min/mg of protein (Fig. 11).

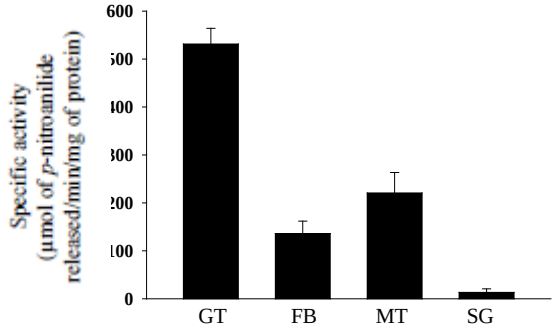

Fig. 11. **Detection of APN enzyme activity in various larval tissues**. APN enzyme activity was assayed using *L*-leucine *p*-nitroanilide as substrate. The specific activity was expressed as µmol of *p*-nitroanilide released/min/mg of proteins. The values represent the mean ± standard deviation of three independent experiments. GT- gut; FB- fat body; MT- Malpighian tubule & SG- salivary gland

3.9. Development of AjAPN4 and AjAPN1 molecular 3D models and their comparison with *B. mori* APN 3D structure

PSI-BLAST against PDB revealed tricorn interacting factor F3 from *Thermoplasma acidophilum* (PDB code: 1Z1W) and human endoplasmic reticulum aminopeptidase-1 (PDB code: 3QNF) to have the best sequence identity and similarity with AjAPN4 and AjAPN1. The sequence identity of AjAPN4 with tricorn interacting factor F3 and human endoplasmic reticulum aminopeptidase-1 were 26% and 27% respectively (Fig. 12A). The sequence alignment of AjAPN1 with tricorn interacting factor F3 showed 28% sequence identity and 44% sequence similarity while with human endoplasmic reticulum aminopeptidase-1, the sequence identity and sequence similarity was 27% and 47% respectively (Fig. 12B). The 3D structure of *B. mori* APN was built based on the crystal structure of the soluble domain of human endoplasmic reticulum aminopeptidase-1 Erap1 (PDB code: 2YD0). The sequence identity and similarly between *B. mori* APN and human Erap1 was 28% and 48% respectively. The characteristic details of the templates are given in table 1. The first 41 amino acid residues of AjAPN1 did not show enough sequence homology with the templates and therefore were not considered in the model. The initial models of AjAPN4, AjAPN1 and *B. mori* APN were generated using MODELLER interfaced by EasyModeller. The whole protein was soaked with 10 Å of water and the whole assembly was energy minimized for 1000 steps of steepest descent and 10000 steps of conjugate gradient minimization methods using CHARMM forcefield of NAMD. The protein was optimized in this step by removing bad contacts and major

errors. The refined models were then validated for their stereo-chemical quality and side chain environment and the results are shown in table 2. The Ramachandran plot of AjAPN4 model showed that only 3 residues (0.4%) are in the disallowed region and 702 residues (89.5%) in the most favored region. The plot of AjAPN1 model showed 6 residues (0.7%) to fall in the disallowed region and 721 residues (87.6%) in the most favored region. In *B. mori* APN model, only 1 residue (0.1%) was in the disallowed region and 705 residues (86.5%) were in the most favored region. The validation results as listed in table 2 show that the models have good stereo-chemical quality.

The 3D structures of AjAPN4 and AjAPN1 were compared with that of *B. mori* APN to find out if the Cry1Aa toxin binding region is structurally conserved in AjAPN4 and AjAPN1. The sequence alignment of AjAPN4, AjAPN1 and *B. mori* APN with the templates revealed that the amino acid residues corresponding to the consensus aminopeptidase activity motif "GAMENWG" and Zn^{++} binding motif "$HEXXHX_{18}E$" were conserved (Figs. 12A & 12B). The residues surrounding these conserved signature motifs were also fairly conserved. The overall fold of the three APN models was found to be conserved (Fig. 13B). The AjAPN4 and AjAPN1 3D structures revealed the presence of four structural domains. The Cry1Aa toxin binding region highlighted in yellow is located in domain I (Fig. 16C; a, b, c). The structures of aminopeptidase enzyme activity and Zn^{++} binding motifs of our models showed high similarity between them and also with the templates. These catalytic motifs are located in domain II (Fig. 14). Domain III, which is composed of several β-sheets, formed the base of the APN structure. The C-terminal domain represented as the domain IV is primarily made up of α-helices that are organized into a super-helix.

The amino acid sequences of AjAPN4, AjAPN1, *B. mori* APN (AAC33301) and *P. xylostella* APN (AAF01259) were aligned and the Cry1Aa toxin binding region was analyzed. Multiple sequence alignment of the 64 amino acid residues of Cry1Aa toxin binding region is represented in figure 16. In this region, the sequence identity between AjAPN4 and *B. mori* APN was only 40% (26 amino acid residues) while the identity between AjAPN4 and *P. xylostella* APN was also only 32% (21 amino acid residues) (Fig. 16A). On the other hand, AjAPN1 and *B. mori* APN shared 81% sequence identity (52 amino acid residues) and with *P. xylostella* APN, the sequence identity was 48% (31 amino acid residues) which include the 27 amino acid residues common to both *B. mori* APN and *P. xylostella* APN (Fig. 16B). The structure of the Cry1Aa toxin binding region of AjAPN1 was highly similar with that of *B. mori* APN (Fig. 16C). The structural

similarity was less between AjAPN4 and *B. mori* APN (Fig. 16C). This structural similarity was further substantiated by *in vitro* Cry1Aa toxin binding to ~110 kDa APN of gut and Malpighian tubule of *A. janata* where AjAPN4 and AjAPN1 are respectively expressed, as well as to gut of *B. mori* (Fig. 16D).

A

```
>P1;1Z1Wmono/1-780
1Z1Wmono 780 residues
-----------------------------------------MEVEKYDLTLDFDIQKRTFNGTETITA
DAGD-----IVLDAVGLQINWMKVNGRDTAFTYDGQTVRAPGDSQ------------P---QKIEISFAGK
VSDSL--SGIY---YAGRENG---MITTHFEATDARRMFPCVDHPAYKAVFAITVVIDKDYD-AISNMP-PK
RIEVSERKVVE-FQDTPRMSTYLLYVGIGKF-RYEYEKYRDIDLILASLKDI--RSKYPLDMARKSVEFYEN
YFGIPY------ALPKMHLISVPEFGAGAMENWGAITFREIYMDI-AENSAVTVKRNSANVIAHEIAHQWFG
DLVTMKWWNDLWLNESFATFMSYKTMDTLFPEWSFWGDFFVSRTSGALRSDSLKNTHPIE-VDVRDPDEISQ
IFDEISYGKGASILRMIEDYAGYEEFRKGISKYLNDHKFGNAEGSDLWTAIEDVSGK-----------PVKR
VMEYWIKNPGYPVIKLKRNGRK--ITMYQTRFLLNGEEEGR--WPVPVNIKKK------DGVERILLEDEAS
I----EADGLIKINADSAGFYRVLYDDATFSDVMGHYRD-----LSPLDRIGLVDDLFAFLLSGHIDPETYR
QRIRNFFDDEDHNVITAIVGQMEYLRMLTHA--FDDDARAFCRSRMQFL---------TGKQDENLKIALGR
VSRLYVMVDESYA---EEMSKLFKDFDSAEPEMRSSIATAYALVTG-------DLKGLLEKFRSVDRDEDRV
RIISAFGKLKSNTDLSTVYGM-VEKTEIKKQDMISFFSSALETLPGR-----EFIFANLDRI----------
---IRLVIRYFTGNRTAS-------RTVEMMIPVIGLDHPDAEDIVRNIGSKN----------ISMGLAKGI
EMLAVNRKLVERIRQTAVK*

>P1;3QNFmono/1-696
3QNFmono 696 residues
--------------------------------PFPWNKIRLPEYVIPVHYDLLIHANLTTLTFWGTTKVEI
TASQPTST-IILHSHHLQISRATL--RKGLSEEPLQVLEHPRQEQIALLAPEPLLVGLP---YTVVIHYAGN
LSETF--HGFYKSTYRTKEGELRILASTQFEPTAARMAFPCFDEPAFKASFSIKIRREPRHL-AISNMPLVK
SVTVAEGLIEDHFDVTVKMSTYLVAFIISDFESVSKITKSGVKVSVYAVPDKINQADYALDAAVTLLEFYED
YFSIPY------PLPKQDLAAIPDFQSGAMENWGLTTYRESALLFDAEKSSASSKLGITMTVAHELAHQWFG
NLVTMEWWNDLWLNEGFAKFMEFVSVSVTHPELKV-GDYFFGKCFDAMEVDALNSSHPVS-TPVEN------
--DDVSYDKGACILNMLREYLSADAFKSGIVQYLQKHSYKNTKNEDLWDSMASIV------------DVKT
MMNTWTLQKGFPLITITVRGRN--VHMKQEHYMKTGYL-----WHVPLTFITSKS----DMVHRFLLKTKTD
VLILPEEVEWIKFNVGMNGYYIVHYEDDGWDSLTGLLKGTHTA-VSSNDRASLINNAFQLVSIGKLSIEKAL
DLSLYLKHETEIMPVFQGLNELIPMYKLMEKRDMNEVETQFKAFLIRLLRDLIDKQTWTDEGSVSERML--R
SQLLLLACVHNYQPCVQRAEGYFRKWKESQIE--------FALCRT-------------------------
------------------------------------------------------------------------
------------------------QNIEE----------------NIGWMD------------------
-------KNFDKIRVWLQS*

>P1;AjAPN4/1-950
AjAPN4 950 residues
MQLLIILSILVGSLVAIPQEDFRSNLEFLEYDSNLGEQHYRLVDTVYPHTMDVDLDVYLDELRFNGFVSIGV
EVRESGLTQIALHQKVQSIQXVNLLTAAGAPV-PLLISEPFTTDDYYELIKINLNSAIPAGNYTITIRYTGV
INENPLDRGFYKGYYFLNNQE-RAYATTQFQPYHARKAFPCFDEPMFKSRYTLAITRDINLSPSYSNMAISA
TVPVGTTRVREEFYPTPIISAYLVAFHVSDFVETEITSTAARPFKIISRPGVIDQHEYAAEIGLKITNELDD
FLGIQYHEMGQGVLMKNDHIALPDFPSGAMENWGMVNYREAYLLYDPDNTNIINKIFIATIMAHELGHKWFG
NLVTCFWWSNLWLNESYASYFEYFGTHWADLALELDEQFVVDYVHSALAADAGAGATPMNWVDVADNPSVTS
HFSTTSYAKGASVLRMMEHFVGTRNFRNALRYYLRDNAYEVGYPIDMYDAFRQAVSEDYTFLQQYPNVDVGA
VFESWVENPGSPVVNINVNHATGAISISQQRYIVTDTQRPNNIWQIPLTWTDQRSLDFTNTRPSRVLTTATD
SITTEAGDYWVLFNVAQSSLYRVNYNDRNWELLADYLKSSNRERIHYLNRAQIVNDLLYFVRSGDVSAEVAF
NVLDFLRYETNYYVWNGALAQIDFLRRRFEH--LPNAHTLFSNYILELMDTVIQHLGFEERATDSTSTILNR
MQILNYACNLGHSGCVLDSQNKWRELRENNVAVPVNL-RRYVYCIGIREGDNTDYNFLFNLYESSENTADMV
IMLRALACTKDEALLNSYLGQSLTNRKIRIHDRTNAWSYALQGNPENLPVVLNYLYQNFEQIRTDYGGPARL
TLAISALSTYLTDFNTIQEYQAWAYENQEELDESFGTAVAVVNAAINNLVWGNANAPEIYNFLLERTVSSST
TFVASTILMLAAMFTHLLR*
```

B

```
>P1;1Z1Wmono/1-780
1Z1Wmono 780 residues
-------------------------------------------------MEVEKYDLTLDFDIQK-----
----RTFNGTETITADAGDIVLDAVGLQINWMKVNG---RDTAFTYDGQTVRAPGDSQ-------------
-------PQKIEISFAGKVSDSLSGIY---YAGRENG---MITTHFEATDARRMFPCVDHPAYKAVFAITVV
IDKDYD-AISNMP-PKRIEVSERKVVE-FQDTPRMSTYLLYVGIGKF-RYEYEKYRDIDLILASLKDI--RS
KYPLDMARKSVEFYENYFGIPYALPKMHLI----SVPEFGAGAMENWGAITFRE--IYMDIAENSAVTVKRN
SANVIAHEIAHQWFGDLVTMKWWNDLWLNESFATFMSYKTMDTLFPEWSFWGDFFVSRTSG-ALRSDSLKNT
HPIEVDVRD-PDEISQIFDEISYGKGASILRMIEDYAGYEEFRKGISKYLNDHKFGNAEGSDLWTAIEDVS-
--------GKPVKRVMEYWIKNPGYPVIKLKR---NGRKITMYQTRFLLNGEEE--GRWPVPVNI--KKKDG
VE-------RILLEDEASI----EADGLIKINADSAGFYRVLYDDATFSDVMGHYR------DLSPLDRIGL
VDDLFAFLLSGHIDPETYRQRIRNFFDDEDHNV-----ITAIVGQMEYL-RMLTHAFD--DDARAFCRSRMQ
FLTGKQ---DENLKIALGRVSRLYVMV------DESYAEEMSKLFKDFDSAEPEMRSSIATAYALVTG----
---DLKGLLEKFRSVDRDEDRVRIISAFGKLKSNTDLS----TVYGMVEKTEIKKQDMISFFSSAL-----E
TLPGREFIFANLDRIIRLV---------------------IRYFTGNRTASRTVEM--------------
-------------------------MIPVIGLDHPDAEDIVRNIGSKNISMGLAKGIEMLAVNRKLVERI
RQTAVK--*

>P1;3QNFmono/1-696
3QNFmono 696 residues
----------------------PFPWNKI----------------RLPEYVIPVHYDLLIHANLTT-----
----LTFWGTTKVEITASQPT-STIILHSHHLQISRATLRKGLSEEPLQVLEHPRQEQIALLA--------P
EPLLVGLPYTVVIHYAGNLSETFHGFYKSTYRTKEGELRILASTQFEPTAARMAFPCFDEPAFKASFSIKIR
REPRHL-AISNMPLVKSVTVAEGLIEDHFDVTVKMSTYLVAFIISDFESVSKITKSGVKVSVYAVPDKINQA
DYALDAAVTLLEFYEDYFSIPYPLPKQDLA----AIPDFQSGAMENWGLTTYRESALLFD-AEKSSASSKLG
ITMTVAHELAHQWFGNLVTMEWWNDLWLNEGFAKFMEFVSVSVTHPELKV-GDYFFGKCFD-AMEVDALNSS
HPVSTPVEN---------DDVSYDKGACILNMLREYLSADAFKSGIVQYLQKHSYKNTKNEDLWDSMASIV-
----------DVKTMMNTWTLQKGFPLITITV---RGRNVHMKQEHYMKTG-----YLWHVPLTFITSKSDM
VH-------RFLLKTKTDVLILPEEVEWIKFNVGMNGYYIVHYEDDGWDSLTGLLK--GTHTAVSSNDRASL
INNAFQLVSIGKLSIEK-ALDLSLYLKHETEIMPVFQGLNELIPMYKLMEKRDMNEVE--TQFKAFLIRLLR
DLIDKQTWTD-EG-SVSERMLRSQLLLLACVHNYQPCVQRAEGYFRKWKESQ--------IEFALC------
-------------------------------------------------RTQNIEENIG---------
------WMDKNFDK-------------------------IRVWLQS-----------------------
------------------------------------------------------------------------
--------*

>P1;AjAPN1/1-994
AjAPN1 994 residues
MASRWFNLLLGVLFIQGYLAFSPIPEERLMDEEWVEYNSMLRDPAYRLPTTTRPSHYAVTLTPYIESVPTGV
TADLFTFDGEATMTIQATEANVNEIRLHCNDLTILELTVH--VATDLTVNLATPGQTYECVMPWSFLTIPLT
TTLNTNLQYVVRSRFRGNLQTNMRGFYRSWYVDSTGNRRWMGTTQFQPGHARQAFPCYDEPGFKARFDITIV
RSPTFSPTLSNMPILSTTTLTNGWVAETFHTSTVTSTYLLAFIVSHYERVASSTDPERPFYIYARDNVGDTG
EWSLEIGEKLLLAMEEYTGYPYYSMTENIIMQQAAIPDFSAGAMENWGLLTYREALILYD-RLNSNHFYRQR
VANIVSHEIAHMWFGKLVTCAWWDNLWLNEGFARFYQYFLTDSVDETLGY-RTRFITEQLQVALLSDSEDSA
HALTNPAVNTPTTVSAHFSTITYAKGAAVLKMTQYLLGEKTYRRGLQSYLQANQYDVAEPEDLFSALDAAAV
VDNALAGYGITIEEYMKTWSEQAGHPLLSVSVDHSTGNMVVTQHRWNVNTGVSAISSLWHVPITW--TRAGA
VDFDNLKPTQILSGTATSINRGSTGREWVIFNKQQSGFYRVNYDSDTWALITQALRDSNSRTQIHEYNRAQI
VDDVFILARAGVLTYTR-AFNILSFLEFEDQYAP----WDAAITGFNFSRRRLAHNTESLEQLHALIYKLSE
AVTRRLGFAEIEGESYMDGLLRMYVNTFLCNVGHEECVQAGRTAFANWKNSGTFIPANM-RPWVYCTGLRYG
DASDFDFFWQQYLATDLASEQVVKLQAAGCTTDEASLGRYLDAITGGADDYQIRDQDIATALSSAITANEVN
TMRAFNWLTNNVERTTLALGSIQTPLSTITQRLLNTEQINTVSAWLQANSASLGTDIYNVGLSGIATSQNNI
AWYNQRISEYNSYFENGYIDETFEDEQTTPAATTEAPTTEADAGTTPDSASIATLSFVTLFVTLALNLAYKL
LSYIYDSL*
```

Fig. 12. **Sequence alignment of AjAPN4 and AjAPN1 with templates using S-alignment software (MODELLER)**. **A)** AjAPN4 with tricorn interacting factor F3 from *Thermoplasma acidophilum* (1Z1W) and human endoplasmic reticulum aminopeptidase-1 (3QNF). **B)** AjAPN1 with tricorn interacting factor F3 from *Thermoplasma acidophilum* (1Z1W) and human endoplasmic reticulum aminopeptidase-1 (3QNF).

Table 1. Template characteristics.

PDB code	Resolution [Å]	R-Value	R-Free
1Z1W	2.70	0.223 (obs.)	0.295
3QNF	3.0	0.231 (obs.)	0.283
2YD0	2.70	0.155 (obs.)	0.215

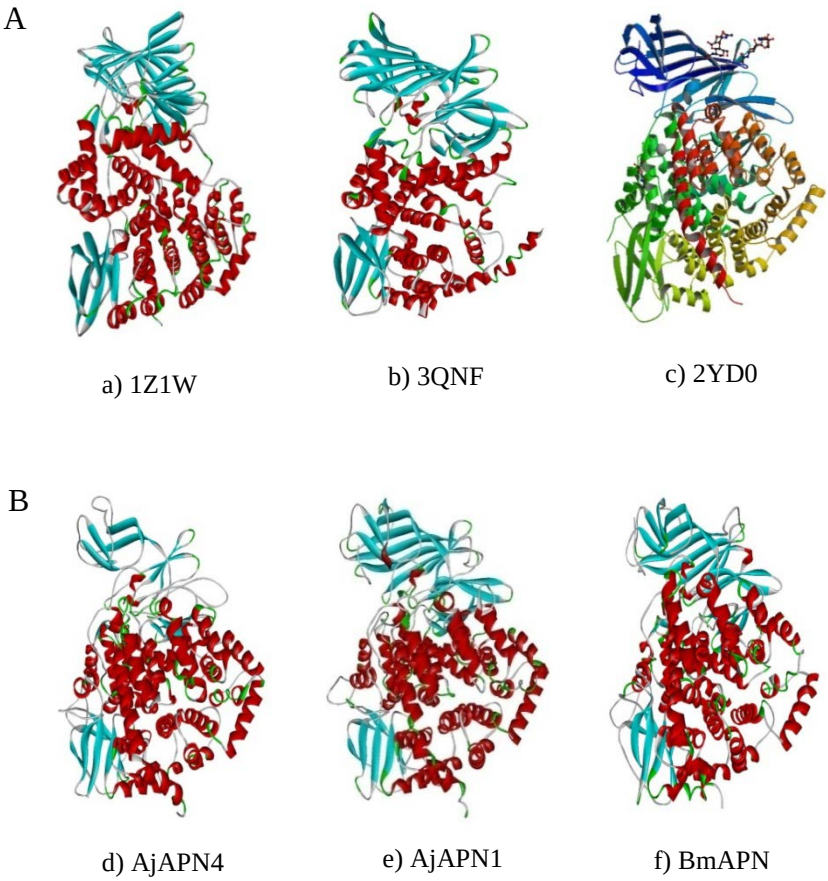

Fig. 13. **3D structures**. **A)** Templates: (a) tricorn interacting factor F3 (1Z1W), (b) human endoplasmic reticulum aminopeptidase-1 (3QNF), (c) soluble domain of human endoplasmic reticulum aminopeptidase-1 Erap1 (PDB code: 2YD0). **B)** Models: **(**d) AjAPN4, (e) AjAPN1 and (f) BmAPN.

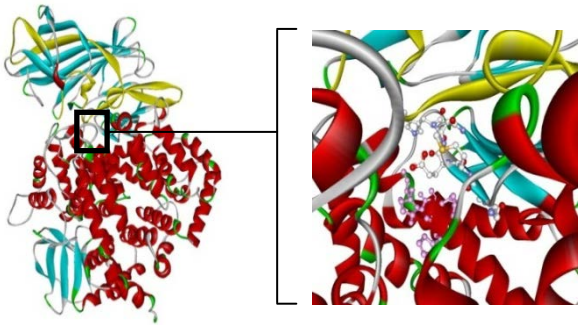

AjAPN1 APN enzyme activity and Zn^{++} binding motifs

Fig. 14. Structure of APN enzyme activity and Zn^{++} binding motifs of AjAPN1. The important residues are shown in ball and stick. The APN enzyme catalytic amino acid residues are shown in white backbone and Zn^{++} binding amino acid residues are highlighted in pink.

Table 2. Validation results of the modeled APNs.

PROTEIN	PROCHECK		ERRAT
	Ramachandran plot (allowed %)	Ramachandran plot (disallowed %)	
AjAPN4	89.5	0.4	83.115
AjAPN1	87.6	0.7	89.963
BmAPN	86.5	0.1	84.871

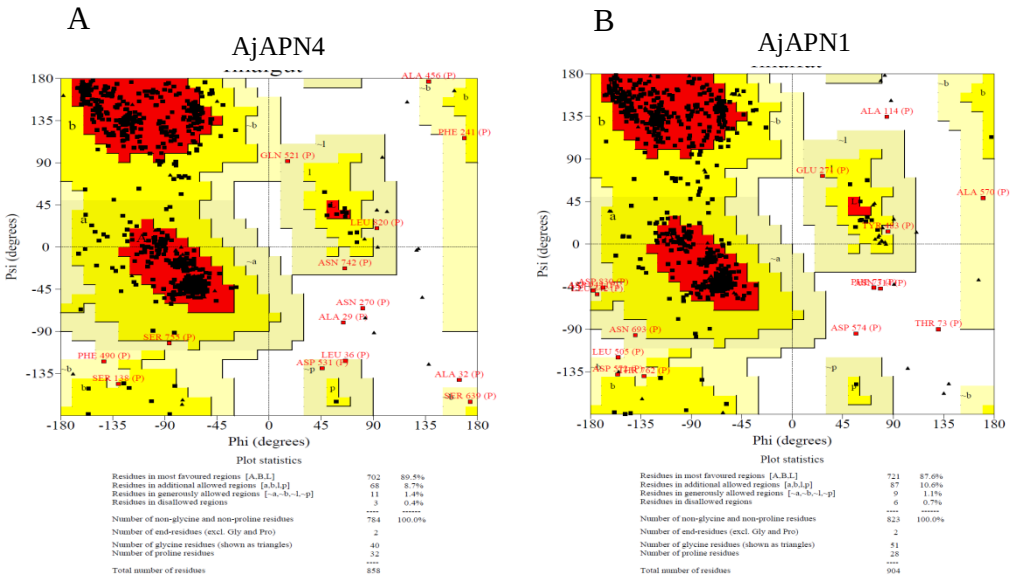

Fig. 15. **Ramachandran plot**. **A)** AjAPN4. **B)** AjAPN1. The amino acid residues in the red shaded region are in most favorable region; amino acid residues in the yellow shaded region are in additionally allowed region; amino acid residues in the cream shaded region are in generously allowed region and those in white shaded region are in the disallowed region.

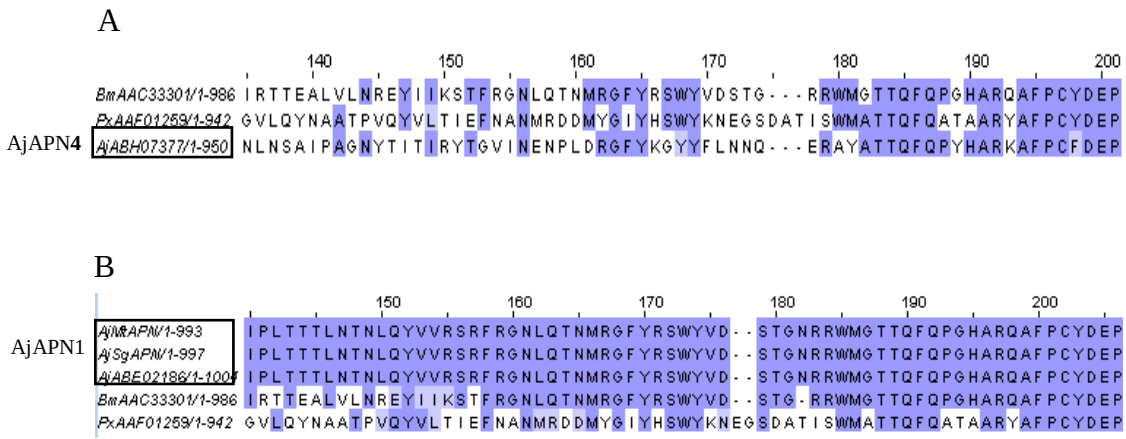

C

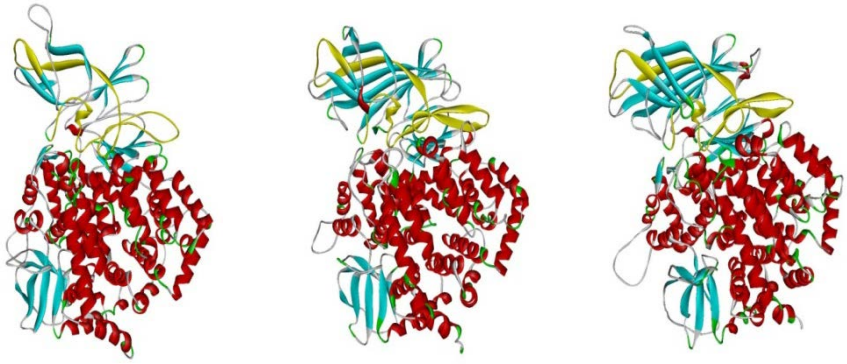

a) AjAPN4 b) AjAPN1 c) BmAPN

D

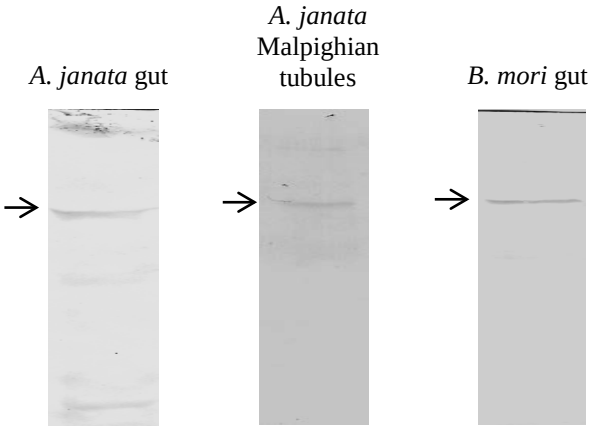

Fig. 16. **Cry1Aa toxin binding analyses**. **A)** Comparison of Cry1Aa toxin binding region of *B. mori* APN and *P. xylostella* APN with AjAPN4. **B)** Comparison of Cry1Aa toxin region of *B. mori* APN and *P. xylostella* APN with AjAPN1. **C)** 3D structures of AjAPN4, AjAPN1 and *B. mori* APN. The secondary structure of the Cry1Aa toxin binding region is highlighted in yellow. **D)** *In vitro* Cry1Aa toxin binding analysis. Note the binding of Cry1Aa to ~110 kDa protein of gut and Malpighian tubule of *A. janata*, where AjAPN4 and AjAPN1 is expressed respectively. Also note the binding of Cry1Aa to ~110 kDa protein of *B. mori* gut, which is reported to contain the Cry1Aa toxin binding region.

4. Discussion

In part 1, we have demonstrated that the delivery of activated Cry toxins into the hemocoel of *A. janata* larvae induced cell death and degeneration in fat body tissue. Cry toxin injection also elicited dose-dependent toxic response in terms of larval mortality, food intake, growth arrest, development of non-viable larval-pupal intermediates and development of defective adults. Binding of Cry toxins to specific receptors is known to be critical for induction of toxicity to the susceptible insects (Hofmann *et al*. 1988; Van Rie *et al*. 1990; Lee *et al*. 1992; Zhang *et al*. 2009). This part of our study was aimed to correlate the pathophysiological state of the larvae with the biochemical events induced by the presence of Cry toxins in the larval hemocoel. *In vitro* ligand blotting analysis revealed specific binding of different Cry toxins i.e. Cry1Aa, Cry1Ab, Cry1Ac and DOR5 Cry toxins to ~110 kDa protein of fat body, Malpighian tubule and salivary gland. BBMV prepared from midgut also showed binding of different Cry toxins to ~110 kDa protein (data not shown) which hints that the interacting protein in all the tissues of *A. janata* could be the same isoform or belonged to different isoforms of a protein with identical binding site. Budatha *et al.* (2007a) demonstrated the interaction of Cry1Aa to 113 kDa and 170 kDa proteins of midgut of *A. janata* suggesting the two proteins to be isoforms of APN. Differential interacting patterns exhibited by the different Cry toxin types in the same tissue protein preparation and the absence of any signal in the control membrane blots where the blots were incubated with the corresponding unlabeled Cry toxins further confirmed specificity in interaction and dismissed the possibility of the outcome as artifactual. The increased interaction of ~110 kDa protein with DOR5 Cry toxins as can be seen from the intensity of the interacting band, either was due to increased binding of toxins or due to more types of binding toxins present in DOR5. The specificity of interaction between the binding protein and Cry toxin was further analyzed by co-immunoprecipitation assay with Cry1Ab as the interacting ligand and using Cry1Ab antibody for pulling down the protein-ligand complex. The ~110 kDa interacting protein was partly confirmed as an APN by detecting it with *A. janata* fat body-specific APN polyclonal antibody, which was generated as described by Budatha *et al* (2007a).

Using degenerate primers designed based on the conserved regions of all the reported lepidopteran midgut APNs including gut-specific APN as well as fat body-specific APN from *A. janata* reported by Budatha *et al.* (2007a), we could amplify a 451bp fragment from gut, fat body, Malpighian tubule and salivary gland of fifth instar *A. janata* larvae. Absence of amplification in testis, ovary and carcass suggest that the APNs

are not ubiquitously present in all the tissues. We obtained full-length cDNA clones from Malpighian tubule and salivary gland using RACE strategy. So far, no proper nomenclature methods are available and hence different APN isoforms in a species are named according to the convenience of the authors (Herrero *et al*. 2005; Angelucci *et al*. 2008). Thus, we named the Malpighian tubule APN clone as "AjMtAPN" and salivary gland APN clone as "AjSgAPN". Molecular characterization of the deduced amino acid sequences of AjMtAPN and AjSgAPN revealed the presence of canonical features of an APN including aminopeptidase activity motif "GAMENWG", Zn^{++} binding motif "$HEXXHX_{18}E$", N-terminal signal peptide, several glycosylation sites and C-terminal GPI-anchor signal. Based on these features, we classify the two sequences as members of gluzincin APN family. APNs are a class of peptidases belonging to a Zn^{++} dependent gluzincin family of metalloproteases M1 type (Albiston *et al*. 2004) and are glycoproteins attached to the cell membranes through a GPI-anchor (Garczynski and Adang, 1995).

Sequence comparison with the reported lepidopteran APNs revealed the conservation of APN signature motifs in all the APNs. Comparative analysis of *A. janata* APNs revealed that AjMgAPN shared 32% sequence identity with AjFbAPN, AjMtAPN and AjSgAPN while AjFbAPN, AjMtAPN and AjSgAPN shared 99% sequence identity between them indicating the presence of two types or isoforms of APN in *A. janata*. In the present study, phylogenetic analysis of the AjMtAPN and AjSgAPN amino acid sequences were performed according to the classification nomenclature proposed by Herrero *et al*. (2005). AjMgAPN belonged to Class 4 while AjFbAPN, AjMtAPN and AjSgAPN belonged to Class 1 in the phylogenetic tree. Hence, we also refer AjMgAPN as "AjAPN4" and AjFbAPN, AjMtAPN and AjSgAPN as "AjAPN1". Presence of a number of APN genes in a species was proposed to have derived from multiple gene duplication (Chang *et al*. 1999) and is evident in a number of lepidopteran insects (Emmerling *et al*. 2001; Herrero *et al*. 2005; Wang *et al*. 2005; Simpson *et al*. 2007; Angelucci *et al*. 2008; Crava *et al*. 2010). Real-time analysis using specific primers for *AjAPN*4 and *AjAPN*1 revealed that *AjAPN*4 was specifically expressed only in the gut while *AjAPN*1 was expressed in fat body, Malpighian tubule, salivary gland and midgut. However, *AjAPN*1 expression was most dominant in the visceral tissues than in gut. Expression of APNs in fat body, Malpighian tubule and salivary gland could have far reaching implication in growth, metamorphosis and reproduction.

As larval fat body is known to be analogous in function to the vertebrate liver and is the primary organ for protein metabolism and storage, the expression of AjAPN1 in fat

body and most importantly in the late larval instars indicate a significant physiological role in insect development. During metamorphosis, APNs are known to be involved in the catabolism of larval storage proteins including hexamerins that are sequestered in the fat body. On the other hand, Malpighian tubule being an excretory organ rather than a digestive system, the function of the APNs in this organ is not clear. However in mammals, APNs are known to play important functions in the kidney (Vlahovic and Stefanovic, 1998) which is the mammalian counterpart of the insect Malpighian tubule. In the kidney, APNs play the function of hydrolysis of small peptides in the Glomerular filtrate (Noven *et al*. 1997). The role of APN in salivary gland is even more elusive. In Lepidoptera, salivary glands are responsible for the secretion of silk that is required for cocoon/puparia formation, which is an important physiological event in metamorphosis. Further investigations are needed to understand its potential role in this organ.

Immunolocalization analysis showed the expression of APN in fat body and Malpighian tubule. The poor fluorescence signals seen in salivary gland could be due to very low level of APN expression in this tissue. In midgut, the intense fluorescence signals observed all along the apical microvillar brush border membranes of the columnar epithelial cells corresponds to the abundant distribution of APN in these sites which is in agreement with similar observations reported from other lepidopteran insects (Chen *et al*. 2005; Valaitis, 2011). The fluorescence signal in fat body tissue sections was prominent on the membranes of the fat cells, more being on the membranes forming the surface of the tissue. In Malpighian tubule, APN was found to be localized both on the basement membranes as well as apical brush border membranes of the single-layered epithelial cells. Unlike in midgut where the APN expression is restricted to the apical brush border membranes, the expression of APN all along the fat cell membranes of fat body tissue and the distribution of APN on both the basement and apical membranes of Malpighian tubule could prove significant in providing easy access to Cry toxins for receptor-Cry toxin interaction. Till date, no reports of such studies in fat body, Malpighian tubule and salivary gland in other insects are available. Western blot analysis of fat body membrane preparation, Malpighian tubule and salivary gland protein homogenates using *A. janata* fat body-specific APN polyclonal antibody (Budatha *et al*. 2007a) also confirmed the presence of ~110 kDa APN in all the three tissues. The antibody cross reacted with three proteins of gut BBMV; a ~110 kDa protein and two lower molecular weight proteins, which might suggest the presence of three different isoforms in gut and only one in other tissues. The cross-reaction of fat body-specific APN polyclonal antibody with the gut-

specific APNs could be attributed to the presence of APN conserved motifs in the 46 kDa fragment against which the antibody was generated. The APN enzyme activity analysis might suggests that AjAPN1 isoform is probably associated with low enzyme activity whereas midgut APN with significantly high level of enzyme activity. The lower levels of APN expression in the non-gut visceral tissues as compared to the midgut could also have resulted in lower levels of enzyme activity. This differential expression of APN in different tissues of *A. janata* could significantly influence their role in insect development and metamorphosis.

In addition to the likely proteolytic role of APNs in fat body, Malpighian tubule and salivary gland, the presence of APNs in these tissues also presents us with a fascinating option to exploit them as Cry toxin target site. APNs as Cry toxin receptors have been established in a number of lepidopteran insects including *Manduca sexta* (Knight *et al*. 1994), *Heliothis virescens* (Gill *et al*. 1995), *Lymantria dispar* (Valaitis *et al*. 1995), *Bombyx mori* (Yaoi *et al*. 1997), *Plutella xylostella* (Luo *et al*. 1997), *Spodoptera litura* (Rajagopal *et al*. 2002) and *Helicoverpa armigera* (Sivakumar *et al*. 2007). Correlation between binding specificity and susceptibility was demonstrated in *B. mori* where high sensitivity to Cry1Aa and less sensitivity to Cry1Ac were associated with high binding and low binding affinities of Cry1Aa and Cry1Ac to APN respectively (Shinkawa *et al*. 1999). *M. sexta* APN bind to Cry1Aa and Cry1Ac with equally high affinities and subsequently, the larvae were found to be highly sensitive to both Cry1Aa and Cry1Ac (Masson *et al*. 1995). The binding regions for Cry1Aa and Cry1Ac on *B. mori* APN were shown to be different (Yaoi *et al*. 1999). All these studies suggest that different Cry toxins have different recognition structures on APN. Yaoi *et al* (1999) identified the region between 135-Ile and 198-Pro on *B. mori* APN (AAC33301) as the Cry1Aa toxin binding region. Sequence alignment of AjAPN1 with *B. mori* APN (Yaoi *et al.* 1999) and *P. xylostella* APN (AAF01259) (Nakanishi *et al*. 1999) and comparison of the 64 amino acid Cry1Aa toxin binding region of these APNs showed 81% and 48% amino acid sequence identity respectively. Of the 64 amino acid residues in this region, 27 amino acid residues were common to *B. mori* and *P. xylostella* APNs and these common amino acid residues were suggested to be important for Cry1Aa toxin binding. Between AjAPN1 and *B. mori* APN, 52 amino acid residues including the 27 amino acid residues which were common to *B. mori* and *P. xylostella* APNs were identical. AjAPN1 and *P. xylostella* APN also shared 31 amino acid residues which also includes the important 27 amino acid residues. Hence we assumed the interaction between Cry1Aa

and ~110 kDa APN of Malpighian tubule and salivary gland to be mediated by the presence of Cry1Aa toxin-binding region. Further, the presence of Cry1A toxin binding region identified in fat body-specific APN and midgut-specific APN isoforms of *A. janata* supported the notion (Budatha *et al*. 2007a). Thus, Cry toxins probably bind to a conserved structure of APN which is specific to the type of Cry toxins and not to all the APNs. For instance, Cry1Aa did not bind to 120 kDa APN from *L. dispar* BBMV (Lee *et al*. 1996). However, it is more important to confirm whether the protein is merely a binding protein or a protein that can confer toxicity upon binding since binding of Cry toxins to non-susceptible insect midguts has also been reported (Wolfersberger *et al*. 1990; Garczynski *et al.* 1991).

Different Cry1A toxins have similar primary sequences and 3D structures and therefore will recognize gut APNs with similar structure (Atsumi *et al*. 2005). The structure of Cry1A binding region of APN mediates the specificity of Cry1A toxin-APN interaction. Till date, crystal structure of insect APN has not been determined. The specific interaction of Cry toxins to ~110 kDa protein (APN) of fat body, Malpighian tubule and salivary gland observed *in vitro* could possibly represent Cry toxin-APN interaction *in vivo*. In the larval hemocoel, fat body, Malpighian tubules and salivary glands are bathed in hemolymph which also increases the chances of Cry toxins interacting with the APNs associated with these tissues. However, the molecular mechanism(s) underlying the toxicity of insects upon delivery of Cry toxins into the hemocoel is not known. Analysis of the structure of this putative APN protein would provide insights on the functional properties of this APN towards understanding of Cry toxin-receptor interaction and its implications.

We used comparative modeling methodology to construct the AjAPN4 and AjAPN1 molecular models based on sequence identity and similarity with the templates. Despite low sequence identity, the model generated may be reasonable because the conservation in the residues corresponding to the APN signature motifs, position specific residues and stereo specific residues were taken into account during the construction of the model. The stereochemical quality of the model was validated using Procheck and Profile3D. In the Ramachandran plot of AjAPN1, only six residues (0.7%) were in the disallowed region where as 87.6% were in the most favored region, which showed that the quality of the model was good. The molecular model of AjAPN4 was better as only three amino acid residues (0.4%) were in the disallowed region and 89.5% were in the most favored region. Cry1Aa toxin binding *B. mori* APN model was also constructed

using the same methodology. The overall folding pattern of AjAPN4, AjAPN1 and *B. mori* APN (AAC33301) 3D structures was highly conserved with the available 3D structures of the experimentally determined gluzincin aminopeptidases. This suggests that the structure of different APNs shared a conserved conformation but the Cry toxin recognition or binding sites could be a region susceptible to change. AjAPN1 and *B. mori* APN shared high sequence and structural similarity in the Cry1Aa toxin binding region, and therefore it is highly probable that both the APNs play similar functions. Besides Cry1 toxins can easily develop toxic activity in a broad spectrum of insect pests by recognizing the conserved structures (Nakanishi *et al*. 1999; Agrawal *et al*. 2002; Kyrieleis *et al*. 2005). The possible role of AjAPN1 as Cry toxin receptor was further supported by *in vitro* binding of Cry1Aa to ~110 kDa protein of Malpighian tubule where AjAPN1 of theoretical weight of 111 kDa was expressed.

Based on the results observed so far, we proposed that Cry toxins upon delivery into the larval hemocoel, specifically interact with fat body tissue, Malpighian tubules and salivary glands through the ~110 kDa protein, which probably is an APN located on the cell membranes of these tissues. The interaction could be responsible for the various toxicity effects induce by Cry toxin delivery. Identification of such molecular targets that allow susceptibility of the insects to Cry toxins would tremendously increase the spectrum of target sites for tackling the ever-increasing problem of insect resistance generated by widespread use of Bt-based biopesticides in crops and organic farming (McGaughey, 1985; Shelton *et al*. 1993; Ferre and Van Rie, 2002; Zhuang and Gill, 2003; Tabashnik *et al*. 2005). The findings from the present study would be useful for designing novel Bt-based delivery strategies that could target these putative sites.

Part 3

Developmental and hormonal regulation of APN expression in *A. janata*

1. Introduction

Aminopeptidases (EC 3.4.11) are a family of enzymes which cleave the N-terminal amino acid residues of polypeptides. They are found in the subcellular organelles, cytosol and bound to membranes of plant and animal cells. They are known to be involved in protein digestion, protein maturation and regulation of peptide hormone levels (Taylor, 1993; Siviter *et al*. 2002). Aminopeptidases N (APNs) are a class of peptidases belonging to a Zn^{++} dependent gluzincin family of metalloproteases M1 type (Hooper, 1994; Albiston *et al*. 2004) which cleave almost all amino acid residues from the N-terminus of oligopeptides, preferentially the neutral amino acids. They are located in the brush border membranes of the alimentary tract of different organisms; including the midgut of insects, especially in lepidopteran larvae, where they are attached to the membrane through a GPI anchor (Garczynski and Adang, 1995).

In the lepidopteran larval midgut, besides their main function in dietary protein digestion (Terra and Ferreira, 1994), membrane-bound APNs are also known to serve as receptors for Cry toxins (Knight *et al*. 1994; Sangadala *et al*. 1994; Gill and Ellar, 2002; Rajagopal *et al*. 2002; Bravo *et al*. 2004, 2007; Budatha *et al*. 2007a). APNs are known to exist in multiple isoforms in each species. To date, over 100 isoforms of lepidopteran APNs have been reported. Nakanishi *et al*. (2002) grouped all the reported lepidopteran APNs into four classes while Herrero *et al*. (2005) classified them into five classes. These isoforms have distinct role in protein digestion and are also known to bind to different Cry toxins (Banks *et al*. 2003; Rajagopal *et al*. 2003). Besides midgut, APNs have also been identified in Malpighian tubule of *Trichoplusia ni* (Wang *et al*. 2005) and fat body of *A. janata* (Budatha *et al*. 2007a) and *S. litura* (Budatha *et al*. 2007b). However till date, majority of studies have concentrated on midgut APNs of lepidopteran larvae primarily to elucidate their role in larval pathogenesis and resistance to different Cry toxins.

During post-embryonic development of insects, variety of tissues play important physiological functions which are primarily governed by interplay between juvenile hormones (JHs) and ecdysteroids through the regulation of a cascade of gene/protein expression. 20-hydroxyecdysone (20E), the major bioactive ecdysteroid orchestrates the molting process, while JH determines the nature of the molt. In the presence of JH, 20E directs larval-larval molt; whereas in the absence of JH, 20E directs larval-pupal and pupal-adult metamorphosis (Riddiford, 1994, 2008). Both of these hormones circulate in the hemolymph throughout the insect's body, hence majority of the tissues get exposed to the same concentrations of hormones, during any developmental time. Prothoracicotropic

hormone (PTTH) in response to neural, hormonal or environmental factors stimulates prothoracic glands to synthesize and release ecdysone into the hemolymph which is further converted into the active form 20-hydroxyecdysone (20E), in mitochondria and microsomes of peripheral tissues like fat body, hemocytes, epidermis *etc*. On the other hand, allotrophic hormone (ATH) as well as allatostatin regulates the synthesis and secretion of JH by the corpora allata which is responsible for preventing metamorphosis in insects. Insect fat body is the major multifunctional organ involved in metabolism and is analogous to vertebrate adipose tissue and liver (Haunerland and Shirk, 1995). Malpighian tubule is the primary excretory organ in insects and is analogous to the kidney of higher vertebrates. Similarly, salivary gland is another major organ in lepidopteran insects, responsible for synthesis and secretion of silk which is used for cocoon/puparia formation, an important event in holometabolous insect development.

Midgut APNs are known to perform multiple physiological activities in insect development. To the best of our knowledge, the role of APNs in non-gut tissues like fat body, Malpighian tubule and salivary gland has not been elucidated till date. Emmerling *et al*. (2001) and Gilliland *et al*. (2002) suggested that the expression of different isoforms of APN may be differentially regulated during larval development. APNs may have distinct roles in visceral tissues and thus play important function in insect growth and development. In part 2, we have demonstrated the presence of two types (isoforms) of APN in *A. janata*- (i) *AjAPN*4, which is gut-specific and (ii) *AjAPN*1, which is primarily found to fat body, Malpighian tubule and salivary gland. In this part of our study, we investigated the developmental and hormonal regulation of *AjAPN*4 and *AjAPN*1 expression during the post-embryonic development of *A. janata*. Methoprene, an analog of JH, was used to mimic the action of JH (Wu *et al*. 2006; Nishiura *et al*. 2007). The data presented in this study revealed that the expression of *AjAPN*4 and *AjAPN*1 is developmentally regulated at transcriptional as well as post-transcriptional levels. Further, the APN enzyme activity in these tissues also showed a similar developmental pattern. However in hemolymph, the APN enzyme activity significantly increased in the stage just prior to pupation and this might facilitate metamorphic changes which occur during larval-pupal transformation. Quantitative PCR analyses revealed that 20E down-regulates and JH up-regulates *AjAPN*4 and *AjAPN*1 mRNA expression in a dose-dependent manner. Our study also revealed the antagonistic effect of JH on 20E depending *AjAPN*4 and *AjAPN*1 mRNA expression. To our knowledge, this is the first report demonstrating the developmental and hormonal regulation of APN expression in a lepidopteran insect.

2. Materials and methods

2.1. Experimental insect

A. janata insects were cultured as described in "Materials and methods" section of part 1. For the present study, third larval instar, fourth larval instar, fifth larval instar, pre-pupa and pupa were used.

2.2. Thorax-ligation and hormone treatment

10 days old fifth instar larvae with body weight of 0.75±0.05 g fresh larval weight were narcotized by placing them on ice for 15 min. Ligation was done by tightly tying a silk thread behind the thoracic region. The tissues anterior to ligation were cut with sterile scissors and the wound was dressed with traces of antibiotic mixture (streptomycin: actinomycin in 1:6 ratio) and sealed with bees wax. These ligatures were kept on petridishes containing moistened filter paper to maintain humidity and to prevent desiccation (Ashok and Dutta-Gupta, 1988). 20E (Sigma Aldrich, USA) was dissolved in ethanol and then diluted in insect Ringer solution. Methoprene, a JH analog (Sigma Aldrich, USA) was dissolved in acetone. After 24 h of thorax-ligation, the larvae were narcotized on ice for 15 min followed by hormone treatment. Each of the ligated larvae was injected with 0.1, 1, 5 and 10 µg of 20E in a volume of 10 µl using a Hamilton microsyringe. The final concentration of ethanol did not exceed 0.05%. Same concentrations of methoprene which was diluted using acetone were topically applied on the dorsal side of each of the ligated larvae. Control larvae were either injected or topically applied with equal volume of the corresponding carrier solvent.

In another set of experiment, thorax-ligated larvae were first injected with 5 µg of 20E which was followed by topical application of the same concentration of methoprene after 5 h. Two different groups of larvae were treated with the same concentration of 20E or methoprene separately. The injection sites were dressed with traces of antibiotic mixture (streptomycin:actinomycin in 1:6 ratio) and sealed with bees wax to avoid any kind of infection.

2.3. Tissue isolation

Larvae of required developmental stages (third instar to pre-pupa) were narcotized by placing on ice for 15-20 min. Midgut, fat body, Malpighian tubule and salivary gland were dissected out in ice-cold insect Ringer solution. The gut tissue was cleared of food content and other attached tissues including peritrophic membranes and Malpighian

tubules. Fat body was also isolated from pupa and adult for certain experiments. The tissues were used for isolation of total RNA and preparation of protein samples for APN enzyme activity assay as well as western blotting. From hormone and/or solvent treated ligated larvae, tissues were isolated at 0, 5, 10, 24 and 48 h post-injection of 20E and 0, 12, 24 and 48 h post-topical application of methoprene and were used for total RNA isolation.

2.4. Collection and preparation of hemolymph sample

The larvae of the appropriate stage(s) were narcotized by placing them on ice for 15-20 min. The prolegs were cut with a sharp scissor and the oozing hemolymph was collected with the help of a capillary tube into centrifuge tubes precoated with 0.025% phenylthiourea. Phenylthiourea prevents tyrosinase activity and melanization of hemolymph. The hemolymph samples were diluted with 10mM Tris-HCl (pH 7.8) and centrifuged at 1000 X g for 3 min at 4ºC to sediment the hemocytes. The supernatant was collected and used immediately.

2.5. Semi-quantitative and real-time PCR analyses

Total RNAs were isolated using TRI reagent ™ (Sigma Aldrich, USA) following the manufacturer's instructions. Quantification of RNA was carried out using Nanodrop 1000 (Thermo Scientific, USA). Quality and integrity of RNA samples were assessed by electrophoresis on a 1% agarose gel. 5 µg of total RNAs from each tissue/organ were reverse-transcribed to corresponding cDNAs using SuperScript III first strand synthesis kit (Invitrogen) following the manufacturers' protocol. For semi-quantitative analysis, we used 5′CTTACTACTGCTACTGACTC3′ and 5′GTTAAGAATGGTAGATGTTGAA3′ as forward and reverse primers respectively, designed to specifically amplify a 441bp *AjAPN*4 fragment from midgut. Further, a specific primer pair of 5′TGGCTGGATATGGTATTACT3′ and 5′GATATTGAATGCTCTGGTGTA3′ was used as a forward and reverse primer respectively to amplify a 476 bp *AjAPN*1 fragment from fat body, Malpighian tubule and salivary gland. We also used forward primer 5′GGTAGTAGACAATGGCTCGGG3′ and reverse primer 5′CCCAGTTAGTGACGATTCCGTG3′ for amplification of a 180 bp fragment of lepidopteran insect β-actin which served as an internal control. Semi-quantitative PCR products were electrophoretically separated using 1% agarose gel. Real-time quantitative PCR reactions were performed in a 20 µl volume using custom Taqman gene expression assay (Applied Biosystems, USA). The forward primer 5′TGCTCAGTCTAGTCTGTA3′,

reverse primer 5′GCCCTGTTCAAATAGTGA3′ and TCCTCTCACGATTGCTGCTCTT as Taqman probe were used for *AjAPN*4 expression analysis. Similarly for *AjAPN*1 expression study, 5′AGGAATACACAGGCTATCCGTACT3′, 5′GGCTGCTTGCTGCATGAT3′ and CAATGACCGAGAACATC were used as forward primer, reverse primer and Taqman probe respectively. Insect 18S RNA was used as internal reference to normalize the transcript expression levels. Analysis was performed in triplicates for each sample of three independent experiments. The results are represented as change in the transcript levels relative to the control using the target gene Ct values normalized to that of 18S RNA gene Ct values using the $2^{(-\Delta\Delta Ct)}$ method described by Livak and Schmittgen (2001). The Applied Biosystems 7500 Fast Real-Time PCR systems machine was used for the real-time PCR quantitative studies.

2.6. Preparation of protein samples

The procedures involved in the preparation of various tissue protein samples have already been described in “Materials and methods” section of part 2. Midgut brush border membrane vesicles (BBMVs) were prepared as described by Wolfersberger *et al*. (1987). Fat body membrane fraction was prepared according to the method of Kirankumar *et al*. (1997). Malpighian tubule and salivary gland protein homogenates were also prepared as described in part 2.

2.7. Western blotting

The midgut BBMV, fat body membrane, Malpighian tubule and salivary gland protein preparations were resolved by 7.5% SDS-PAGE and electro-blotted to nitrocellulose membranes using trans-blot apparatus (Bio-Rad) according to the procedure of Towbin *et al*. (1979). The blots were processed with 5% skimmed-milk powder (w/v) in Tris buffered-saline (10mM Tris-HCl, pH 7.4, 150mM NaCl) supplemented with 0.1% Tween-20 (TBST) for 1 h at room temperature to block the non-specific binding sites. The blots were incubated with *A. janata* midgut-specific APN polyclonal antibody (1:8000 dilutions) (Budatha *et al*. 2007a) and *A. janata* fat body-specific APN polyclonal antibody (1:10000 dilutions) (Budatha *et al*. 2007a) in TBST containing 5% milk powder (w/v) for overnight for detection of midgut-specific APN and visceral tissue-specific APN, respectively. The antibodies bound to APN proteins were detected using ALP-conjugated goat anti-rabbit IgG and the specific cross-reactivity was visualized with ALP substrate, NBT-BCIP (Sigma Aldrich, USA).

2.8. APN enzyme activity assay

APN enzyme activity assay was performed as primarily described by Garczynski and Adang (1995). The detailed procedure has been described in "Materials and methods" section of part 2. The molar absorbance co-efficient of *p*-nitroanilide was taken as 9.9×10^{-3} mol/L (Malik and Riazuddin, 2001) for calculation. The specific activity was expressed as µmol of *p*-nitroanilide released/min/mg of proteins.

2.9. Statistical analysis

Data are expressed as mean ± standard deviation of three independent experiments (n=3). Differences between groups were analyzed for statistical significance by One-Way ANOVA followed by Students-Newman-Keuls (SNK) test using SigmaPlot 11.0 software. A probability of $p > 0.05$ is considered statistically significant.

3. Results

3.1. Developmental expression of AjAPN4 and AjAPN1

Semi-quantitative (Fig. 1A) and real-time quantitative (Fig. 1B) PCR analyses detected a relatively high *AjAPN*4 transcript level in the gut of all the larval stages studied. The transcript level increased gradually from third larval instar to fifth larval instar and then decreased in pre-pupal stage. Western blot results (Fig. 1C) corroborated well at protein level. Further the APN enzyme activity profile (Fig. 1D) also matched with protein profile, showing a gradual increase in activity during larval development from third to fifth larval instar. The activity decreased significantly in pre-pupal stage.

In fat body, the expression of *AjAPN*1 mRNA was fairly low when compared with other tissues like Malpighian tubule and salivary gland. Results presented in figures 1A and 1B clearly showed slow but gradual increase in the transcript level from third to fifth larval instar which then decreased at pre-pupal stage. Fat body tissue undergoes remodeling during pupal-adult transformation. Analysis of *AjAPN*1 expression during pupal stage detected low *AjAPN*1transcript level, which however peaked up and increased to a moderate level in adult. Western blot (Fig. 1C) and APN enzyme activity (Fig. 1D) analyses further revealed similar pattern both at protein content as well as enzyme activity levels. The APN protein content in fat body during pupal stage was undetectable (Fig. 1C), but very low activity was detected (Fig. 1D). The protein content as well as enzyme activity when detected in adult fat body was quite low as compared to the larval stages (Figs. 1C & 1D).

The *AjAPN*1 transcript profiling in Malpighian tubule revealed that the expression of *AjAPN*1 was much higher in this tissue when compared to fat body and salivary gland. The mRNA, protein and enzyme activity of AjAPN1 in Malpighian tubule increased gradually from third larval instar to fifth larval instar; maximum expression being detected at the fifth instar (Figs. 1A, 1B, 1C, 1D), remained more or less the same throughout the fifth instar and then declined significantly in pre-pupal stage.

In salivary gland, AjAPN1 protein expression and enzyme activity profiles during larval development (Figs. 1C & 1D) were similar to the corresponding transcript expression profile (Figs. 1A & 1B). However, AjAPN1 protein and enzyme activity levels were extremely low in this tissue when compared to fat body and Malpighian tubule. Lower panels in all the semi-quantitative gels and western blots represent β-actin, which was used as internal control.

APN enzyme activity analysis of the larval hemolymph revealed a fairly low enzyme activity in the early larval instars (Fig. D). However there was a 3.5-fold increase from fourth to fifth larval instar and further 2.5-fold increase from fifth larval instar to pre-pupa, reaching its highest at this stage. At pre-pupal stage, the APN enzyme activity levels in hemolymph, fat body and Malpighian tubule are comparable. The activity of the enzyme was expressed as µmol of *p*-nitroanilide released/min/mg of protein. Thus, we found quite a reverse developmental activity profile in hemolymph from the ones observed in the other APN expressing tissues (Fig. 1D).

A)

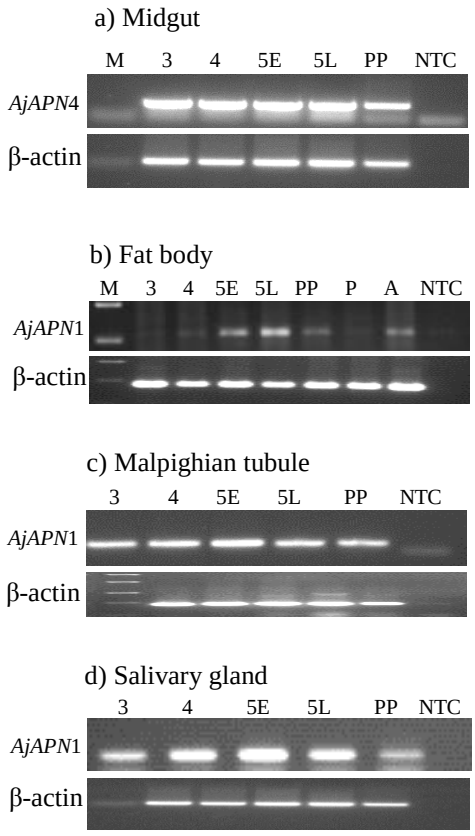
a) Midgut
M 3 4 5E 5L PP NTC
AjAPN4
β-actin
b) Fat body
M 3 4 5E 5L PP P A NTC
AjAPN1
β-actin
c) Malpighian tubule
3 4 5E 5L PP NTC
AjAPN1
β-actin
d) Salivary gland
3 4 5E 5L PP NTC
AjAPN1
β-actin

B)

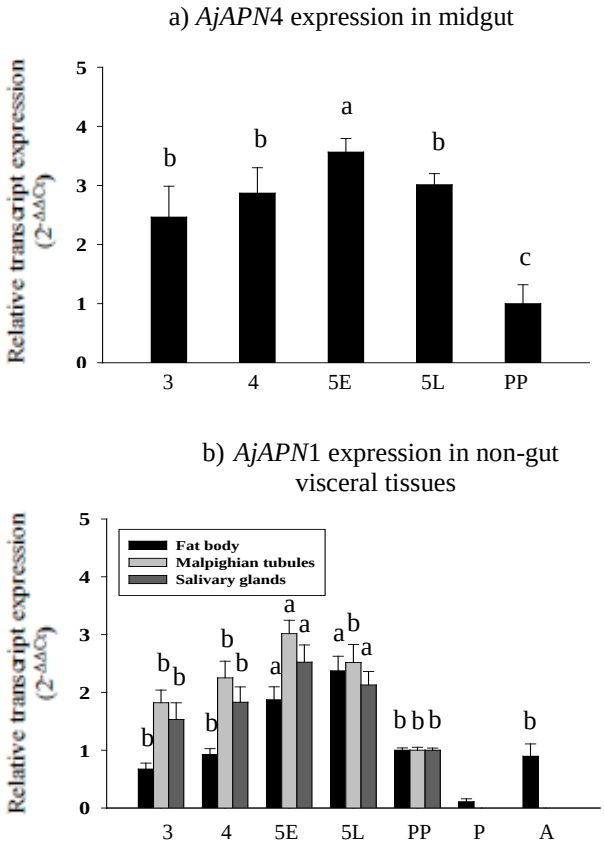
a) AjAPN4 expression in midgut
Relative transcript expression (2-ΔΔCt)
0 1 2 3 4 5
b b a b c
3 4 5E 5L PP
b) AjAPN1 expression in non-gut visceral tissues
Fat body
Malpighian tubules
Salivary glands
Relative transcript expression (2-ΔΔCt)
0 1 2 3 4 5
b b b b b a a a a b a b b b b
3 4 5E 5L PP P A

C)

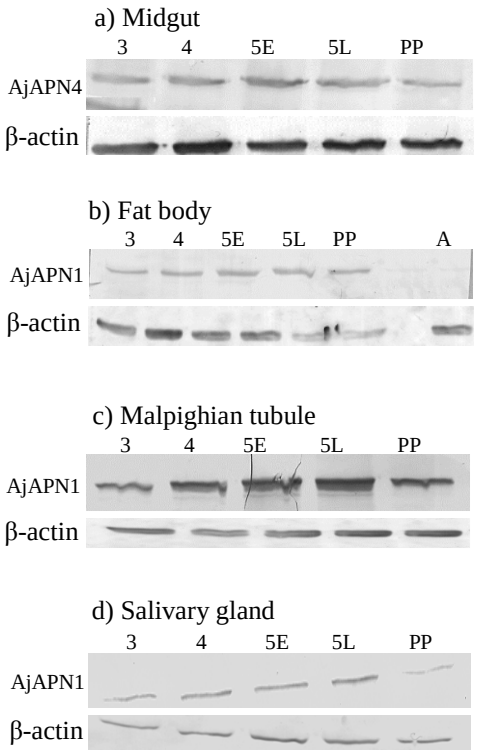

D)

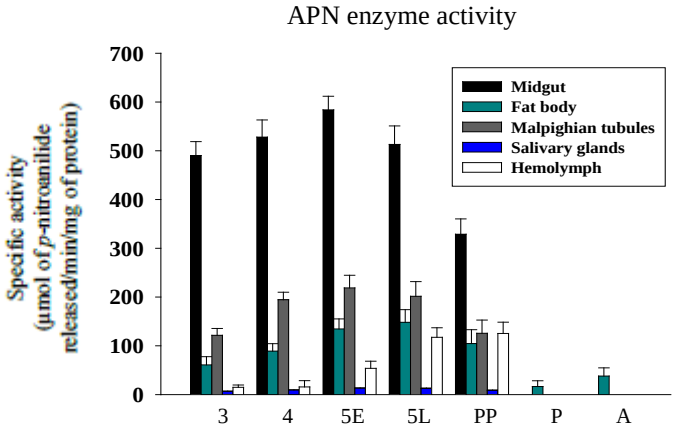

Fig. 1. **Developmental changes of *AjAPN*4 and *AjAPN*1 expression in *A. janata*. A)** Semi-quantitative PCR analysis. β-actin was used as an internal endogenous control. **B)** Real-time quantitative PCR analysis. Tissues from four larvae of every developmental stage were pooled together for each sample. The values represent mean ± standard deviation of three independent experiments. Statistical significance between the developmental stages was tested by performing One-Way ANOVA followed by SNK test using SigmaPlot 11.0 software. Means designated with different letters indicate statistical significance ($P<0.05$). 18sRNA was used as an internal endogenous control. Changes in *AjAPN*4 and *AjAPN*1 expression throughout the

larval developmental stages are shown relative to pre-pupal stage. **C)** Western blot analysis of APN expression in gut, fat body, Maplighian tubule and salivary gland (upper panels). β-actin represents endogenous control (lower panels). **D)** APN enzyme activity analysis of midgut BBMVs, fat body membrane, Malpighian tubule and salivary gland protein homogenates, and hemolymph. 3-third instar, 4-fourth instar, 5E-early fifth instar, 5L-late fifth instar and PP-pre-pupa, P-pupa and A-adult.

3.2. Hormonal regulation of *AjAPN*4 and *AjAPN*1 expression

Semi-quantitative and real-time quantitative PCR methods were employed to analyze the effect of 20E and methoprene (a JH analog) on *AjAPN*4 and *AjAPN*1 gene expression. For this experiment, fifth instar larvae were thorax-ligated (Fig. 2A) and maintained for 24 h before use, which was primarily to deplete endogenous hormones including ecdysteroids. Injection of 20E to the 24 h post thorax-ligated larvae (Fig. 2B) down-regulated *AjAPN*4 gene expression in gut (Figs. 3A & 3B) and *AjAPN*1 gene expression in fat body (Figs. 4A & 4B), Malpighian tubule (Figs. 5A & 5B) and salivary gland (Figs. 6A & 6B) in a dose-dependent manner. Significant reduction in the *AjAPN*4 transcript level in gut was observed only with higher doses of 5 and 10 µg with a minimum exposure time of 24 h (Figs. 3A & 3B). Injection dose of 0.1 µg/larvae did not alter the transcript levels of *AjAPN*4 in gut (Figs. 3A & 3B) and *AjAPN*1 in fat body (Figs. 4A & 4B) and Malpighian tubule (Figs. 5A & 5B). However in salivary gland (Figs. 6A & 6B), after 48 h post-injection, we observed significant effect even at this concentration. This study shows that 20E doses of 1, 5 and 10 µg/larvae were able to significantly suppress the expression of *AjAPN*1 after 24 h. Furthermore, none of the 20E concentrations tested altered the transcript levels at 5 h post-injection. The transcript levels in all the tissues decline gradually with the increase in exposure time to hormone and highest suppression was seen at 48 h post-injection. Thus, the effect of 20E on *AjAPN*1 expression appeared to be dose and time-dependent. Among the *AjAPN*1 expressing tissues, *AjAPN*1 expression level in fat body was most affected by 20E treatment (Figs. 4A & 4B).

Topical application of methoprene to 24 h post thorax-ligated larvae displayed an inductive effect on the transcript levels of *AjAPN*4 in gut (Figs. 7A & 7B) and *AjAPN*1 in fat body (Figs. 8A & 8B), Malpighian tubule (Figs. 9A & 9B) and salivary gland (Figs. 10A & 10B). The transcript levels of both the isoforms were enhanced at a dose as low as 0.1 µg/ larva. The effect was observed to be dose-dependent with higher doses of 1, 5 and 10 µg up-regulating the transcript levels significantly. The effect of the treatment appears

to differ from tissue to tissue. In gut and Malpighian tubule, none of the doses were able to significantly up-regulate expression at 12 h post-treatment. On the other hand, in fat body and salivary gland, 10 µg dose up-regulated expression at 12 h post-treatment. Further, we observed that the enhancing effect of methoprene on *AjAPN*1expression did not increase at doses higher than 5 µg. We further observed that *AjAPN*1 was more responsive to methoprene treatment than *AjAPN*4 gene expression. Figure 2A depicts the method used for ligation of larvae to deplete the endogenous hormone titer (including JH).

To determine the combined effect of 20E and methoprene on transcript levels, each of the larvae were first injected with 5 µg of 20E which were then topically applied with 5 µg of methoprene after 5 h (Figs. 11A & 11B). The larvae which were injected with 5 µg of 20E alone showed significant down-regulation of *AjAPN*4 transcripts in gut 24 h post hormone treatment. Similarly, we also observed a significant down-regulation of *AjAPN*1 transcripts in fat body, Malpighian tubule and salivary gland after 24 h of 20E treatment. Methoprene has an opposite effect on *AjAPN*4 and *AjAPN*1 expression. These results matched well with the results obtained in previous sections. Larvae which were topically applied with 5 µg of methoprene alone resulted in significant up-regulation of *AjAPN*4 expression (1.6-fold increase) in gut, and *AjAPN*1 expression in fat body (1.7-fold increase), Malpighian tubule (2.3-fold increase) and salivary gland (2.3-fold increase) after 24 h of hormone treatment. However, topical application of methoprene (5µg/larvae) to the 20E injected larvae (5µg/larvae) resulted in significant inhibition of 20E-supressed *AjAPN*4 expression (30%) in gut and *AjAPN*1 expression in fat body (40%), Malpighian tubule (35%) as well as salivary gland (30%). Thus, methoprene antagonized the effect of 20E on *AjAPN*4 and *AjAPN*1 expression. This data clearly suggests that these morphogenetic hormones (20E+JH) most likely counteract the effect of each other while regulating the expression of the two APN isoforms during post-embryonic development of *A. janata.*

A)

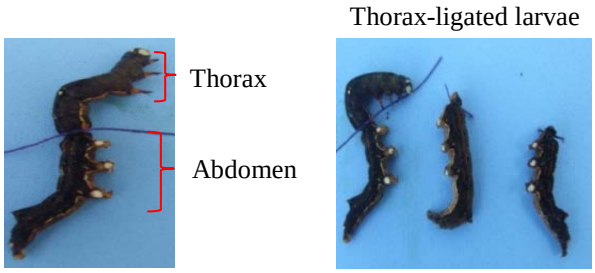

B)

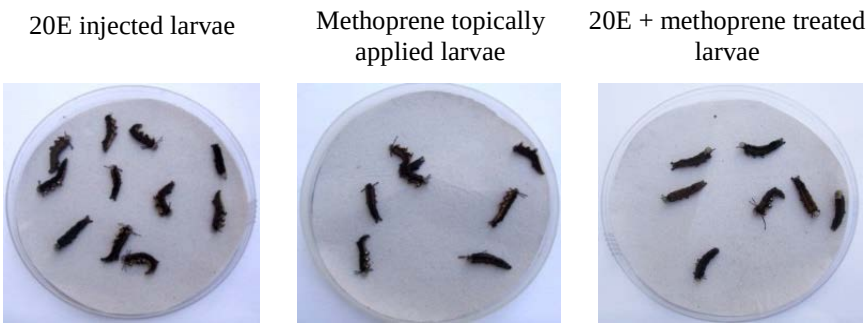

Fig. 2. **Thorax-ligation and hormone treatment**. **A)** Thorax-ligation of larvae. Ligation was done by tightly tying a silk thread behind the thorax region. The tissues anterior to ligature were cut with sterile scissor and the wound was dressed with traces of antibiotic mixture and sealed with bees wax. These ligatures were kept for 24 h on petridishes containing moistened filter paper to maintain humidity and to prevent desiccation. **B)** Hormone treated larvae. The first group of isolated abdomens/ligatures were injected with 20E; the second group of larvae were topically applied with methoprene and the third group of ligated larvae were first injected with 20E followed by methoprene treatment.

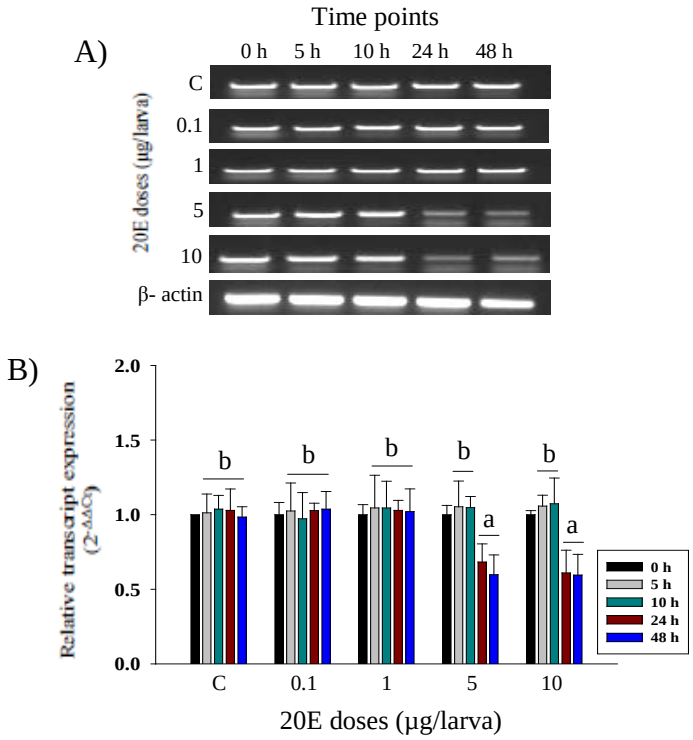

Fig. 3. **Effect of 20E on *AjAPN*4 expression in gut of fifth instar larvae**. Tissues isolated from four ligated larvae were pooled together for each sample. Transcript expression was analyzed at 5 h, 10 h, 24 h and 48 h post-injection of 20E at concentrations of 0.1, 1, 5 and 10 µg/larva. The control larvae were injected with equal volumes of the carrier solvent. **A)** Semi-quantitative RT-PCR. β-actin was used as an internal endogenous control. **B)** Real-time quantitative RT-PCR. 18sRNA was used as an internal endogenous control. *AjAPN*4 expression is demonstrated as fold change relative to 0 h of the control. The values represent mean ± standard deviation of three independent experiments. Significance between groups was tested by One-Way ANOVA followed by SNK test using SigmaPlot 11.0 software. Means designated with different letters indicate statistical significance ($P<0.05$).

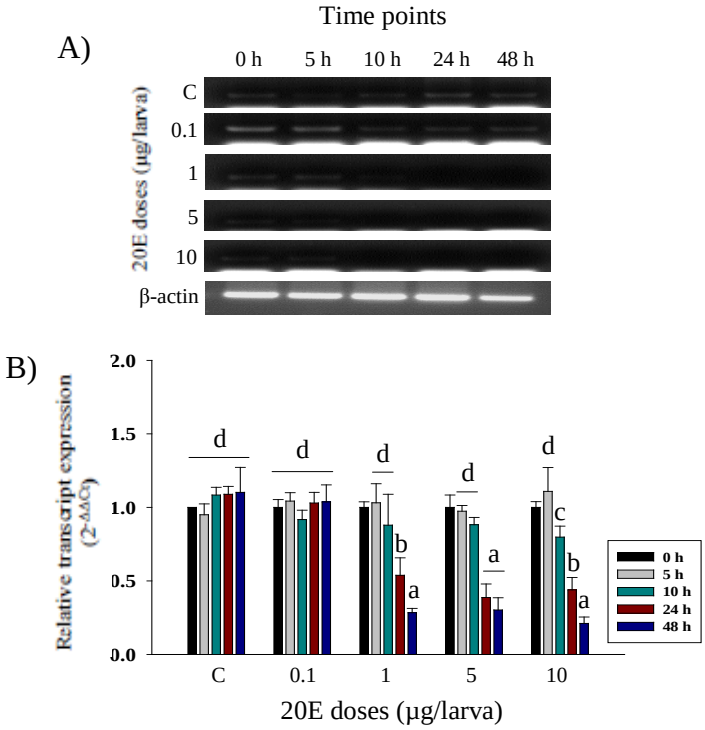

Fig. 4. **Effect of 20E on *AjAPN*1 expression in fat body of fifth instar larvae**. Tissues isolated from four ligated larvae were pooled together for each sample. Transcript expression was analyzed at 5 h, 10 h, 24 h and 48 h post-injection of 20E at concentrations of 0.1, 1, 5 and 10 µg/larva. The control larvae were injected with equal volumes of the carrier solvent. **A)** Semi-quantitative RT-PCR. β-actin was used as an internal endogenous control. **B)** Real-time quantitative RT-PCR. 18sRNA was used as an internal endogenous control. *AjAPN*1 expression is demonstrated as fold change relative to 0 h of the control. The values represent mean ± standard deviation of three independent experiments. Significance between groups was tested by One-Way ANOVA followed by SNK test using SigmaPlot 11.0 software. Means designated with different letters indicate statistical significance ($P<0.05$).

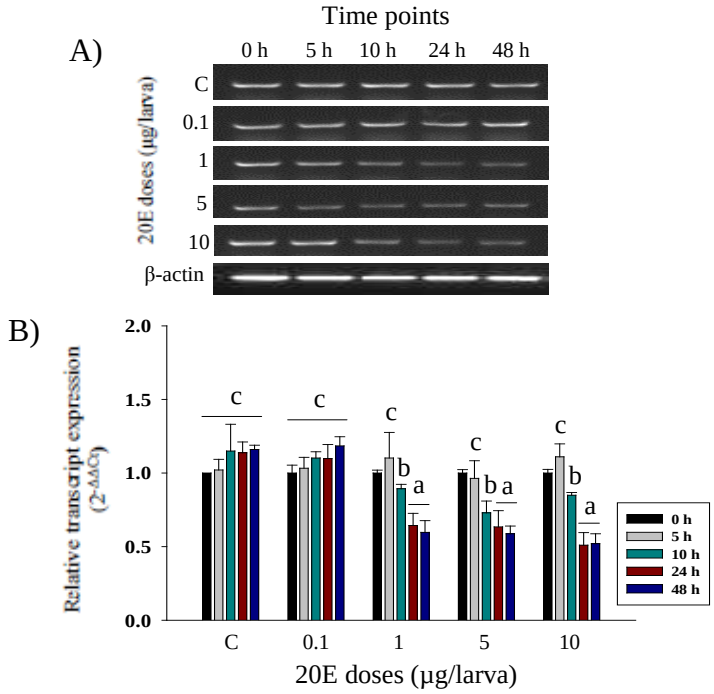

Fig. 5. **Effect of 20E on *AjAPN*1 expression in Malpighian tubule of fifth instar larvae**. Tissues isolated from four ligated larvae were pooled together for each sample. Transcript expression was analyzed at 5 h, 10 h, 24 h and 48 h post-injection of 20E at concentrations of 0.1, 1, 5 and 10 µg/larva. The control larvae were injected with equal volumes of the carrier solvent. **A)** Semi-quantitative RT-PCR. β-actin was used as an internal endogenous control. **B)** Real-time quantitative RT-PCR. 18sRNA was used as an internal endogenous control. *AjAPN*1 expression is demonstrated as fold change relative to 0 h of the control. The values represent mean ± standard deviation of three independent experiments. Significance between groups was tested by One-Way ANOVA followed by SNK test using SigmaPlot 11.0 software. Means designated with different letters indicate statistical significance ($P<0.05$).

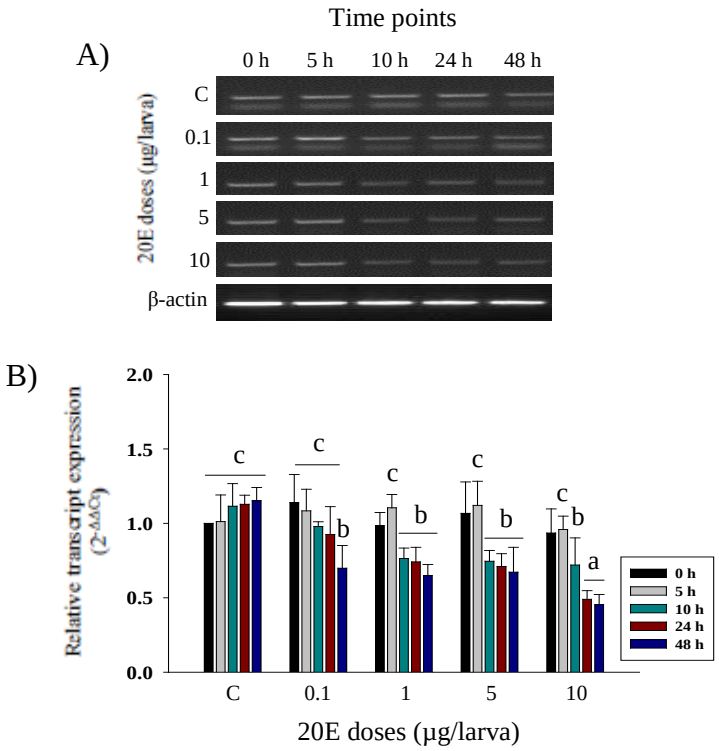

Fig. 6. **Effect of 20E on *AjAPN*1 expression in salivary gland of fifth instar larvae**. Tissues isolated from four ligated larvae were pooled for each sample. Transcript expression was analyzed at 5 h, 10 h, 24 h and 48 h post-injection of 20E at concentrations of 0.1, 1, 5 and 10 µg/larva. The control larvae were injected with equal volumes of the carrier solvent. **A)** Semi-quantitative RT-PCR. β-actin was used as an internal endogenous control. **B)** Real-time quantitative RT-PCR. 18sRNA was used as an internal endogenous control. *AjAPN*1 expression is demonstrated as fold change relative to 0 h of the control. The values represent mean ± standard deviation of three independent experiments. Significance between groups was tested by One-Way ANOVA followed by SNK test using Sigma Plot 11.0 software. Means designated with different letters indicate statistical significance ($P<0.05$).

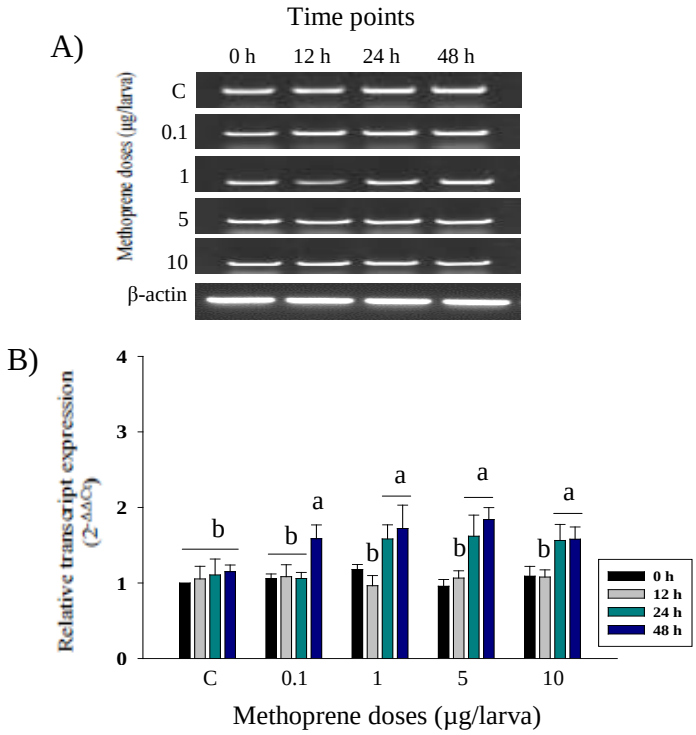

Fig. 7. **Effect of methoprene on *AjAPN*4 expression in gut of fifth instar larvae**. Tissues isolated from four ligated larvae were pooled for each sample. Transcript expression was analyzed at 12 h, 24 h and 48 h post-topical application of methoprene at concentrations of 0.1, 1, 5 and 10 µg/larva. The control larvae were topically applied with equal volumes of the carrier solvent. **A)** Semi-quantitative RT-PCR. β-actin was used as an internal endogenous control. **B)** Real-time quantitative RT-PCR. 18sRNA was used as an internal endogenous control. *AjAPN*4 expression is demonstrated as fold change relative to 0 h of the control. The values represent mean ± standard deviation of three independent experiments. Significance between groups was tested by One-Way ANOVA followed by SNK test using SigmaPlot 11.0 software. Means designated with different letters indicate statistical significance ($P<0.05$).

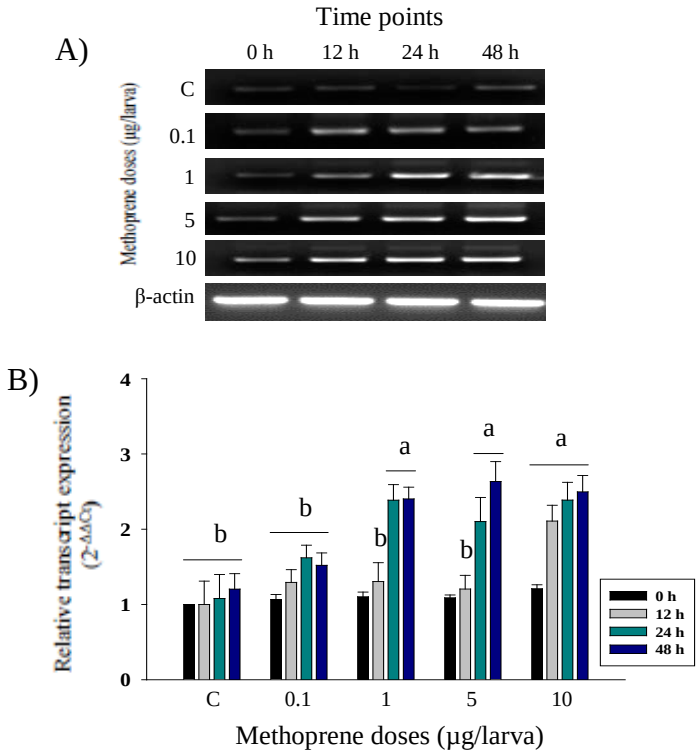

Fig. 8. **Effect of methoprene on *AjAPN*1 expression in fat body of fifth instar larvae**. Tissues isolated from four ligated larvae were pooled for each sample. Transcript expression was analyzed at 12 h, 24 h and 48 h post-topical application of methoprene at concentrations of 0.1, 1, 5 and 10 µg/larva. The control larvae were topically applied with equal volumes of the carrier solvent. **A)** Semi-quantitative RT-PCR. β-actin was used as an internal endogenous control. **B)** Real-time quantitative RT-PCR. 18sRNA was used as an internal endogenous control. *AjAPN*1 expression is demonstrated as fold change relative to 0 h of the control. The values represent mean ± standard deviation of three independent experiments. Significance between groups was tested by One-Way ANOVA followed by SNK test using SigmaPlot 11.0 software. Means designated with different letters indicate statistical significance ($P<0.05$).

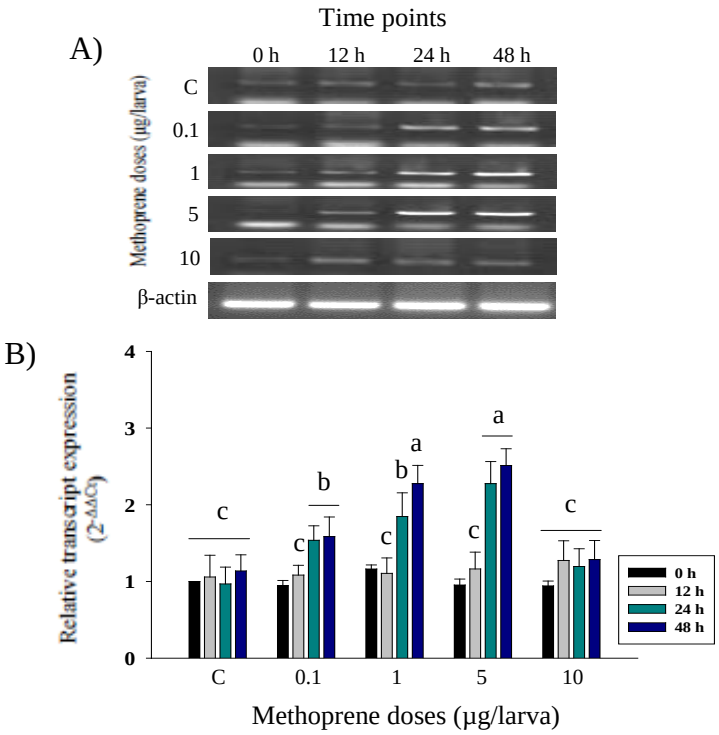

Fig. 9. **Effect of methoprene on *AjAPN*1 expression in Malpighian tubule of fifth instar larvae**. Tissues isolated from four ligated larvae were pooled for each sample. Transcript expression was analyzed at 12 h, 24 h and 48 h post-topical application of methoprene at concentrations of 0.1, 1, 5 and 10 µg/larva. The control larvae were topically applied with equal volumes of the carrier solvent. **A)** Semi-quantitative RT-PCR. β-actin was used as an internal endogenous control. **B)** Real-time quantitative RT-PCR. 18sRNA was used as an internal endogenous control. *AjAPN*1 expression is demonstrated as fold change relative to 0 h of the control. The values represent mean ± standard deviation of three independent experiments. Significance between groups was tested by One-Way ANOVA followed by SNK test using SigmaPlot 11.0 software. Means designated with different letters indicate statistical significance ($P<0.05$).

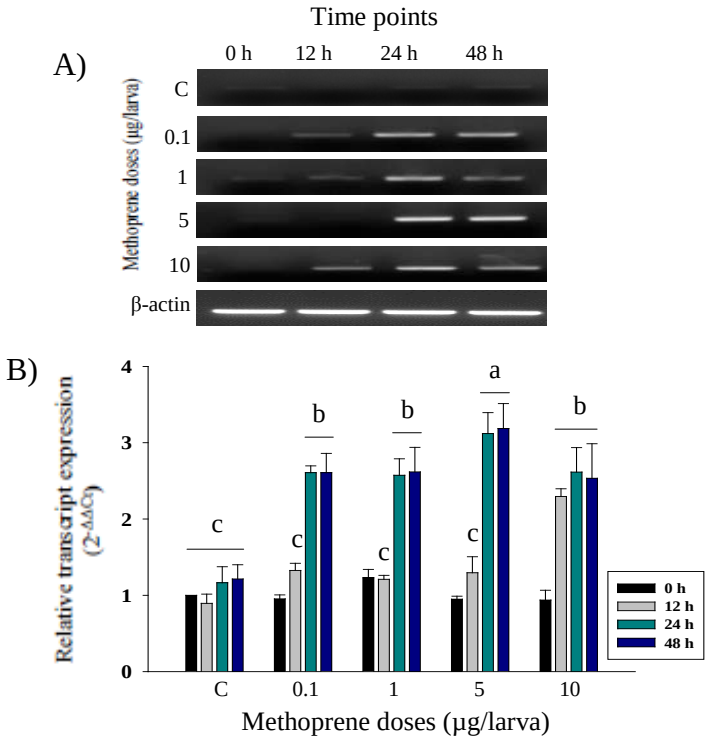

Fig. 10. **Effect of methoprene on *AjAPN*1 expression in salivary gland of fifth instar larvae**. Tissues isolated from four ligated larvae were pooled for each sample. Transcript expression was analyzed at 12 h, 24 h and 48 h post-topical application of methoprene at concentrations of 0.1, 1, 5 and 10 µg/larva. The control larvae were topically applied with equal volumes of the carrier solvent. **A)** Semi-quantitative RT-PCR. β-actin was used as an internal endogenous control. **B)** Real-time quantitative RT-PCR. 18sRNA was used as an internal endogenous control. *AjAPN*1 expression is demonstrated as fold change relative to 0 h of the control. The values represent mean ± standard deviation of three independent experiments. Significance between groups was tested by One-Way ANOVA followed by SNK test using SigmaPlot 11.0 software. Means designated with different letters indicate statistical significance ($P<0.05$).

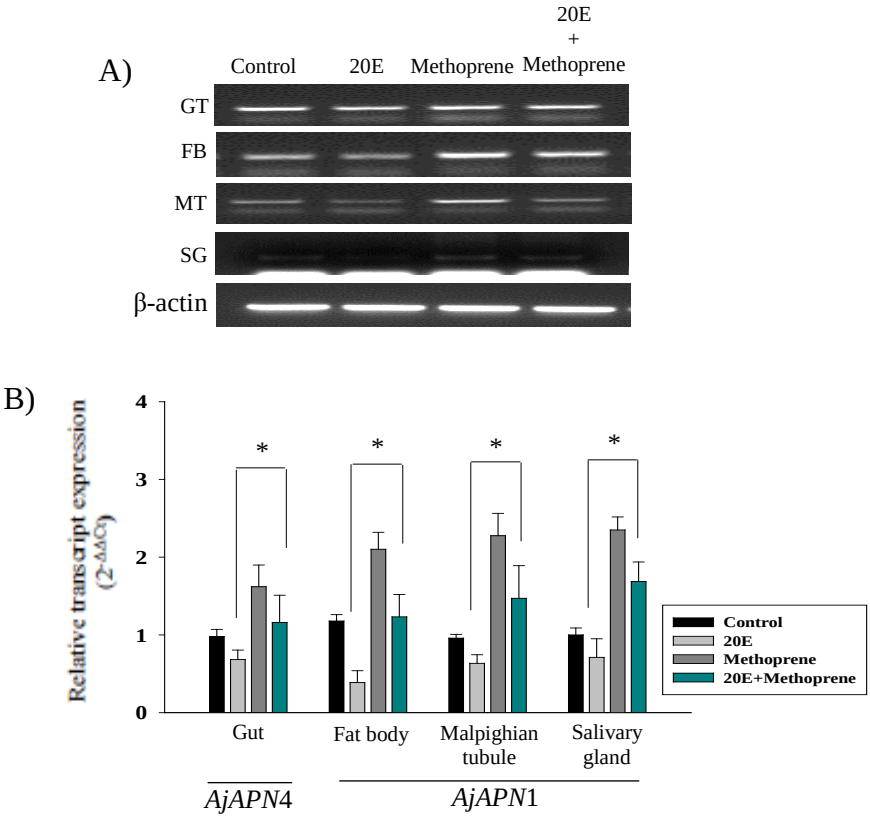

Fig. 11. **Regulation of *AjAPN*4 and *AjAPN*1 expression in *A. janata* by 20E and JH**. For this experiment, ligated fifth instar larvae were initially injected with 5 µg of 20E followed by topical application of 5 µg of methoprene after 5 h and transcript expression analysed after 24 h. **A)** Semi-quantitative PCR analysis. β-actin was used as an internal endogenous control. **B)** Real-time quantitative RT-PCR analysis. Tissues from four larvae were pooled together for each sample. Mean ± standard deviation of three independent experiments is represented. Statistical significance between treatment groups was tested by performing One-Way ANOVA followed by SNK test using SigmaPlot 11.0 software. Means designated with different letters indicate statistical significance ($P<0.05$). 18sRNA was used as an internal endogenous control. *AjAPN*4 and *AjAPN*1 expression are demonstrated as fold change relative to 0 h of the control. GT-gut, FB-fat body, MT-Malipighian tubule and SG-Salivary gland.

4. Discussion

In the present study, we investigated the developmental and hormonal regulation of *AjAPN*4 and *AjAPN*1 expression in *A. janata*. Using gene specific primers for *AjAPN*4 and *AjAPN*1, the expression of the two isoforms was found to be tissue-specific. *AjAPN*4 was specifically expressed only in gut while *AjAPN*1 was predominantly expressed in the visceral tissues like fat body, Malpighian tubule and salivary gland. This tissue-specific distribution of the two isoforms of APN may be indicative of their specific physiological roles in these tissues. The major role played by midgut APNs is digestion of dietary proteins (Terra and Ferreira, 1994). We found that in *A. janata*, *AjAPN*4 transcript expression in gut was relatively high throughout its larval stages, which was similarly demonstrated by high protein expression and its enzyme activity at these stages. Its expression gradually increased from third to fifth larval instar which are actively feeding stages and then decreased in pre-pupa, which is a non-feeding stage. This high activity throughout the larval stages may imply its important physiological role in the intermediary digestion of proteins during the feeding stages. In insects, aminopeptidases are usually known to be more active than carboxypeptidases (Terra and Ferreira, 1994). This high expression of APNs in larval gut of *A. janata* further substantiates its high susceptibility to Cry1Aa, Cry1Ab, Cry1Ac and DOR5 Cry toxins seen in toxin feeding assays (data shown in part 1), as APNs are well reported Cry toxin receptors. We have demonstrated the binding of these toxins to the ~120 kDa APN of *A. janata* midgut BBMV (data presented in part 2). Thus in *A. janata* midgut, AjAPN4 might assume a dual role of a digestive enzyme as well as a Cry toxin receptor.

APNs are known to perform multiple physiological activities but majority of reports are related to midgut APNs. Wang *et al*. (2005) reported the presence of APN in Malpighian tubule of *Trichoplusia ni*. However, they did not show its expression in other visceral tissues like the fat body, salivary gland and body carcass. From our laboratory, Budatha *et al*. (2007) reported the presence of a novel form of APN in the larval fat body of *A. janata*. In the present study, we found that this isoform of APN is also expressed in Malpighian tubule and salivary gland of *A. janata*. In fat body, maximum transcript level was detected during fifth larval instar. APN protein and enzyme activity analyses also showed highest expression during this stage. The specific activity (µmol of *p*-nitroanilide released/min/mg of protein) of APN found in the fat body of fifth instar larvae was about 35% of the activity detected in the midgut of the same stage. Fat body performs a myriad of developmentally specific metabolic activities that produce, store or release components

central to the prevailing nutritional requirements and/or metamorphic events of the insect (Price, 1973; Wyatt, 1974; Burmester and Scheller, 1999). The role of fat body might also change as the insect progresses through development and is involved in homeostatic maintenance of hemolymph proteins, lipids and carbohydrates (Haunerland and Shirk, 1995). Fat body is known to be functionally most active during the late larval stages, in this case in *A. janata*, from fourth larval instar to pre-pupal stage where the expression of *AjAPN*1 transcript and APN protein as well as enzyme activity levels were observed to be high. As larval fat body is known to be analogous in function to the vertebrate liver and is an essential organ for protein metabolism and storage, the expression of AjAPN1 in fat body and most importantly during these late larval stages indicate a significant physiological role in fat body. AjAPN1, along with other proteases present in the fat body of *A. janata* might also be involved in the catabolism of larval storage proteins like hexamerins. Storage proteins, predominantly the hexamerins are sequestered by the fat body cells at the onset of metamorphosis (Burmester and Scheller, 1997; Kiran Kumar *et al*. 1997). The GPI-anchored APNs present on the membrane of fat body cells may also be involved in the uptake of hexamerins by fat body (Budatha *et al*. 2011). Interestingly, AjAPN1 expression which was absent at pupal stage was found to reappear again in adult; however the exact role of which need to be elucidated. However though, in adult females, the fat body is known to convert pre-vitellogenins to vitellogenins which are well known yolk polypeptides secreted into the hemolymph (Haunerland and Shirk, 1995).

Using semi-quantitative and real-time quantitative PCR analyses, we found that the *AjAPN*1 transcript level in Malpighian tubule gradually increased from third to early fifth larval instar which then decreased during late fifth larval instar and becomes fairly low at pre-pupal stage. Immunoblot and APN enzyme activity analyses also revealed similar pattern. The specific activity (µmol of *p*-nitroanilide released/min/mg of protein) of the enzyme in Malpighian tubule of the fifth instar, the larval stage at which highest activity was detected and it was about 47% of the activity seen in the midgut of the same stage. The enzyme activity in Malpighian tubule seen in *A. janata* is very high when compared with that of reported for *Trichoplusia ni* (Wang *et al.* 2005) where it is only about 8% of that found in the midgut. Since Malpighian tubule is the major excretory organ of the larval forms, the function of the APNs in these organs is not clear at the moment. However, in higher animals including mammals, the primary source of APNs is the gastrointestinal tract and the kidney. Mammalian APNs are known to play important

functions in the kidney (Vlahovic and Stefanovic, 1998). In the kidney, APNs were shown to be localized on the brush border membranes of the proximal tubules which are functionally analogous to the individual Malpighian tubule, and play a role in hydrolysis of small peptides in the glomerular filtrate (Noven *et al*. 1997). A GPI anchor as detected in the AjAPN1 deduced amino acid sequence by computational analysis and immunofluorescence localization of APN expression on the apical and basal membranes of epithelial cells of the tubules (data shown in part 2) also draw similarity with mammalian kidney. The developmental expression profile of AjAPN1 indicates its biochemical and functional importance in larval growth and development. However, further investigation is required to understand, whether they also play a similar kind of function as that of mammalian kidney APNs.

Developmental expression profile of AjAPN1 in salivary gland was similar to that of Malpighian tubule. Highest expression both at transcript and protein levels was seen during fifth larval instar. During this larval instar, the specific enzyme activity (µmol of *p*-nitroanilide released/min/mg of protein) of APN in salivary gland was found to be very low when compared with the activity levels in gut, fat body as well as Malpighian tubule and it is only about 13% of the activity seen in fifth instar larval gut. Salivary gland is a vital organ in insects, and in lepidopteran insects, the glands are commonly known as labial glands or silk glands. They get fairly enlarged as they synthesize and secrete silk for the formation of puparia/cocoon, a structure in which a holometabolan insect undergoes larval-pupal-adult metamorphosis. The silk glands (salivary gland) in lepidopteran larvae also produce variety of other proteins like protease inhibitors, antibacterial proteins along with silk proteins which have different types of functions. In a recent study in *Corcyra cephalonica*, our group demonstrated the sequestration and secretion of hexamerins from insect hemolymph to the salivary secretion (Manohar *et al*. 2010). In this study, we report the developmental regulation of AjAPN1 expression in salivary gland of *A. janata.*

The APN enzyme activity analysis of *A. janata* larval hemolymph revealed a fairly low enzyme activity during the early larval instars which then increased gradually from fourth to fifth larval instar and reached its highest during the late fifth larval instar and thereafter; it was more or less at the same level during pre-pupal stage. The presence of aminopeptidase-like activity in the larval hemolymph of *Lymantria dispar* has also been reported earlier (Masler *et al*. 1997). This observation tempt us to suggest that the APNs synthesized in the visceral tissues like fat body, Malpighian tubule and salivary

gland might be released into the hemolymph and possibly play a role during post-embryonic development especially during larval-pupal transformation and pupal-adult metamorphosis.

In order to study the hormonal regulation of *AjAPN*4 and *AjAPN*1 expression at mRNA level, thorax-ligated larvae were used. Thorax-ligation primarily blocks the supply of hormones from the prothoracic gland and corpora allata to the abdomen. Ashok and Dutta-Gupta (1988) have shown that endogenous circulating 20E and JH levels in lepidopteran larvae are completely abolished 24 h post thorax-ligation. As in previous section, we have seen that the APN expression is developmentally regulated, and development in holometabolous insects including lepidopteran insects is regulated by interplay between two morphogenetic hormones - JH and 20E (Riddiford, 1994, 2008). Here, we analyzed the effect of exogenous hormone/hormone analog treatment on the regulation of *A. janata* APNs. This is the first study on 20E and JH regulation of insect APNs.

In the present study, semi-quantitative and real-time quantitative PCR analyses showed that only high doses of 20E and a prolonged exposure time could suppress *AjAPN*4 expression in gut. However similar analyses revealed that a much lower dose of 20E could significantly down-regulate *AjAPN*1 transcript levels in fat body, Malpighian tubule and salivary gland. Fat body was more sensitive to 20E treatment when compared to other tissues. Ecdysteroids are known to regulate variety of genes in different tissues during post-embryonic development of lepidopteran insects (Hiruma, 2003). Earlier reports show down-regulation of salivary gland proteins in *D. melanogaster* (Crowley and Meyerowitz, 1984) as well as silk protein genes in *C. cephalonica* (Chaitanya and Dutta-Gupta, 2010; Chaitanya *et al*. 2011). This 20E effect was shown to be mediated by the presence of ecdysone nuclear receptors (EcR) (Yao *et al*. 1992; Riddiford *et al*. 2000; Elmogy *et al*. 2004; King-Jones and Thummel, 2005; Flatt *et al*. 2006; Sun and Song, 2006) or non-genomic actions not mediated by nuclear hormone receptor signaling (Elmogy *et al*. 2004; Srivastava *et al*. 2005). Although ecdysteroid hormone can bind to EcR on its own (Grebe *et al*. 2004), this binding is increased by the interaction of EcR with *ultraspiracle* gene product (USP) (Koelle *et al*. 1991; Yao *et al*. 1993), which is also a member of another nuclear receptor superfamily. Ecdysteroid binding to EcR/USP heterodimer increases the affinity of the heterocomplex to 20E-response elements (Koelle *et al*. 1991; Yao *et al*. 1993) and affect transcription of specific genes. However, the presence of 20E-response elements in *AjAPN*4 and *AjAPN*1 sequences has not been

established yet. Identification and analysis of ecdysone response elements in these genes could help understand the differential response of the two APN isoforms to 20E treatment.

Semi-quantitative and real-time quantitative PCR results following hormone treatment with increasing doses of methoprene showed an inducing effect on *AjAPN*4 and *AjAPN*1 expression at transcript level. We observed a significant dose-dependent increase in the *AjAPN*1 transcript level from 0.1 µg to 5 µg dose in all the *AjAPN*1 expression tissues. However, at 10 µg dose, we observed a decline in the transcript levels suggesting that this gene respond only to an optimum concentration of JH and the inhibition seen might be associated with receptor desensitization, a very common phenomenon seen with very high concentration of hormone during treatment. All the three *AjAPN*1 expressing visceral tissues appear to be quite sensitive to methoprene treatment unlike the gut, where induction of *AjAPN*4 expression was much less. The reason might be that the two APN isoforms respond differently to methoprene. It is interesting to note that irrespective of the doses given, significant response to methoprene treatment was observed only after 24 h. Our observation of high responsiveness of *AjAPN*4 and *AjAPN*1 in all the tissues to methoprene treatment indicates their expression to be more of larval-specific. Such a prominent effect is most likely mediated by JH nuclear receptors present in the cells of these tissues (Riddiford *et al*. 2001; Berger and Dubrovsky, 2005; Dubrovsky, 2005; King-Jones and Thummel, 2005; Flatt *et al*. 2006; Iwema *et al*. 2007). However till date, identity of JH receptors has still not been resolved properly. The action of JH via non-genomic pathways involving membrane receptors (rather than nuclear receptors) and protein kinase C (PKC) signaling have been demonstrated (Wheeler and Nijhout, 2003; Kethidi *et al*. 2006).

Post-embryonic development in insects involving larval molt, larval-pupal transformation and pupal-adult metamorphosis is regulated by a precise interplay between the titer of 20E and JH through the regulation of a cascade of stage-specific expression of different genes at transcriptional as well as translational levels (Riddiford *et al*. 1981; Riddiford, 1993; Nijhout, 1994; Dubrovsky, 2005, Truman and Riddiford, 2007) but not at replication level (Dyer *et al*. 1981). In the present study, we investigated the transcriptional regulation of *AjAPN*4 and *AjAPN*1 expression when both methoprene and 20E are present at the same time. Methoprene treatment to the 20E injected insects revealed the antagonistic effect of JH on 20E-suppressed *AjAPN*4 and *AjAPN*1 mRNA expression. Thus, methoprene and 20E could counteract each other. The counteractive

effect of methoprene and ecdysteroids has been reported in other insect genes like small heat shock protein gene expression (Berger *et al*. 1992). Similar kind of effect was also reported in *Aedes aegypti* where methoprene was found to block midgut remodeling by interfering with 20E action (Wu *et al*. 2006). During molting and pupation, when the levels of JH are low and 20E are high, many genes involved in energy metabolism are down-regulated (White *et al*. 1999; Beckstead *et al*. 2005; Tian *et al*. 2010) via EcR-USP (Beckstead *et al*. 2005). In *B. mori*, two-third of the genes which get down-regulated during the pre-pupal stage was involved in energy metabolism where 20E-trigerred molting and pupation tempered metabolic activity by affecting fat body (Tian *et al*. 2010). In our present study, developmental expression profiles of the two APN isoforms in all the tissues also demonstrated that their expression levels at transcript, protein and activity were high during the fifth larval instar but diminished significantly as the larvae enters pre-pupal stage. Besides, down-regulation of *AjAPN*4 and *AjAPN*1 expression by 20E in the absence of methoprene and up-regulation of *AjAPN*4 and *AjAPN*1 expression by methoprene in the absence of 20E is also indicative of their role in energy metabolism, especially in gut and fat body. These results demonstrated the contrast function of JH and 20E in *A. janata*. However, in *D. melanogaster*, a dipteran, APNs were shown to have activities during metamorphosis and were found to be inducible by 20E (Hall *et al*. 1988; Siviter *et al*. 2002), but in *A. janata*, APN enzyme activity in these tissues was found to be low during pre-pupal stage, which normally have a very high titer of ecdysteroids (Sakurai *et al*. 1998) as well as APN gene expression was inhibited by 20E.

Hence, we suggest *AjAPN*4 and *AjAPN*1 as larval genes predominantly expressed during larval instars and are regulated by JH, while during larval-pupal transformation, these genes are inhibited by ecdysone. The expression of these two isoforms might possibly have some biochemical and physiological role in these tissues/organs and contribute to overall growth, development and metamorphosis of lepidopteran insects.

Part 4

Functional elucidation of *AjAPN*1 expression in visceral tissues of *A. janata*

1. Introduction

Insect midgut aminopeptidases play an important physiological role in the intermediary digestion of dietary proteins (Terra and Ferreira, 1994). Disruption of the function of midgut aminopeptidases was proposed to induce a detrimental effect on larval growth and development, leading to larval death (Reed *et al*. 1999). Insect digestive aminopeptidases belong to the aminopeptidase N (APN) class of metalloproteases M1 type (Adang, 2004). The APNs are Zn^{++} dependent (Hooper, 1994) and located on the brush border membranes of the insect gut epithelial cells, where they are attached to the membrane through a GPI anchor (Garczynski and Adang, 1995; Albiston *et al*. 2004). During the digestion process, they cleave almost all types of amino acid residues from the N-terminus of oligopeptides, preferentially the neutral amino acids. However, besides their role in dietary protein digestion, they have been reported to act as Cry toxin receptors and the binding of which, is known to induce toxic effects to the feeding insects (Knight *et al*. 1994; Bravo *et al*. 2007). Upon ingestion by the larval forms of the susceptible insects, they are solubilized in the alkaline medium of the gut and processed by the gut proteases to yield the active toxins (Hofte and Whiteley, 1989; Gill *et al*. 1992). The active toxins then bind to the specific receptors located on the brush-border membranes of the midgut epithelial cells, resulting in cell lysis and causing death of the insects (Ferre and Van Rie, 2002). Midgut APNs have been identified as Cry1A receptors in a number of lepidopteran insects including *Manduca sexta* (Knight *et al*. 1994), *Bombyx mori* (Yaoi *et al*. 1997), *Heliothis virescens* (Gill *et al*. 1995), *Lymantria dispar* (Valaitis *et al*. 1995) and *Plutella xylostella* (Luo *et al*. 1997). The presence of APN in non-gut tissues like Malpighian tubule of *Trichoplusia ni* (Wang *et al*. 2005) and fat body of *A. janata* (Budatha *et al*. 2007a) and *S. litura* (Budatha *et al*. 2007b) have been reported. In previous section of our study (part 2), we have cloned and characterized full-length cDNA sequences of APNs from Malpighian tubule and salivary gland of *A. janata.* Amino acid sequence analysis and comparison confirmed the APNs of fat body, Malpighian tubule and salivary gland as being the same gene in this species which we have designated as *AjAPN*1. The insect fat body is an organ analogous to the vertebrate adipose tissue and liver, and it functions as a major organ for nutrient storage and energy metabolism (Haunerland and Shirk, 1995; Burmester and Scheller, 1999). They also participate in other physiological functions such as innate immunity and detoxification (Haunerland and Shirk, 1995). Pioneering studies in the fruitly *D. melanogaster* have demonstrated that fat body which is regulated by several hormonal and nutritional signals

to be the central organ for insect development and metamorphosis (Shingleton, 2005; King-Jones and Thummel, 2005). Besides, in the insect hemocoel, there are also other organs like Malpighian tubule, salivary gland, ovary and testis which play different important functions during post-embryonic development and adult reproduction. Till date, the role of APNs in these tissues has not been elucidated in any insects.

Cheon *et al*. (1997) demonstrated the pore forming ability of Cry toxins on *in vitro* cultured fat body cells, which suggested the possibility of Cry toxin binding to the fat body membrane proteins and causing toxic effects to the cells. Transgenic expression of *M. sexta* APN in *D. melanogaster* induced sensitivity to the lepidopteran-specific insecticidal Cry1Ac which otherwise is not toxic (Gill and Ellar, 2002). Similarly, Sivakumar *et al*. (2007) also demonstrated that Sf21 insect cells expressing *H. armigera* APN which were sensitive to Cry1Ac, upon down-regulation by RNA interference (RNAi) using double-stranded RNA resulted in reduced sensitivity to Cry1Ac. These studies suggest the possibility of Cry toxins causing insecticidal effects in the tissues where APNs are expressed. Using *in vitro* ligand blot and immunoprecipitation analyses (part 2), we demonstrated the interaction of various Cry toxins with the ~110 kDa APN of larval fat body, Malpighian tubule and salivary gland of *A. janata*. Previously we have also localized the expression of APN on the cell membranes of fat body cells and epithelial cells of Malpighian tubule (part 2).

Successful gene silencing in Lepidoptera by RNAi was first reported by Bettencourt *et al*. (2002). Since then, a number of successful as well as unsuccessful experiments have been carried out to study gene function in a number of lepidopteran species including the non-model insects (Terenius *et al*. 2011). RNAi-mediated knockdown of genes in Lepidoptera either by oral ingestion (Turner *et al*. 2006; Tian *et al*. 2009; Whyard *et al*. 2009) or by intra-hemocoelic injection (Rajagopal *et al*. 2002; Eleftherianos *et al*. 2006; Huang *et al.* 2007; Sivakumar *et al*. 2007; Tang *et al*. 2010) have always been used to identify potential target genes for control of these pests. Using RNAi strategy, the functional role of midgut APNs as Cry toxin receptor has been demonstrated in *S. litura* (Rajagopal *et al*. 2002) and *H. armigera* (Sivakumar *et al*. 2007). In the present study, we employed RNAi strategy to investigate the possible function of non-gut visceral APN (designated as *AjAPN*1) which is expressed in fat body, Malpighian tubule and salivary gland of *A. janata*. The ultimate objective of the study was to explore novel avenues to identify molecular targets and exploit them for the management of agriculturally important pests. Here we show that hemocoelic injection of

double-stranded *AjAPN*1 siRNA to third instar larvae significantly down-regulated the expression of this gene in fat body and Malpighian tubule but not in the salivary gland. Consequently, reduced *AjAPN*1 expression in fat body and Malpighian tubule was associated with high larval mortality rate, growth arrest and prolonged larval duration, development of smaller pupae and higher incidence of non-viable larval-pupal intermediates formation. In surviving adults, fertility and fecundity was also significantly compromised. *In vitro* ligand blotting analysis from knockdown larval tissues showed reduced interaction of Cry1Ab with the ~110 kDa APN correlating well with its reduced expression. Our results clearly suggest that *AjAPN*1 expression in fat body and Malpighian tubule play important physiological role in growth, development as well as metamorphosis of *A. janata*. Further in the present study, the possibility of *AjAPN*1 as a Cry toxin receptor in these tissues is also highlighted.

2. Materials and Methods

2.1. Insect culture

A. janata insects were cultured as described in "Materials and methods" section of part 1. For the present study, the "third instar", "fourth instar" and "fifth instar" larvae, each larva weighing 0.2±0.03g, 0.4±0.04g and 0.75±0.03g respectively were used.

2.2. Preparation of *A. janata AjAPN*1 and *GFP* siRNA duplexes

Based on the complete cDNA sequence of *AjAPN*1 cloned from fat body, Malpighian tubule and salivary gland of *A. janata*, *AjAPN*1 siRNA duplex of 19-nt each of sense and antisense strands was designed, synthesized, quantified and commercially supplied by Sigma Aldrich (USA). The siRNA duplex sequence used for the injection experiment comprised 5′CUCUUUCAAACAUGCCGAUdTdT3′ and 5′AUCGGCAUGUUUGAAAGAGdTdT3′ as a sense and antisense sequence respectively. The siRNA was targeted to the specific sequence region "CTCTTTCAAACATGCCGAT" of *AjAPN*1. The integrity and quality of the double-stranded siRNA was analyzed by non-denaturing polyacrylamide gel electrophoresis and visualized using UV shadowing.

For the control, a double-stranded *GFP* siRNA comprising 5′GAACUUCAGGGUCAGCUUGCC3′ and 5′GCAAGCUGACCCUGAAGUUCA3′ as sense and antisense strands respectively were prepared as described by Donzé and Picard, (2002).

2.3. Injection of double-stranded *AjAPN*1 siRNA and control siRNA to *A. janata* larvae

The injection assay was initially carried out with the fifth instar larvae, followed by fourth instar and later with third instar larvae. The larvae were narcotized by placing them on ice for 30 min. The double-stranded siRNA of target and control gene were dissolved in DEPC treated water and each larva was injected with 1, 2.5 and 5 µg of siRNA/100 mg body weight. For each dose, 18 larvae were intrahemocoelically injected through the dorsal side of the larvae. Injection was carried out with a home-assembled microsyringe (Fig. 1A). A glass needle prepared with a micropipette puller (Model P-2000, Sutter Instruments Co. USA) was fitted to a Hamilton microsyringe holder through a sterile plastic tube to generate the injection microsyringe. After injection, the wounds were sealed immediately with bees wax. Maximum care was taken to incur minimum injury and loss of hemolymph. Larvae showing sign of hemolymph leakage after withdrawal of the needle were discarded. Further, soon after sealing the wounds, the larvae were placed again on ice for 15-20 min and transferred back to the rearing chamber provided with fresh castor leaves. The experiment was repeated three times independently to obtain reproducible results.

2.4. Isolation of larval tissues

66 h post-injection, four larvae from each dose were chilled on ice for 15-20 min, and various tissues like fat body, Malpighian tubule and salivary gland were dissected out using ice-cold insect Ringer solution. The tissues were rinsed properly with Ringer solution and the tissues from four larvae were pooled together for the isolation of total RNA and preparation of protein samples for ligand binding, western blotting and APN enzyme activity analyses.

2.5. Semi-quantitative and real-time PCR analyses of *AjAPN*1 gene silencing

Total RNA from various tissue samples were isolated using TRI reagent ™ (Sigma Aldrich, USA) and following the manufacturer's instructions. The RNA quantity was determined by Nanodrop 1000 (Thermo Scientific, USA). Quality and integrity of RNA were also assessed by denaturing electrophoresis on a 1% agarose gel. The total RNA was reverse transcribed to corresponding cDNA using SuperScript III first strand synthesis kit (Invitrogen). For semi-quantitative RT-PCR analysis, a primer pair of 5′TGGCTGGATATGGTATTACT3′ and 5′GATATTGAATGCTCTGGTGTA3′ was used as forward and reverse primer respectively to amplify a 476 bp fragment of *AjAPN*1 from fat body, Malpighian tubule and salivary gland post-injection of the siRNA

duplexes. A primer pair of 5′GGTAGTAGACAATGGCTCGGG3′ and 5′CCCAGTTAGTGACGATTCCGTG3′ was used as forward and reverse primer respectively to amplify a 180 bp fragment of lepidopteran insect β- actin for use as an internal control.

Real-time PCR analysis was performed in a 20 µl reaction volume using a custom-made Taqman gene expression assay (Applied Biosystems, USA). A forward primer 5′AGGAATACACAGGCTATCCGTACT3′, a reverse primer 5′GGCTGCTTGCTGCATGAT3′ and a Taqman probe "CAATGACCGAGAACATC" were used for the analysis of expression levels of *AjAPN*1 in fat body, Malpighian tubule and salivary gland post-injection of *AjAPN*1 siRNA. Insect 18S RNA was used as an internal reference to normalize the *AjAPN*1 transcript levels. *AjAPN*1 transcript levels of the *AjAPN*1 siRNA injected larvae are presented as change in the transcript levels relative to the *GFP* siRNA injected larvae using the $2^{-\Delta\Delta Ct}$ method described by Livak and Schmittgen (2001). The real-time expression analysis of each sample was performed in triplicates for three independent experiments. The Applied Biosystems 7500 Fast Real-Time PCR machine was used for the real-time PCR studies.

2.6. Preparation of protein samples

Fat body membrane fraction was prepared according to the method of Kirankumar *et al*. (1997). The procedure involved in the preparation of Malpighian tubule and salivary gland protein homogenates has also been described in "Materials and methods" section of part 2.

2.7. Western blot and APN enzyme activity analyses of *AjAPN*1 silencing

Fat body membrane, Malpighian tubule and salivary gland protein preparations of the *AjAPN*1 siRNA injected and control larvae were electrophoretically separated by 7.5% SDS-PAGE and transferred (electro-blotted) onto nitrocellulose membrane (Pall-Life Sciences, USA) using trans-blot apparatus (Bio-Rad) following the procedure of Towbin *et al*. (1979). The protein blots were incubated with 5% skim milk powder (w/v) in Tris buffered-saline (10mM Tris-HCl, pH 7.4, 150mM NaCl) supplemented with 0.1% Tween-20 (TBST) for 1 h at room temperature to block the non-specific binding sites. The blots were incubated with *A. janata* fat body APN-specific polyclonal antibody (1:10000 dilutions) (Budatha *et al*. 2007a) in TBST containing 5% milk powder (w/v) for overnight. The antibodies bound to APN proteins were detected using ALP-conjugated with goat anti-rabbit IgG (Bangalore Genei, India) for 1 h at room temperature. The

specific cross-reactivity was visualized with ALP substrate, NBT-BCIP (Sigma Aldrich, USA).

APN enzyme activity of fat body, Malpighian tubule and salivary gland protein preparations of the *AjAPN*1 siRNA and control siRNA injected larvae was examined as described by Garczynski and Adang (1995). The molar absorbance co-efficient of *p*-nitroanilide was taken as $9.9x10^{-3}$ mol/L (Malik and Riazuddin, 2001). The specific activity was expressed as µmol of *p*-nitroanilide released/min/mg of proteins.

2.8. *In vitro* ligand blot analysis

The detailed methodology involved in the preparation and purification of activated Cry1Ab and the subsequent biotinylation of the activated toxins have already been described in "Materials and methods" section of part 1. Fat body membrane, Malpighian tubule and salivary gland protein preparations (30 µg each) of experimental and control larvae were separated by 7.5% SDS-PAGE and electro-transferred onto nitrocellulose membranes (Pall-Life Sciences, USA). The membranes were blocked in a blocking buffer [3% (w/v) BSA in 0.01M Tris-buffered saline (TBS, pH 7.4)] for 1 h, followed by incubation in a blocking buffer containing biotin-labeled Cry1Ab toxins (200ng/mL) separately for 1 h. Following this, the blots were washed with TBS supplemented with 0.1% Tween-20 (TBST), and then incubated for 2 h in a blocking buffer containing streptavidin-ALP conjugate (1:1000 dilutions). Cry1Ab toxin-bound proteins were detected using the ALP substrate, NBT-BCIP (Sigma Aldrich, USA).

2.9. Evaluation of phenotypic differences between target and control siRNA injected insects

The phenotypic differences between *AjAPN*1 and *GFP* siRNA injected larval groups were investigated by examining larval mortality, larval growth, pupal weights and analysis of larval-pupal as well as pupal-adult metamorphosis. The larval growth of both the experimental and control groups were recorded at every 24 h for 5 days. Larval mortality was calculated 2 day post-injection. Phenotypic features of experimental and control insects were recorded and analyzed every 2 day until all adults eclosed. We also compared the fecundity of the adults between the two groups. All the photographs were taken with FinePix S9600 digital camera.

2.10. Statistical analysis

Data were expressed as mean ± standard deviation of three independent experiments (n=5). Differences between groups were analyzed for statistical significance by One-Way ANOVA followed by Students-Newman-Keuls (SNK) test using SigmaPlot 11.0 software. A probability of $p > 0.05$ was considered statistically significant.

3. Results

3.1. Expression analyses after siRNA injection

The integrity of the 19 oligomer duplex *AjAPN*1 siRNA used for the injection assay was analyzed and confirmed by non-denaturing polyacrylamide gel electrophoresis (PAGE) and visualized by UV shadowing (Fig. 1A; i). 3 day post-injection, we analyzed the *AjAPN*1 transcript levels in fat body, Malpighian tubule and salivary gland using semi-quantitative and real-time quantitative RT-PCR methods. The fourth and fifth instar larvae which were injected with 1, 2.5 and 5 µg of siRNA/100 mg body weight did not show any alteration in the transcript levels (data not presented). We then selected third instar larvae for the injection studies. The third instar larvae which were injected either with 1 or 2.5µg/100 mg body weight also did not show any reduction in the transcript levels. However, the third instar larvae which were injected with 5 µg/100 mg body weight showed a substantial decrease in the *AjAPN*1 mRNA level of fat body and Malpighian tubule. The fold decrease was 1.9 and 2.8 in fat body and Malpighian tubule respectively (Figs. 1B & 1C). However, the reduction in the transcript level of salivary gland was not significant (Figs. 1B & 1C). We also evaluated the silencing efficiency of the target siRNA at protein and enzyme activity levels. Western blot analysis of fat body membrane fraction, Malpighian tubule and salivary gland protein preparations (30 µg) from siRNA injected insects showed a significant reduction in fat body and Malpighian tubule of target siRNA injected insects as compared to the control siRNA injected insects (Fig. 1D). Nearly complete silencing was seen in Malpighian tubule (Fig. 1D). APN enzyme activity of fat body and Malpighian tubule protein preparations of the target siRNA injected larvae were significantly lower than the controls (Fig. 1E). The reduction in the APN enzyme activity of the target siRNA injected larvae as compared to the controls was 50% for fat body and 56% for Malpighian tubule. The specificity of RNAi silencing was demonstrated by the injection of *GFP* siRNA where there was no significant change in the transcript, protein and enzyme activity levels (Figs. 1B, 1C &1D).

3.2. Effects of *AjAPN*1 gene silencing on mortality, larval growth, pupation and metamorphosis of *A. janata*

The physiological consequences of decreased *AjAPN*1 expression in visceral tissues were assessed by examining larval mortality, larval growth, percentage of successful pupation and pupal weights. The larval mortality calculated 2 day post-injection revealed 42% death in the target siRNA injected insects, while in the controls, it was only 5% (Figs. 2A & 2B). The larval body weight recorded at every 24 h of post-injection showed a significant inhibition of growth in the *AjAPN*1 siRNA injected larvae. The injury caused by the injection resulted in brief cessation of feeding even in the control larvae. However 12 h post-injection, almost all the control larvae began to feed voraciously and grew normally throughout the larval stages with each larva weighing approximately 0.78±0.03 g at the fifth instar i.e., 5 day post-injection. In contrast, all the *AjAPN*1 siRNA injected larvae either fed less or did not feed and showed growth arrest throughout the larval stages. 5 day post-injection, each larva still weighed only 0.37±0.04 g (Fig. 2C). Feeding inhibition and the subsequent larval growth arrest delayed the pupation by 4-5 days in experimental insects when compared with control animals. Of the surviving larvae, only 25% of the experimental larvae were able to pupate normally, while 87% of the control larvae successfully developed into healthy pupae (Fig. 2D). A high percentage of the target siRNA injected larvae could not complete the larval-pupal transformation and died as “larval-pupal intermediates” exhibiting both larval as well as pupal phenotypes (Fig. 2F). Treated larvae developed into smaller pupae with a body weight around 0.58±0.05 g per pupa, while the control pupae were larger in size and weighed around 0.75±0.03 g per pupa (Fig. 2F). Thus, a significant reduction in the pupal weights was observed (Fig. 2E). The adults that emerged from pupae of the siRNA injected insects were found to be either smaller in size or defective and laid negligible number of eggs (data not presented). The fertility of the adults and fecundity of the eggs were highly reduced as no neonate larvae could emerge from these eggs.

A) (i)

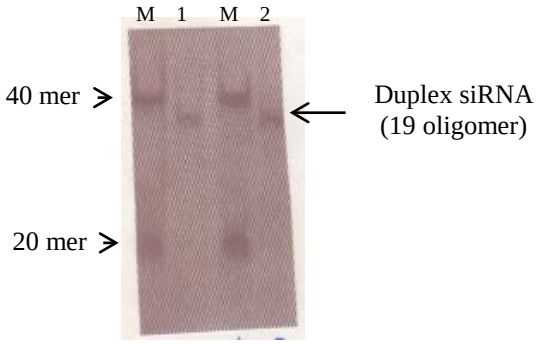

(ii)

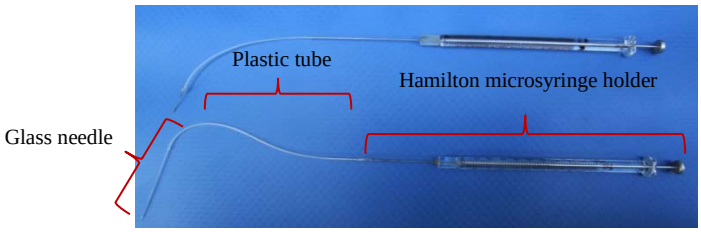

1 or 2.5 or 5 µg siRNA /100 mg body weight

↓

3rd instar
(5 days old)

↓

Molecular and physiological analyses

B)

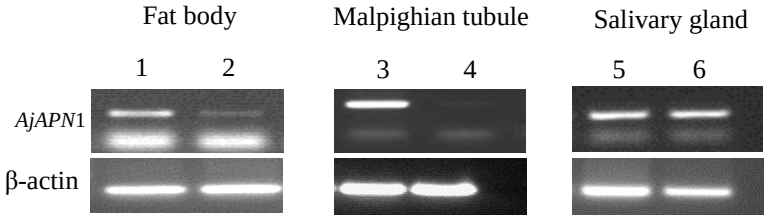
Fat body
Malpighian tubule
Salivary gland
1
2
3
4
5
6
AjAPN1
β-actin

C)

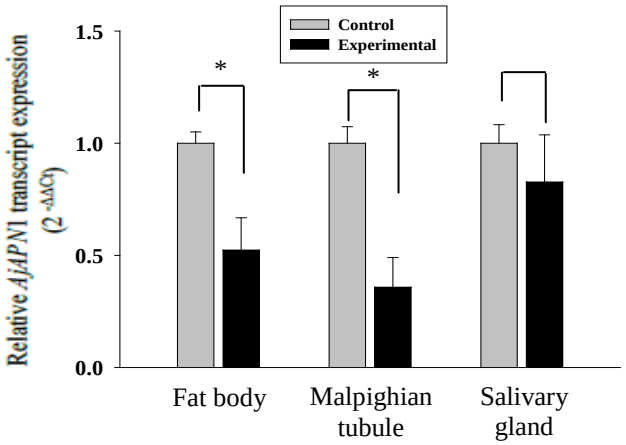
Control
Experimental
Relative AjAPN1 transcript expression
(2 -ΔΔCt)
1.5
1.0
0.5
0.0
*
*
Fat body
Malpighian tubule
Salivary gland

D)

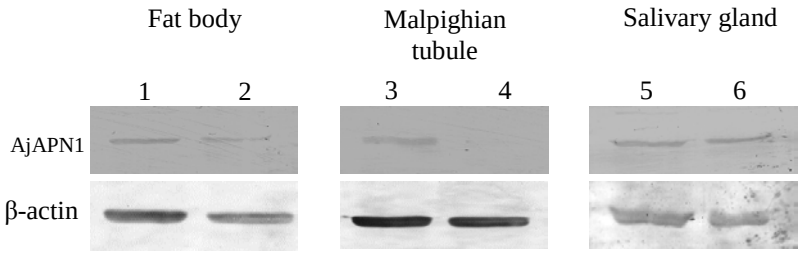
Fat body
Malpighian tubule
Salivary gland
1
2
3
4
5
6
AjAPN1
β-actin

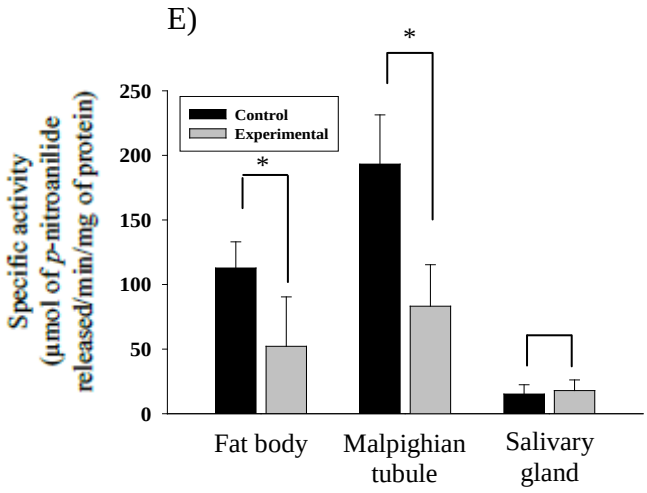

Fig. 1. RNAi-mediated knockdown of *AjAPN*1 transcript and its encoded protein. **A)** (i) Analysis of the integrity of double-stranded *AjAPN*1 siRNA oligonucleotides by non-denaturing polyacrylamide gel electrophoresis and visualization by UV shadowing; Lanes M: oligonucleotide marker, Lanes 1 & 2: double-stranded *AjAPN*1 siRNA. (ii) Flowchart depicting the methodology involved in the study. Home-assembled set-up, where a Hamilton microsyringe holder fitted to a glass needle through a sterile plastic tube was used for injection. The glass needles were generated with a micropipette puller (Model P-2000, Sutter Instruments Co. USA). **B)** Semi-quantitative PCR analysis of *AjAPN*1 transcript levels in different tissues. β-actin was used as an internal endogenous control (lower panel). **C)** Real-time quantitative PCR analysis of *AjAPN*1 transcript levels. Fat body, Malpighian tubule and salivary gland tissues from four larvae were pooled together for each sample. 18sRNA was used as an internal endogenous control. *AjAPN*1 transcript level is demonstrated as fold change relative to the control. **D)** Western blot analysis. Fat body, Malpighian tubule and salivary gland protein preparations were pooled together from four larvae. Note the reduction in ~110 kDa APN of fat body and Malpighian tubule of the *AjAPN*1 siRNA injected insects. β-actin expression was used as an internal endogenous control (lower panel). **E)** APN enzyme activity analysis. Note the decrease in the APN enzyme activity of fat body and Malpighian tubule of the *AjAPN*1 siRNA injected insects. The values are presented as mean ± standard deviation of three independent experiments. Significance between groups was tested by ANOVA followed by SNK test using SigmaPlot 11.0 software. * indicate statistical significance ($P<0.05$). Lanes 1, 3 & 5: double-stranded *GFP* siRNA injected (Control) and Lanes 2, 4 & 6: double-stranded *AjAPN*1 siRNA injected (Experimental) insects.

A)

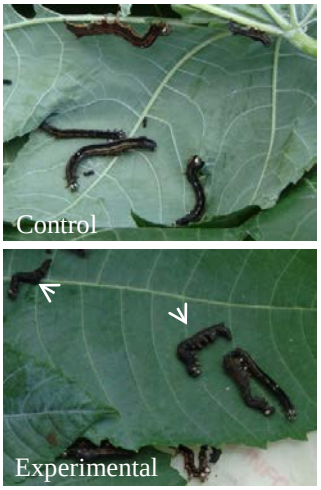
Control
Experimental

B)

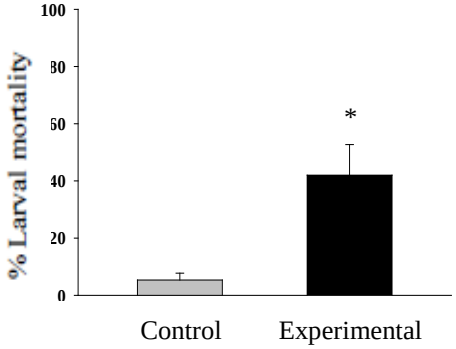
% Larval mortality
100
80
60
40
20
0
*
Control
Experimental

C)

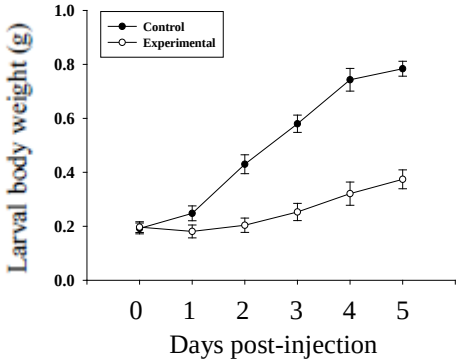
Larval body weight (g)
1.0
0.8
0.6
0.4
0.2
0.0
Control
Experimental
0
1
2
3
4
5
Days post-injection

D)

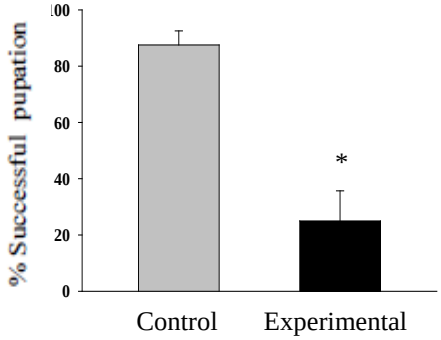
% Successful pupation
100
80
60
40
20
0
*
Control
Experimental

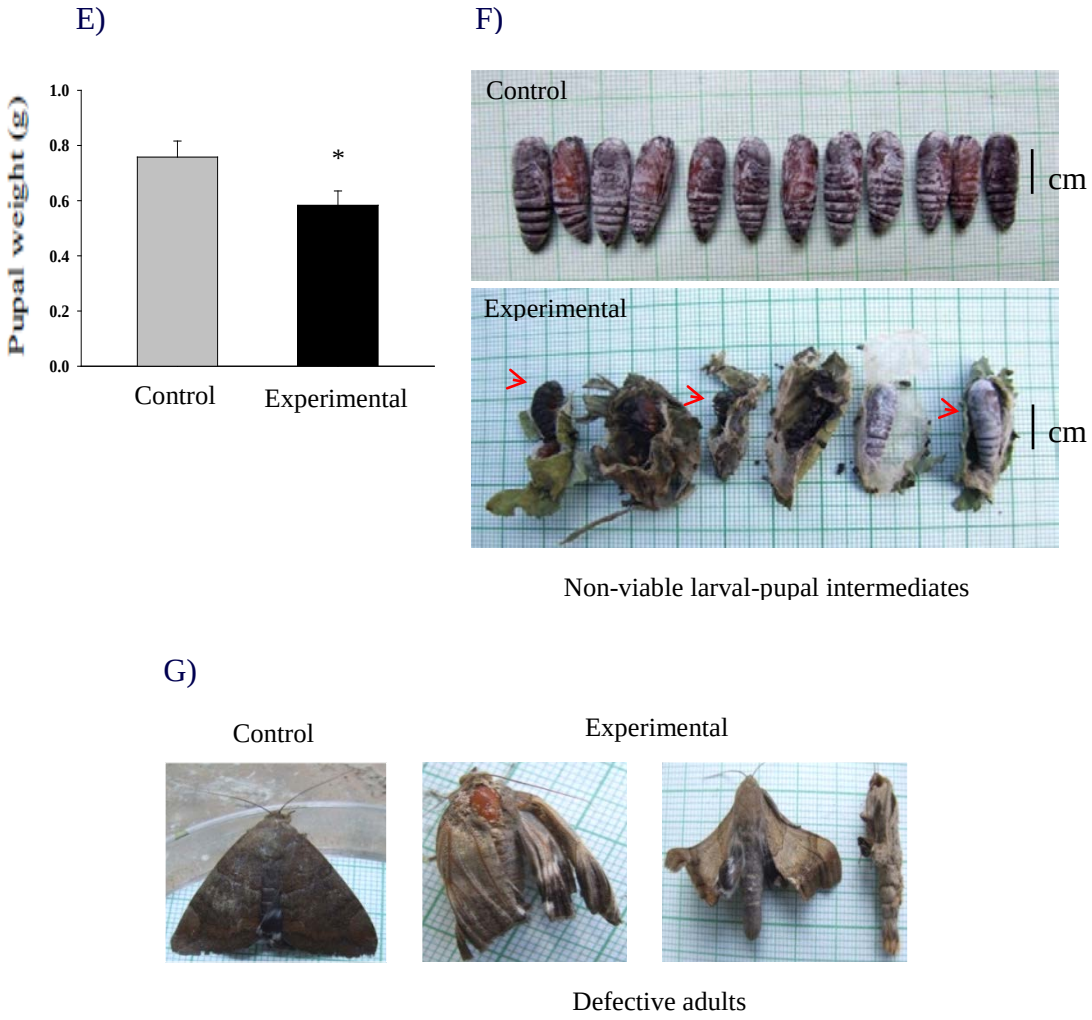

Fig. 2. **Effects of *AjAPN*1 RNAi on *A. janata* development**. **A)** Feeding inhibition; arrows indicate inactive and non-feeding larvae following *AjAPN*1 siRNA injection. **B)** Percentage larval mortality. **C)** Inhibition of larval growth. **D)** Percentage of successful pupation in control and target siRNA injected larvae. **E)** Weight of pupae that developed from the siRNA injected larvae. **F)** Development of non-viable larval-pupal intermediates and defective pupae. **G)** Development of defective adults. Each of the third instar larvae were injected with 1 or 2.5 or 5 µg of double-stranded *AjAPN*1 siRNA/100 mg body weight in a volume of 8 µl DEPC treated water. Simultaneously, the control larvae were injected with the same concentration and volume of *GFP* siRNA duplex. The larval growth was monitored by recording the weight of each larva after every 24 h for 5 days. Larval mortality was calculated 2 day post-injection. Pupal weights and percentage of successful pupation were compared between the control and experimental groups. Larval-pupal intermediate phenotypes were photographed. Values represented are mean ± standard deviation of three independent experiments. Significance between groups was tested by ANOVA followed by SNK test using SigmaPlot 11.0 software. * indicate statistical significance ($P<0.05$). Each injection dose was performed with 18 larvae.

3.3. Effect of *AjAPN*1 silencing on interaction with Cry toxins

To correlate the specificity of RNAi and interaction with Cry toxins, equal amounts of visceral tissue protein preparations (30 µg) of target and control siRNA injected insects were separated by 7.5% SDS-PAGE, transferred onto nitrocellulose membranes and analyzed by *in vitro* ligand blot. The blots were analyzed for interaction with biotinylated Cry1Ab. Overlay of 200ng/mL of insecticidal Cry1Ab on the blots revealed a comparatively lower interaction of Cry1Ab with the ~110 kDa APN protein of fat body and Malpighian tubule of the target siRNA injected insects. In salivary gland, the interaction of Cry1Ab was low and showed no reduction in the intensity of the interacting band of the experimental insects compared to the control insects. Reduced binding of Cry1Ab to ~110 kDa APN directly correlated with the reduced expression of the target protein in the experimental insects.

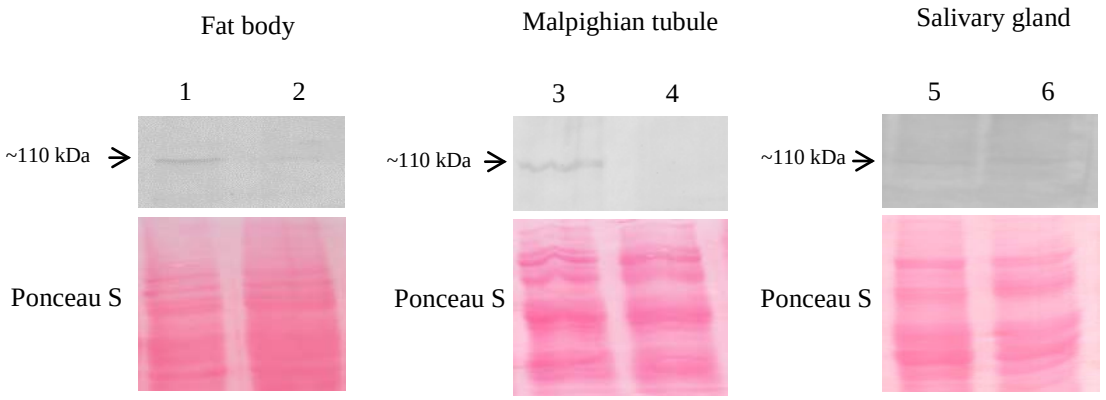

Fig. 3. *In vitro* ligand binding analysis. Fat body membrane, Malpighian tubule and salivary gland protein preparations (30 µg each) of *AjAPN*1 siRNA injected and control siRNA injected larvae were separated by 7.5% SDS-PAGE and transferred onto nitrocellulose membrane. The blots were incubated with biotin-labelled Cry1Ab toxins (200ng/mL) followed by incubation with streptavidin-ALP conjugate (1:1000 dilutions) and visualized with NBT-BCIP. Note the reduced binding of Cry1Ab to ~110 kDa APN of fat body and Malpighian tubule of the *AjAPN*1 siRNA injected larvae. Lower panels in each blot represent equal loading of proteins in each lane (Ponceau S stained blots). Lanes 1, 3 & 5: *GFP* siRNA injected (Control), Lanes 2, 4 & 6: *AjAPN*1 siRNA injected (Experimental) insects.

4. Discussion

Cry proteins produced by a gram positive soil bacterium *Bacillus thuringiensis* (*Bt*) are toxic to a wide range of insects including those belonging to the order Lepidoptera (Crickmore *et al*. 1998). *Bt* formulations of *kurstaki* strains 4D17 and 4D21, and local strains including DOR5 isolate were found to be effective against *A. janata* (Vimala-Devi *et al*. 2001). In part 1, we have already demonstrated by laboratory feeding bioassays that compared to *S. litura* and *H. armigera*, which are common polyphagous pest, *A. janata* was relatively more sensitive to purified recombinant Cry1Aa, Cry1Ab and Cry1Ac toxins as well as to DOR5 Cry toxins. *Bt*-based commercial formulations are still not being used widely for the control of *A. janata*, hence this pest might not have been exposed to *Bt* toxins and as a result, the larvae are more susceptible to the Cry toxins. Ingested Cry toxins are known to bind to the midgut brush border membrane anchored-receptors mainly APNs, thereby inducing gut paralysis and causing death of the larvae (Schnepf *et al.* 1998; Ferre and Van Rie, 2002). In lepidopteran insect, midgut APNs are more widely studied for their role as Cry toxin receptors (Knight *et al*. 1994; Yaoi *et al*. 1997; Gill *et al*. 1995; Valaitis *et al*. 1995; Luo *et al*. 1997) rather than their role in dietary protein digestion (Terra and Ferreira, 1994, Angelucci *et al*. 2008). Intrahemocoelic injection of purified Cry1Aa, Cry1Ab, Cry1Ac and DOR5 Cry toxins to *A. janata* larvae was found to induce variety of toxin-specific effects. These included induction of high larval mortality, inhibition of food intake, growth arrest, formation of non-viable larval-pupal intermediates, development of smaller pupae and emergence of defective adults. In addition, we also showed extensive tissue degeneration and cell death in fat body upon Cry toxin injection (part 1). In part 2, we have reported the presence of two different isoforms of APN in *A. janata* - (i) *AjAPN*4 which is primarily expressed in the gut of all the larval instars while (ii) *AjAPN*1 is expressed predominantly in the larval visceral tissues like fat body, Malpighian tubule and salivary gland. The role of APNs in non-gut tissues is relatively unknown and unexplored. Ligand blot analysis showed that activated Cry1Aa, Cry1Ab, Cry1Ac and DOR5 Cry toxins bind to the ~110 kDa protein (APN) of fat body, Malpighian tubule and salivary gland (part 2).

RNAi strategy has been successfully employed in a number of lepidopteran insects to study gene function (Bellés, 2010; Terenius *et al.* 2010). In the present study, we employed the same strategy to evaluate the potential function of *AjAPN*1 in fat body, Malpighian tubule and salivary gland of *A. janata*. Based on recent findings, Terenius *et al.* (2010) suggested that fairly high concentrations of dsRNA are required to achieve

high degree of silencing in lepidopteran insect, either by feeding or by hemocoelic injection. Furthermore, in an earlier study on *H. armigera* (Kumar *et al.* 2009), it was found that feeding of short siRNAs induced high levels of silencing while long dsRNA was not very effective. Hence in the present study, we opted for siRNA rather than the more commonly used long dsRNA for Lepidoptera. Initially, we injected *AjAPN*1 siRNA duplexes at concentrations of 1, 2.5 and 5 µg/100 mg body weight to fifth and fourth instar larvae. We did not observe any reduction in the transcript and protein levels of AjAPN1 in any of the tissues even after 2 day post-injection (data not shown). However after 3 days, there was a minor reduction in the expression level of AjAPN1 in all the three tissues which possibly might be due to the normal developmental regulation of the gene rather than the consequence of RNAi. In part 3, we have already reported that during normal development of *A. janata*, *AjAPN*1 expression both at the mRNA and protein levels gradually increases from neonate to early fifth instar (Malpighian tubule and salivary gland) or late fifth instar (fat body) and then decreases as the larval development progresses. In contrary to the present study, in other lepidopteran species like *S. litura* (Rajagopal *et al*. 2002) and *H. armigera* (Sivakumar *et al*. 2007), successful silencing of midgut APNs were achieved when siRNA was injected into the first day of fifth instar larvae and analyzed after 2 days. RNAi experiments conducted so far in various lepidopteran species revealed that genes expressed in hemocytes, fat body, midgut, pheromone gland and brain were relatively easier to silence than the genes expressed in the larval epidermis and wing (Terenius *et al*. 2010). Besides, different developmental stages of the same species seem to also affect the degree of susceptibility to RNAi. For instance in *S. littoralis*, silencing of a *period* gene was achieved when dsRNA was injected into the adult hemocoel (Kotwica *et al*. 2009), but Iga *et al*. (2010) were unsuccessful in achieving knockdown of the *halloween* genes by dsRNA when injected into the larval hemocoel. As we did not observe any effect on the *AjAPN*1 expression in fifth and fourth larval instars, we selected younger age larvae i.e., third instar larva and injected 1, 2.5 and 5 µg siRNA/100 mg body weight of larvae. Analysis after 66 h showed a significant 1.9 and 2.8-fold decrease in *AjAPN*1 transcript levels of fat body and Malpighian tubule respectively. However the change in salivary gland was not significant. Consequently, we observed a corresponding decrease in the protein expression level in these two tissues i.e., fat body and Malpighian tubule. APN enzyme activity analysis revealed 50% and 56% reduction in fat body and Malpighian tubule respectively. The controls used in the experiment confirmed that the responses were specific to the gene for

which it was employed. We assume that the difference in the susceptibility of the developmental stages by an unknown mechanism to be the cause of such an outcome. Thus, we observed that the susceptibility of a species to siRNA of the same gene could also depend on the stage of growth and development. Reports suggest that midgut APN genes of different species of Lepidoptera show variation in the susceptibility to systemic RNAi. As earlier reports suggested, hemocoelic injection of dsRNA to fifth instar larvae of *S. litura* (Rajagopal *et al*. 2002) and *H. armigera* (Sivakumar *et al*. 2007) resulted in high degree of APN gene silencing but not in *Ostrinia nubilalis*, *S. exigua* and *E. postvittana* (Terenius *et al*. 2010) which corroborated well with our observation in *A. janata* where *AjAPN*1 silencing could not be achieved when *AjAPN*1 siRNA was injected into fifth instar larvae. All these studies along with our present report clearly suggest wide variation in lepidopteran gene silencing with siRNA application.

In *A. janata*, both gut (Budatha *et al.* 2007a) and visceral APN isoforms identified in the present study, display all the canonical features of an APN including the aminopeptidase motif "GAMENWG", Zn^{++} binding motif "$HEXXHX_{18}H$", N-terminal signal peptide, several glycosylation sites and C-terminal GPI-anchor signal. However, both the isoforms share only 32% amino acid sequence identity. The sequence identity with other known lepidopteran midgut APNs was also less than 50%. Since the APN sequences of the non-gut tissues from species other than *A. janata* are unavailable, we could not confirm if all the non-gut tissue APNs are identical. Thus, the RNAi effect seen in fat body as well as Malpighian tubule and not in salivary gland suggest that RNAi efficiency also depend on the nature of the tissue. All these suggest that performing RNAi experiments in Lepidoptera is not as straight-forward as known for insect like *Drosophila* of order Diptera. With these results, we also report gene silencing in Malpighian tubule for the first time.

The results observed at the molecular level were further supported by the physiological observations. Reduced expression of *AjAPN*1 in fat body and Malpighian tubule induced significant percentage of larval mortality, growth arrest and prolonged larval duration which consequently might have been responsible for the development of non-viable, malformed larval-pupal intermediates suggesting *AjAPN*1 to play an important role in *A. janata* development. Besides, the adults that emerged from the *AjAPN*1 knockdown insects had fairly lowered fertility and laid a negligible number of eggs. Further the fecundity of the laid eggs was very poor and no neonate larvae were

found to emerge from these eggs which might be due to the failure of mating associated with defective adult structures.

Since the injection of *AjAPN*1 siRNA into the third instar larvae resulted in high larval mortality, we could not conduct Cry toxin hemocoelic delivery-based larval toxicity assay as the effects of the two could not be differentiated either at morphological or at phenotypical level. Instead we performed *in vitro* Cry toxin binding assay using biotinylated Cry1Ab toxin which revealed reduced interaction of Cry1Ab with the ~110 kDa APN protein of fat body and Malpighian tubule of the knockdown larvae correlating well with the reduction in the transcript and protein levels of the target gene. In salivary glands, there was no difference in the intensity of interaction between the treated and the control larvae. These results further demonstrate that the binding of Cry toxins to ~110 kDa APN protein is a specific interaction and once again supports its potential role as a Cry toxin receptor in these tissues.

In conclusion, the results of our study clearly suggest APN to play an important physiological role in fat body and Malpighian tubule thereby, contributing significantly to the overall growth and development in *A. janata*. Secondly, the visceral tissue-specific APN could also act as receptor for Cry toxins. This provides a high prospect of visceral tissue APNs as a potential target molecule for development of a novel strategy for Bt-based management of important agricultural pest like *A. janata*.

Summary and conclusions

Part 1: Toxicity effects of Cry toxins upon hemocoelic delivery to *A. janata* larvae

The first investigation was aimed to find out whether other modes of delivery of Cry toxins to the larval forms of insects, other than oral ingestion, could induce insecticidal effects. Upon injection of activated Cry1Aa, Cry1Ab, Cry1Ac and DOR5 Cry toxins individually to third instar larvae of *A. janata* at various concentrations of 0.1, 0.5, 1, 5 and 10 µg/0.2 g body weight, we observed high percentage of larval mortality, inhibition of food intake, slower growth rate and development of smaller pupae in a dose-dependent manner. DOR5 Bt isolate, whose lepidopteran-specific *cry* gene profile showed the presence of *cry1*Aa, *cry1*Ab, *cry1*C, *cry1*I, *cry2*A, *cry2*B and vegetative insecticidal protein (*vip*) genes obviously was found to be more potent than Cry1Aa, Cry1Ab and Cry1Ac toxins injected individually. Histological analyses of the toxin injected larvae revealed morphological and structural changes in gut, fat body, Malpighian tubule and salivary gland. In fat body, extensive degeneration and disintegration was evident from the appearance of numerous fragmented nucleus and large cytoplasmic cavities. Almost negative MTT staining and detection of a number of TUNEL-positive signals in the damaged tissue further confirmed apoptotic cell death in fat body of the Cry toxin injected larvae. Significant elevation in the level of acid phosphatase activity primarily in the fat body tissue and not in other tissues; indicates the involvement of lysosomal enzymes in Cry toxin-induced cell death in fat body. TUNEL-negative signals and the absence of significant changes in the acid phosphatase activity levels in gut, Malpighian tubule and salivary gland clearly ruled out the involvement of apoptotic and/or autophagic modes of cell death in these tissues upon Cry toxin injection. However, presence of cell debris in the gut lumen and the disorganization of the Goblet and columnar epithelial cells indicate loss of gut tissue structure and damage. The large pores and cavities seen in the epithelium of Malpighian tubule and the significant reduction in the size of salivary gland clearly show that these tissues are far from being normal. The involvement of different modes of cell death and degeneration in these tissues, other than apoptosis is probable. A relatively high percentage of the surviving larvae developed into non-viable larval-pupal intermediates exhibiting “incomplete ecdysis” phenotype. However, surviving insects metamorphosed and gave rise smaller pupae, and the number of adults that emerged from them were defective, exhibiting phenotypic features like small and curly wing, presence of higher number of pilliform or hair-like scales (only lamellar or blade-like scales in controls) and defective antenna,

which clearly indicate defective metamorphosis. These abnormal adults failed to mate and reproduce. A 6-fold decrease in total protein content and a significant reduction in hexamerin content in the hemolymph also supported degeneration and loss of function of fat body upon Cry toxin delivery. The fat body being the principle metabolic organ in insect that synthesize, release and store variety of macromolecules including proteins, this damage could be responsible for the impaired development and metamorphosis. Thus, based on these results, we infer that the larval mortality, the inability of the surviving insects to complete larval-pupal and pupal-adult metamorphosis and also the reproductive failure of the resultant adults are the consequences of morphological changes and tissue degeneration of the vital larval cells/tissues/organs induced by Cry toxins upon hemocoelic delivery.

Part 2: Identification and characterization of Cry toxin targets in *A. janata*

In this part, our aim was to find out whether the toxicity effects induced by hemocoelic delivery of Cry toxins to the larval forms of *A. janata* was possibly due to its interaction with putative proteins expressed in the larval visceral tissues like fat body, Malpighian tubule and salivary gland. *In vitro* ligand binding analysis using biotinylated Cry1Aa, Cry1Ab, Cry1Ac and DOR5 Cry toxins revealed binding of these Cry toxins to ~110 kDa protein of fat body, Malpighian tubule and salivary gland. Lepidopteran APNs are reported to have a molecular weight of ~110-120 kDa. The specificity of interaction was further analyzed by co-immunoprecipitation assay with Cry1Ab as the interacting ligand and using purified Cry1Ab antisera for pulling down the protein-ligand complex. The ~110 kDa interacting protein was partly confirmed as APN by detecting with *A. janata* fat body-specific APN polyclonal antibody. Full-length APN cDNAs were cloned and characterized from Malpighian tubule and salivary gland. Molecular characterization of the deduced amino acid sequences of Malpighian tubule APN (AjMtAPN) and salivary gland APN (AjSgAPN) revealed the presence of all the canonical features of an APN including aminopeptidase motif "GAMENWG", Zn^{++} binding motif "$HEXXHX_{18}E$", N-terminal signal peptide, several glycosylation sites and C-terminal GPI-anchor signal. Sequence comparative analysis of *A. janata* APNs revealed 99% amino acid sequence identity between AjFbAPN (fat body APN), AjMtAPN and AjSgAPN, while the sequence identity of the non-gut visceral tissue APNs with AjMgAPN (*A. janata* midgut APN) was only 32%, indicating the presence of two types of APN in *A. janata*. Sequence

comparison with the reported lepidopteran APNs also revealed the conservation of APN signature motifs. AjFbAPN, AjMtAPN and AjSgAPN belonged to Class 1 and AjMgAPN belonged to Class 4 of APN classification. We named AjFbAPN, AjMtAPN and AjSgAPN as "AjAPN1" and AjMgAPN as "AjAPN4". AjAPN4 was specifically expressed only in gut, while AjAPN1 was distributed in fat body, Malpighian tubule, salivary gland and midgut. The distribution of APN expression in these tissues was also confirmed by immunofluorescence, western blot and APN enzyme activity analyses. To have better insights of their potential function as Cry toxin receptors, we constructed 3D molecular models of AjAPN4 and AjAPN1 by comparative modeling method. Analysis of the molecular models revealed that the overall folding pattern of AjAPN4 and AjAPN1 was highly conserved with the available 3D structure of experimentally determined gluzincin aminopeptidases. AjAPN1 and *B. mori* APN shared high sequence and structural similarity in the Cry1Aa toxin binding region. The similarity was less between AjAPN4 and *B. mori* APN. The possible role of AjAPN1 as Cry toxin receptor was further supported by *in vitro* binding of Cry1Aa to ~110 kDa protein of Malpighian tubule where AjAPN1 with theoretical weight of 111 kDa was expressed. All these observations therefore strongly support their potential role as Cry toxin receptors.

Part 3: Developmental and hormonal regulation of APN expression in *A. janata*

In insects, post-embryonic development involving larval molt, larval-pupal transformation and pupal-adult metamorphosis is regulated by a precise interplay between the titre of JH and 20E through the regulation of a cascade of stage-specific expression of different genes. Midgut APNs are known to perform multiple physiological activities in insect development. In this part of our study, we investigated the developmental and hormonal regulation of *AjAPN*4 and *AjAPN*1 expression during the post-embryonic development of *A. janata*. The expression of *AjAPN*4 in gut as well as *AjAPN*1 in fat body, Malpighian tubule and salivary gland increased gradually from third larval instar to fifth larval instar and then decreased in prepupal stage. This expression pattern was observed at mRNA, protein as well as APN enzyme activity levels, thus revealing that the expression of *AjAPN*4 and *AjAPN*1 is developmentally regulated at transcriptional as well as post-transcriptional levels. In order to study the hormonal regulation of *AjAPN*4 and *AjAPN*1 expression in these tissues at mRNA level, the larvae were thorax-ligated, which primarily blocks the supply of hormones from the prothoracic gland and corpora allata to

the abdomen. The isolated abdomens were injected with 20E and/or topically applied with methoprene (JH analog). Quantitative RT-PCR analyses revealed that 20E down-regulate and JH up-regulate *AjAPN*4 and *AjAPN*1 mRNA expression in a dose-dependent manner. Topical application of methoprene to the 20E injected insects revealed the antagonistic effect of JH on 20E-suppressed *AjAPN*4 and *AjAPN*1 mRNA expression. Hence, based on the developmental profile and hormonal studies, we suggest *AjAPN*4 and *AjAPN*1 as larval genes predominantly expressed during larval instars and regulated by JH while during larval-pupal transformation, they are inhibited by ecdysteroids.

Part 4: Functional elucidation of *AjAPN*1 expression in non-gut visceral tissues of *A. janata*

*AjAPN*1 is expressed predominantly in the larval visceral tissues like fat body, Malpighian tubule and salivary gland of *A. janata*. The role of APNs in the non-gut tissues is relatively unknown and unexplored. For this part of our study, we employed RNAi-mediated silencing strategy to evaluate the potential role of *AjAPN*1 expression in fat body, Malpighian tubule and salivary gland of *A. janata*. Injection of *AjAPN*1 double-stranded siRNA to third instar larvae at 5µg/100 mg body weight showed a substantial decrease in the *AjAPN*1 mRNA level of fat body and Malpighian tubule after 66 h. The fold decrease was 1.9 and 2.8 in fat body and Malpighian tubule respectively. Consequently, we observed a corresponding decrease in the protein expression level in fat body and Malpighian tubules. APN enzyme activity analysis also revealed 50% and 56% reduction in fat body and Malpighian tubule respectively. The results observed at the molecular level were further supported by the physiological observations. Reduced expression of *AjAPN*1 in fat body and Malpighian tubules induced significant percentage of larval mortality, growth arrest, prolonged larval duration and development of smaller pupae. A high percentage of the target siRNA injected larvae could not complete the larval-pupal transformation and died as “larval-pupal intermediates” exhibiting both larval as well as pupal phenotypes. Besides, the adults that emerged from the *AjAPN*1 knockdown insects had fairly low fertility and laid negligible number of eggs. Further the fecundity of the laid eggs was very poor and no neonate larvae were found to emerge from these eggs. All these observations suggest *AjAPN*1 expression in these tissues to play an important role in *A. janata* development. Since the injection of *AjAPN*1 siRNA to the third instar larvae resulted in high larval mortality, we could not conduct Cry toxin

hemocoelic delivery-based larval toxicity assay as the effects of the two could not be differentiated either at morphological or phenotypical level. Instead we performed *in vitro* ligand binding assay using biotinylated Cry1Ab toxins which revealed reduced interaction of Cry1Ab with the ~110 kDa protein (APN) of fat body and Malpighian tubule of the knockdown larvae correlating well with the reduction in the transcript and protein levels of the target gene. In salivary glands, there was no difference in the intensity of interaction between the treated and the control larvae. These results further demonstrate that the binding of Cry toxins to ~110 kDa APN protein is a specific interaction and once again supports its potential role as a Cry toxin receptor in these tissues.

Based on the results obtained from all the four studies, we made two major conclusions- (i) Visceral tissue specific APNs play important physiological role during the development of insects and (ii) APNs in these tissues could also act as Cry toxin receptors, and hence they could be exploited as an effective targets for designing novel *Bt*-based control strategies for effective management of lepidopteran pests.

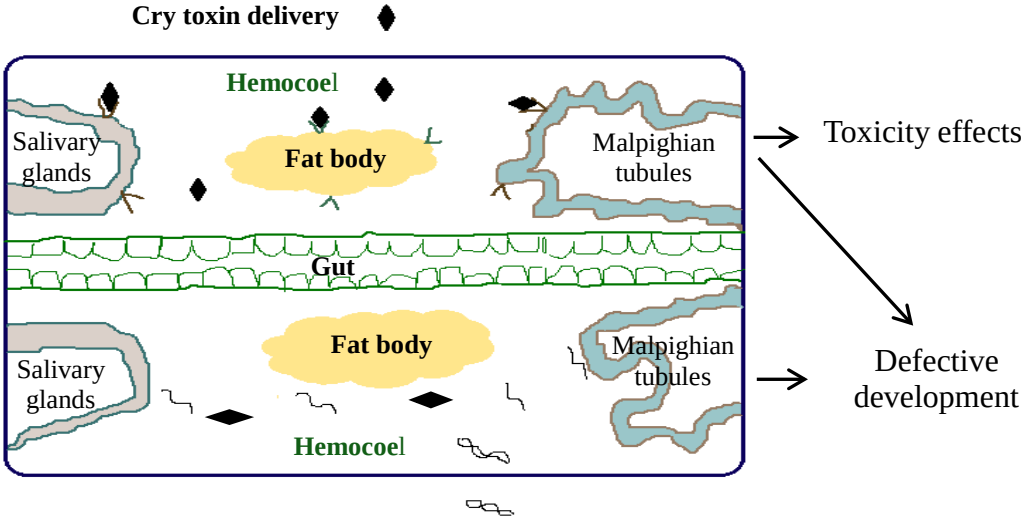

Fig.1. Proposed model for the role of non-gut visceral APNs in lepidopteran insects and their exploitation for targeted delivery of Cry toxin for management of insect pests.

References

Adang, M.J. (2004) Insect aminopeptidase N. In: Barret, A.J., Rawlings, N.D., Woessner, J.F. (Eds.), Handbook of proteolytic enzymes, Vol. 1. *Elsevier Academic Press, New York*, 296-299.

Agrawal, N., Malhotra, P., Bhatnagar, R.K. (2002) Interaction of gene-cloned and insect cell-expressed aminopeptidase N of *Spodoptera litura* with insecticidal crystal Cry1C protein. *Applied and Environmental Microbiology*, 68, 4583-4592.

Albiston, A.L., Ye, S., Chai, S.Y. (2004) Membrane bound members of the M1 family more than aminopeptidase. *Protein Peptide Letters*, 11, 491-500.

Altschul, S.F., Gish, W., Miller, W., Myers, E.W., Lipman, D.J. (1990) Basic local alignment search tool. *Journal of Molecular Biology*, 215, 403-410.

Amano, H., Yamagiwa, M., Akao, T., Mizuli, E., Ohba, M., Sakai, H. (2005) A novel 29-kDa crystal protein from *Bacillus thuringiensis* induce caspase activation and cell death of Jurkat T-cells. *Bioscience, Biotechnology and Biochemistry*, 69, 2063-2072.

Angelucci, C., Barret-Wilt, G.A., Hunt, D.F., Akhurst, R., East, P.D., Gordon, K.H.J., Campbell, P.M. (2008) Diversity of aminopeptidases, derived from four lepidopteran gene duplications, and polycalins expressed in the midgut of *Helicoverpa armigera*: Identification of proteins binding the δ-endotoxin Cry1Ac of *Bacillus thuringiensis*. *Insect Biochemistry and Molecular Biology*, 38, 685-696.

Angst, B.D., Marcozzi, C., Magee, A.I. (2001) The cadherin superfamily: diversity in form and function. *Journal of Cell Sciences*, 114, 629-641.

Arif, A., Vasanthi, P., Hansen, I.A., Scheller, K., Dutta-Gupta, A. (2004) The insect hemolymph protein HP19 mediates the non-genomic effect of ecdysteroids on acid phosphatase activity. *Journal of Biological Chemistry*, 279, 28000-28008.

Aronson, A. I., Angelo, N., Holt, S. C. (1971). Regulation of extracellular protease production in *Bacillus cereus* T: Characterization of mutants producing altered amounts of protease. *Journal of Bacteriology*, 106, 1016-1025.

Arpaia, S., DE Marzo, L., DI Leo, G.M., Santoro, M.E., Mennella, G., Van Loon, J.J.A. (2000) Feeding behavior and reproductive biology of Colorado potato beetle adults fed transgenic potatoes expressing the *Bacillus thuringiensis* Cry3B endotoxin. *Entomologia Experimentalis et Applicata*, 95, 31-37.

Ashok, J.B., Dutta-Gupta, A. (1988) Ecdysteroid mediated fat body acid phosphatase activity during larval development of rice moth, *Corcyra cephalonica*. *Biochemistry International*, 17, 1087-1091.

Ashok, M., Dutta-Gupta, A. (1991) *In vitro* effect of non-steroidal ecdysone agonist RH 5849 on fat body acid phosphatase activity in rice moth, *Corcyra cephalonica* (Insecta). *Biochemistry International*, 24, 69-75.

Ashok, M., Dutta-Gupta, A. (Ray) (1988) Ecdysteroid mediated fat body acid phosphatase activity during larval development of rice moth, *Corcyra cephalonica* (Lepidoptera). *Biochemistry International*, 17, 1087-1091.

Atsumi, S., Mizuno, E., Hara, H., Nakashini, K., Kitami, M., Miura, M., Tabunoki, H., Watanabe, A., Sato, R. (2005) Location of the *Bombyx mori* aminopeptidase N type 1 binding site on *Bacillus thuringiensis* Cry1Aa toxin. *Applied and Environmental Microbiology*, 71, 3966-3977.

Banks, D., Hua, G., Adang, M. (2003) Cloning of a *Heliothis virescens* 110 kDa aminopeptidase N and expression in *Drosophila* S2 cells. *Insect Biochemistry and Molecular biology*, 33, 499-508.

Bates, S.L., Zhao, J.Z., Roush, R.T., Shelton, A.M. (2005) Insect resistance management in GM crops: past, present and future. *Nature Biotechnology*, 23, 57-62.

Beckstead, R.B., Lam, G., Thummel, C.S. (2005) The genomic response to 20-hydroxyecdysone at the onset of *Drosophila* metamorphosis. *Genome Biology*, 6, R99

Bellés, X. (2010) Beyond *Drosophila*: RNAi *in vivo* and functional genomics in insects. *Annual Reviews of Entomology*, 55, 111-128.

Berger, E.M., Dubrovsky, E.B. (2005) Juvenile hormones – molecular actions and interactions during development of *Drosophila melanogaster*. *Vitamins and Hormones*, 73, 175-215.

Berger, E.M., Goudie, K., Klieger, L., Berger, M., DeCato, R. (1992) The juvenile hormone analogue, methoprene, inhibits ecdysterone induction of small heat shock protein gene expression. *Developmental Biology*, 151, 410-418.

Berman, H.M., Westbrook, J., Feng, Z., Gilliland, G., Bhat, T.N., Weissig, H., Shindyalov, I.N., Bourne, P.E. (2000) The Protein Data Bank. *Nucleic Acids Research*, 28, 235-242.

Beron, C.M., Curatti, L., Salerno, G.L. (2005) New strategy for identification of novel *cry*-type genes from *Bacillus thuringiensis* strains. *Applied and Environmental Microbiology*, 71, 761-765

Bettencourt, R., Terenius, O., Faye, I. (2002) Hemolin gene silencing by dsRNA injected into *Cecropia* pupae is lethal to next generation embryos. *Insect Molecular Biology*, 11, 267-271.

Bitondi, M.M., Nascimento, A.M., Cunha, A.D., Guidugli, K.R., Nunes, F.M., Simoes, Z.L. (2006) Characterization and expression of the Hex 110 gene encoding a glutamine-rich hexamerin in the honey bee, *Apis mellifera*. *Archives of Insect Biochemistry and Physiology*, 63, 57-72.

Bravo, A., Gill, S.S., Soberon, M. (2007) Mode of action of *Bacillus thuringiensis* Cry and Cyt toxins and their potential for insect control. *Toxicon*, 49, 423-435.

Bravo, A., Gomez, I., Conde, J., Munoz-Garay, C., Sanchez, J., Miranda, R., Zhuang, M., Gill, S.S., Soberon, M. (2004) Oligomerization triggers binding of a *Bacillus thuringiensis* Cry1Ab pore-forming toxin to aminopeptidase N receptor leading to insertion into membrane microdomains. *Biochemica Biophysica Acta*, 1667, 38-46.

Budatha, M., Meur, G., Dutta-Gupta, A. **(**2007a) A novel aminopeptidase in the fat body of the moth *Achaea janata* as a receptor for *Bacillus thuringiensis* Cry toxins and its comparison with midgut aminopeptidase. *Biochemical Journal*, 405, 287-297.

Budatha, M., Meur, G., Kirti, P.B., Dutta-Gupta, A. (2007b) Characterization of *Bacillus thuringiensis* Cry toxin binding novel GPI anchored aminopeptidase from fat body of the moth, *Spodoptera litura*. *Biotechnology Letters*, 29, 1651-1657.

Budatha, M., Ningshen, T.J., Dutta-Gupta, A. (2011) Is hexamerin receptor a GPI-anchored protein in *Achaea janata* (Lepidoptera: Noctuidae)? *Journal of Biosciences*, 36, 545-553.

Burmester, T. (2001) Molecular evolution of the arthropod hemocyanin superfamily. *Molecular Biology and Evolution*, 18, 184-195.

Burmester, T., Scheller, K (1999) Ligands and receptors: Common theme in insect storage protein transport. *Naturwissenschaften*, 86, 468-474.

Burmester, T., Scheller, K. (1997) Conservation of hexamerin endocytosis in diptera. *European Journal of Biochemistry*, 244, 713-720.

Ceron, J., Anabel, O., Rodolfo, Q., Leopoldo, G., Alejandra, B. (1995) Specific PCR primers directed to identify *cry*1 and *cry*111 genes within a *Bacillus thuringiensis* strain collection. *Applied and Environmental Microbiology*, 61, 3826-3831.

Cerstians, A., Verleyen, P., Van Rie, J., Van Kerkhove, E., Schwartz, J., Laprade, R., De Loof, A., Schoofs, L. (2001) Effect of *Bacillus thuringiensis* Cry1 toxins in insect hemolymph and their neurotoxicity in brain cells of *Lymantria dispar*. *Applied and Environmental Microbiology*, 9, 3923-3927.

Chaitanya, R.K., Dutta-Gupta, A. (2010) Light chain fibroin and P25 genes of *Corcyra cephalonica*: Molecular cloning, characterization, tissue-specific expression, synchronous developmental and 20-hydroxyecdysone regulation during the last instar larval development. *General and Comparative Endocrinology*, 167, 113-121.

Chaitanya, R.K., Sridevi, P., Senthilkumaran, B., Gupta, A.D. (2011) 20-Hydroxyecdysone regulation of H-fibroin gene in the stored grain pest *Corcyra cephalonica*, during the last instar larval development. *Steroids*, 76, 125-134.

Chang, W.X.Z., Gahan, L.J., Tabashnik, B.E., Heckel, D.G. (1999) A new aminopeptidase from diamondback moth provides evidence for a gene duplication event in Lepidoptera. *Insect Biochemistry and Molecular Biology*, 8, 171-177.

Chen, J., Brown, M.R., Hua, G., Adang, M.J. (2005) Comparison of the localization of *Bacillus thuringiensis* Cry1A delta endotoxins and their binding proteins in larval midgut of tobacco hornworm *Manduca sexta*. *Cell Tissue Research*, 321, 123-129.

Cheon, H.M., Kim, H.J., Kang, S.K., Seo, S.J (1997) Effect of *Bacillus thuringiensis* delta-endotoxin on insect fat body structure. *Korean Journal of Biological Sciences*, 1, 507-513.

Chinzei, Y. (1975) Induction of histolysis by ecdysterone *in vitro*: breakdown of anterior silk gland in silkworm, *Bombyx mori* (Lepidoptera: Bombycidae). *Applied Entomology and Zoology*, 10, 136-138.

Clarke, T.E., Clem, R.J. (2003) Insect defenses against virus infection: the role of apoptosis. *International Reviews of Immunology*, 22, 401-424.

Colombani, J., Bianchini, L., Lavalle, S., Pondeville, E., Dauphin-Villemant, C., Antoniewski, C., Carre, C., Noselli, S., Leopold, P. (2005) Antagonistic actions of ecdysone and insulin determine final size in *Drosophila*. *Science*, 310, 667-670.

Colovos, C., Yeates, T.O. (1993) Verification of protein structures: patterns of non-bonded atomic interactions. *Protein Science*, *2*, 1511-1519.

Crava, C.M., Bel, Y., Lee, S.F., Manachini, B., Heckel, D.G., Escriche, B. (2010) Study of the aminopeptidase N gene family in the lepidopterans *Ostrinia nubilalis* (Hübner) and *Bombyx mori* (L.) : Sequences, mapping and expression. *Insect Biochemistry and Molecular Biology*, 40, 506-515.

Crickmore, N., Zeigler, D.R., Feitelson, J., Schnepf, E., Van Rie, J., Lereclus, D., Baum, J., Dean, D.H. (1998) Revision of the nomenclature for the *Bacillus thuringiensis* pesticidal crystal proteins. *Microbiology and Molecular Biology Reviews*, 62, 807-813.

Croft, B.A. (1990) Developing a philosophy and program of pesticide resistance management In: Pesticide resistance in Arthropods, Roush, R.T. and Tabashnik, B.E., Eds. Chapman and Hall, New York, NY, 277-296.

Crowley, T.E., Meyerowitz, E.M. (1984) Steroid regulation of RNAs transcribed from the *Drosophila* 68C polytene chromosome puff. *Developmental Biology*, 102, 110-121.

Davey, K.G. (2000) The modes of action of juvenile hormones: some questions we ought to ask. *Insect Biochemistry and Molecular Biology*, 30, 663-669.

de Maagd, R.A., Bravo, A., Berry, C., Crickmore, N., Schnepf, H.E. (2003) Structure, diversity and evolution of protein toxins from spore forming entomopathogenic bacteria. *Annual Reviews of Genetics*, 37, 409-433.

Donzé, O., Picard, D. (2002) RNA interference in mammalian cells using siRNAs synthesized with T7 RNA polymerase. *Nucleic Acid Research*, 2002, 30, 10 e46.

Dubrovsky, E.B. (2005) Hormonal cross-talk in insect development. *Trends in Endocrinology and Metabolism*, 16, 6-11.

Dyer, K.A., Thornhill, W.B., Riddiford, L.M. (1981) DNA synthesis during change to pupal commitment of *Manduca sexta* epidermis. *Developmental Biology*, 84, 425-431.

Eguchi, M. (1995) Alkaline phosphatase isozymes in insects and comparison with mammalian enzyme. *Comparative Biochemistry and Physiology*-B, 111, 151-162.

Eleftherianos, I., Millichap, P.J., ffrench-Constant, R.H., Reynolds, S.E. (2006) RNAi suppression of recognition protein mediated immune responses in the tabacco hornworm *Manduca sexta* causes increased susceptibility to the insect pathogen *Photorhabdus*. *Developmental and Comparative Immunology*, 30, 1099-1107.

Elmogy, M., Iwami, M., Sakurai, S. (2004) Presence of membrane ecdysone receptor in the anterior silk gland of the silkworm *Bombyx mori*. *European Journal of Biochemistry*, 271, 3171-3179.

Emmerling, M., Chandler, D., Sandeman, M. (2001) Molecular cloning of three cDNAs encoding aminopeptidases from the midgut of *Helicoverpa punctigera*, the Australian native budworm. *Insect Biochemistry and Molecular Biology*, 31, 899-907.

Eswar, N., Webb, B., Marti-Renom, M.A., Madhusudhan, M.S., Eramian, D., Shen, M.Y., Pieper, U., Sali, A. (2007) Comparative protein structure modeling using MODELLER. *Current Protocols in Protein Science*, Chapter 2, Unit 2.9.

Fabrick, J., Tabashnik, B. (2007) Binding of *Bacillus thuringiensis* toxin Cry1Ac to multiple sites of cadherin in pink bollworm. *Insect Biochemistry and Molecular Biology*, 37, 97-106.

Federici, B.A. (2005) Insecticidal bacteria: an overwhelming success for invertebrate pathology. *Journal of Invertebrate Pathology*, 89, 30-38.

Feng, G., Yu, Q., Hu, C., Wang, Y., Yuan, G., Chen, Q., Yang, K., Pang, Y. (2007) Apoptosis is induced in the haemolymph and fat body of *Spodoptera exigua* larvae upon oral inoculation with *Spodoptera litura* nucleopolyhedrovirus. *Journal of General Virology*, 88, 2185-2193.

Fernandez, L.E., Aimanova, K.G., Gill, S.S., Bravo, A., Sóberon, M. (2006) A GPI-anchored alkaline phosphatase is a functional midgut receptor of Cry11Aa in *Aedes aegypti* larvae. *Biochemical Journal*, 394, 77-84.

Ferre, J., Real, M.D., Van Rie, J., Jansens, S., Peferoen, M. (1991) Resistance to *Bacillus thuringiensis* in a field population of *Plutella xylostella* is due to change in a midgut membrane receptor. *Proceedings of the National Academy of Sciences USA*, 88, 5119-5123.

Ferre, J., Van Rie, J. (2002) Biochemistry and genetics of insect resistance to *Bacillus thuringiensis*. *Annual Reviews of Entomology*, 47, 501-533.

Finney, D.J. (1952) In probit analysis, 2nd ed. Cambridge, UK: Cambridge University Press.

Flatt, T., Moroz, L.L., Tatar, M., Heyland, A. (2006) Comparing thyroid and insect hormone signaling. *Integrative and Comparative Biology*, 46, 777-794.

French, E.W. (1950) A study of the biology and morphology of *Achaea janata* (Linn.), a cotocaline moth, as it occurs in Hawaii. M.S. Thesis, University of Hawaii.

Funk, C.J. (2001) Alkaline phosphatase activity in whitefly salivary glands and saliva. *Archives of Insect Biochemistry and Physiology*, 46, 165-174.

Gaikwad, B.B., Bilapate, G.G. (1992) Parasitization of *Achaea janata* and estimation of yield losses on castor. *Journal of Marathwada Agriculture University*, 17, 195-196.

Garczynski, S. F., Crim, J.W., Adang, M.J. (1991) Identification of putative brush border membrane binding proteins specific to *Bacillus thuringiensis* delta-endotoxin by protein blot analysis. *Applied and Environmental Microbiology*, 57, 2816-2820.

Garczynski, S.F., Adang, M.J. (1995) *Bacillus thuringiensis* Cry1A(c) δ-endotoxin binding APN in the *Manduca sexta* midgut has a glycosyl-phosphatidylinositol anchor. *Insect Biochemistry and Molecular Biology*, 25, 409-415.

Garner, K.J., Hiremath, S., Lentoma, K., Valaitis, A.P. (1999) Cloning and complete sequence characterization of two gypsy moth aminopeptidase-N cDNAs including the receptor for *Bacillus thuringiensis* Cry1Ac toxin. *Insect Biochemistry and Molecular Biology*, 29, 527-535.

Gill, M., Ellar, D. (2002) Transgenic *Drosophila* reveals a functional *in vivo* receptor for the *Bacillus thuringiensis* toxin Cry1Ac. *Insect Molecular Biology*, 11, 619-625.

Gill, S., Cowles, E.A., Pietrantonio, P.V. (1992) The mode of action of *Bacillus thuringiensis* delta-endotoxins. *Annual Reviews of Entomology*, 37, 615-636.

Gill, S.S., Cowles, E.A., Francis, V. (1995) Identification, isolation, and cloning of *Bacillus thuringiensis* Cry1Ac toxin-binding protein from the midgut of the lepidopteran insect, *Heliothis virescens*. *Journal of Biological Biochemistry*, 270, 27277-27282.

Gilliland, A., Chambers, C.E., Bone, E.J., Ellar, D.J. (2002) Role of *Bacillus thuringiensis* Cry1 delta endotoxin binding in determining potency during lepidopteran larval development. *Applied and Environmental Microbiology*, 68, 1509-1515.

Gómez, I., Dean, D.H., Bravo, A., Soberón, M. (2003) Molecular basis for *Bacillus thuringiensis* Cry1Ab specificity, two structural determinants in the *Manduca sexta* Bt-R_1 receptor interact with α-8 and 2 in domain II of Cry1Ab toxicity. *Biochemistry*, 42, 10482-10489.

Gómez, I., Oltean, D.I., Sánchez, J., Gill, S.S., Bravo, A., Soberón, M. (2001) Mapping the epitope in cadherin-like receptors involved in *Bacillus thuringiensis* Cry1A toxin interaction using phage display. *Journal of Biological Chemistry*, 276, 28906-28912.

Gómez, I., Sánchez, J., Miranda, R., Bravo, A., Soberón, M. (2002) Cadherin-like receptor facilitates proteolytic cleavage of helix α-1 in domain I and oligomer pre-pore formation of *Bacillus thuringiensis* Cry1Ab toxin. *FEBS Letters*, 513, 242-246.

Goodman, W.G. (1983) Hemolymph transport of ecdysteroids and juvenile hormones. In " *Insect Endocrinology*", (Eds. Downer, R.H., Laufer, H.), 2, 49-57, Alan Liss Pub., New York.

Gould, F. (1998) Sustainability of transgenic insecticidal cultivars: integrating pest genetics and ecology. *Annual Reviews of Entomology*, 43, 701-726.

Grebe, M., Fauth, T., Spindler-Barth, M. (2004) Dynamic of ligand binding to *Drosophila melanogaster* ecdysteroid receptor. *Insect Biochemistry and Molecular Biology*, 34, 981-989.

Griffitts, J.S., Haslam, S.M., Yang,T., Garczynski, S.F., Mulloy, B., Morris, H., Cremer, P.S., Dell, A., Adang, M.J., Aroian, R.V. (2005) Glycolipids as receptors for *Bacillus thuringiensis* crystal toxins. *Science*, 307, 922-925.

Gudderra, N.P., Sonenshine, D.E., Apperson, C.S., Roe, R.M. (2002) Tissue distribution and characterization of predominant hemolymph carrier proteins from *Dermacentor variabilis* and *Ornithodoros parkeri*. *Journal of Insect Physiology*, 48, 161-170.

Hall, N.A. (1988) Peptidases in *Drosophila melanogaster* II. The variation of peptidase activities during development. *Insect Biochemistry*, 18, 145-155.

Hansen, I.A., Meyer, S.R., Schafer, I., Scheller, K. (2002) Interaction of the anterior fat body protein with the hexamerin receptor in the blowfly *Calliphora vicina*. *European Journal of Biochemistry*, 269, 954-960.

Haunerland, N.H., Shirk, P.D. (1995) Regional and functional differentiation in the insect fat body. *Annual Reviews of Entomology*, 40, 121-145.

Henrikson, P.A., Clever, U. (1972) Protease activity and cell death during metamorphosis in the salivary gland of *Chironomus tentans*. *Journal of Insect Physiology*, 18, 1981-2004.

Herrero, S., Gechev, T., Bakker, P.L., Moar, W.J., de Maagd, R.A. (2005) *Bacillus thuringiensis* Cry1Ca-resistant *Spodoptera exigua* lacks expression of one of four aminopeptidase N genes. *BMC Genomics*, 6:96.

Hiruma, K. (2003) Juvenile hormone action in insect development. In: Henry, H.L., Norman, A.W., (Eds.) *Encyclopedia of hormones and related cell regulators*, 2, Academic Press, San Diego, 528-535.

Hofmann, C., Vanderbruggen, H., Hofte, H., Van Rie, J., Jansens, S., Van Mellaert, H. **(**1988) Specificity of *Bacillus thuringiensis* delta endotoxins is correlated with the presence of high-affinity binding sites in the

brush border membrane of target insect midguts. *Proceedings of National Academy of Sciences USA*, 85, 7844-7848.

Hofte, H., Whiteley, H.R. (1989) Insecticidal crystal proteins of *Bacillus thuringiensis*. *Microbiological Reviews*, 53, 242-255.

Hooper, N.M. (1994) Families of zinc metalloproteases. *FEBS Letters*, 354, 1-6.

Huang, J., Zhang, Y., Li, M., Wang, S., Liu, W., Couble, P., Zhao, G., Huang, Y. (2007) RNA interference-mediated silencing of the *bursicon* gene induces defects in wing expansion of silkworm. *FEBS Letters*, 581, 697-701.

Humphrey, W., Dalke, A., Schulten, K. (1996) "VMD – Visual Molecular Dynamics" *Journal of Molecular Graphics*, 14, 33-38.

Hussein, H. M., Habustova, O., Turanli, F., Sehnal, F. (2006) Potato expressing beetle-specific *Bacillus thuringiensis* Cry3Aa toxin reduces performance of a moth. *Journal of Chemical Ecology*, 32.

Iga, M., Smagghe, G. (2010) Identification and expression profile of *halloween* genes involved in ecdysteroid biosynthesis in *Spodoptera littoralis*. *Peptides*, 31, 456-467.

Iwema, T., Billas, I.M.L., Beck, Y., Bonneton, F., Nierengarten, H., Chaumot, A., Richards, G., Laudet, V., Moras, D. (2007) Structural and functional characterization of a novel type of ligand-independent RXR-USP receptor. *The EMBO Journal*, 26, 3770-3982.

Janmaat, A.F., Myers, J. (2003) Rapid evolution and the cost of resistance to *Bacillus thuringiensis* in green house populations of cabbage loopers, *Trichoplusia ni*. *Proceedings of the Royal Society London B: Biological Sciences*, 270, 2263-2270.

Jiménez-Juárez, , N., Muñoz-Garay, C., Gómez, I., Saab-Rincon, G., Damian-Alamazo, J.Y., Gill, S.S., Soberón, M., Bravo, A. (2007) *Bacillus thuringiensis* Cry1Ab mutants affecting oligomer formation are non-toxic to *Manduca sexta* larvae. *Journal of Biological Chemistry*, 282, 21222-21229.

John, R., Sonenshine, D.E., Hynes, W.L. (2001) Identification of a defensin from the hemolymph of the American dog tick, *Dermacentor variabilis*. *Insect Biochemistry and Molecular Biology*, 31, 857-865.

Juarez-Perez, V. M., Ferrandis, M.D., Frutos, R. (1997) PCR-based approach for detection of novel *Bacillus thuringiensis cry* genes. *Applied and Environmental Microbiology*, 63, 2997-3002

Jurat-Fuentes, J.L., Adang, M.J. (2004) Characterization of a Cry1Ac-receptor alkaline phosphatase in susceptible and resistant *Heliothis virescens* larvae. *European Journal of Biochemistry*, 271, 3127-3135.

Jurat-Fuentes, J.L., Adang, M.J. (2007) "A proteomic approach to study Cry1Ac binding proteins and their alterations in resistant *Heliothis virescens* larvae". *Journal of Invertebrate Pathology*, 95, 187-191.

Kado, C.I., Liu, S.T. (1981) Rapid procedure for detection and isolation of large and small plasmids. *Journal of Bacteriology*, 145, 1365-1373

Kanost, M.R., Kawooya, J.K., Ryan, R.D., Van Heusden, M.C., Ziegler, R. (1990) Insect hemolymph proteins. *Advances in Insect Physiology*, 22, 299-366.

Kanost, M.R., Sparks, K.A., Wells, M.A. (1995) Isolation and characterization of apolipophorin-III from the giant water bug (*Lethocerus medius*). *Insect Biochemistry and Molecular Biology*, 25, 759-764.

Kegley, S.E., Wise, L.J. (1998) Pesticides in fruits and vegetables. Sausalito, CA: University Science Books.

Kethidi, D.R., Li, Y., Palli, S.R. (2006) Protein kinase C mediated phosphorylation blocks juvenile hormone action. *Molecular Cell Endocrinology*, 247, 127-134.

King-Jones, K., Thummel, C.S. (2005) Developmental biology: Less steroids make bigger flies. *Science*, 310, 630-631.

King-Jones, K., Thummel, C.S. (2005) Nuclear receptors – a perspective from *Drosophila*. *Nature Reviews Genetics*, 6, 311-323.

KiranKumar, N., Ismail, S.M., Dutta-Gupta, A. (1997) Uptake of storage proteins in the rice moth: *Corcyra cephalonica* Identification of storage protein binding proteins in the fat body cell membranes. *Insect Biochemistry and Molecular Biology*, 27, 671-679.

Knight, P., Crickmore, N., Ellar, D.J. (1994) The receptor for *Bacillus thuringiensis* Cry1Ac delta-endotoxin in the brush border membrane of the lepidopteran *Manduca sexta* is aminopeptidase N. *Molecular Microbiology*, 11, 429-436.

Knight, P., Knowles, B., Ellar, D. (1995) Molecular cloning of an insect aminopeptidase N that serves as a receptor for *Bacillus thuringiensis* Cry1A(c) toxin. *Journal of Biological Chemistry*, 270, 17765-17770.

Kochan, G., Krojer, T., Harvey, D., Fischer, R., Chen, L., Vollmar, M., von Delft, F., Kavanagh, K.L., Brown, M.A., Bowness, P., Wordsworth, P., Kessler, B.M., Oppermann, U. (2011) Crystal structures of the endoplasmic reticulum aminopeptidase-1 (ERAP1) reveal the molecular basis for N-terminal peptide trimming. *Proceedings of National Academy of Science USA*, 108, 7745-7750.

Koelle, M.R., Talbot, W.S., Segraves, W.A., Bender, M.T., Cherbas, P., Hogness, D.S. (1991) The *Drosophila* EcR gene encodes an ecdysone receptor, a new member of the steroid receptor superfamily. *Cell*, 67, 59-77.

Kotwica, J., Bebas, P., Gvakharia, B.O., Giebultowicz, J.M. (2009) RNA interference of the *period* gene affects the rhythm of sperm release in moths. *Journal of Biological Rhythms*, 24, 25-34.

Krishnamoorthy, M., Jurat-Feuntes, J., McNall, R.J., Andacht, T., Adang, M. (2007) Identification of novel Cry1Ac binding proteins in midgut membranes from *Heliothis virescens* using proteomic analyses. *Insect Biochemistry and Molecular Biology*, 37, 189-201.

Kumar, M., Gupta, G.P., Rajam, M.V. (2009) Silencing of acetylcholinesterase gene of *Helicoverpa armigera* by siRNA affects larval growth and its life cycle. *Journal of Insect Physiology*, 55, 273-278.

Kumaraswami, N.S., Maruyama, T., Kurabe, S., Kishimoto, T., Mitsu, T., Hori, H. (2001) Lipids of brush border membrane vesicles (BBMV) from *Plutella xylostella* resistant and susceptible to Cry1Ac delta-endotoxin of *Bacillus thuringiensis*. *Comparative Biochemistry and Physiology-B*, 129, 173.

Kuntal, B.K., Aparoy, P., Reddanna, P. (2010) EasyModeller: A graphical interface to MODELLER. *BMC Research Notes*, 3, 226–230.

Kyrieleis, O.J.P., Goettig, P., Kiefersauer, R., Huber, R., Brandstetter, H. (2005) Crystal structures of the tricorn interacting factor F3 from *Thermoplasma acidophilum*, a zinc aminopeptidase in three different conformations. *Journal of Molecular Biology*, 349, 787-800.

Lakshminarayana, M., Raoof, M.A. (2005) Insect pests and diseases of castor and their management. *Directorate of Oilseeds Research, Hyderabad*, 78.

Laskowski, R.A., MacArthur, M.W., Moss, D.S., Thornton, J.M. (1993) PROCHECK: A program to check the stereochemical quality of protein structures. *Journal of Applied Crystallography*, 26, 283-291.

Lee, D.W., Akao, T., Yamashita, S., Katayama, H., Maeda, M., Saitoh, H., Mizuki, E., Ohba, M. (2000) Non-insecticidal parasporal proteins of a *Bacillus thuringiensis* serovar *shandongiensis* isolate exhibit a preferential cytoxicity against human leukemic T-cells. *Biochemical and Biophysical Research Communications*, 272, 218-223.

Lee, M. K., Milne, R. E., Ge, A. Z., Dean, D.H. (1992) Location of a *Bombyx mori* receptor binding region on a *Bacillus thuringiensis* delta-endotoxin. *Journal of Biological Chemistry*, 267, 3115-3121.

Lee, M.K., You, T.H., Young, B.A., Cotrill, J.A., Valaitis, A.P., Dean, D.H. (1996) Aminopeptidase N purified from Gypsy moth brush border membrane vesicles is a specific receptor for *Bacillus thuringiensis* Cry1Ac toxin. *Applied and Environmental Microbiology*, 62, 2845-2849.

Lee, Y.L., Baehriecke, E.H. (2001) Steroid regulation of autophagic programmed cell death during development. *Development*, 128, 1443-1451.

Livak, K.J., Schmittgen, T.D. (2001) Analysis of relative gene expression data using real-time quantitative PCR and the 2(-Delta Delta C(T)) method. *Methods*, 25, 402-408.

Lomate, P.R., Hivrale, V.K. (2010) Partial purification and characterization of *Helicoverpa armigera* (Lepidoptera: Noctuidae) active aminopeptidase secreted in midgut. *Comparative Biochemistry and Physiology* - Part B: *Biochemistry and Molecular Biology*, 155, 164-170.

Lou, K., Tabashnik, B.E., Adang, M.J. (1997) Binding of *Bacillus thuringiensis* Cry1Ac toxin to aminopeptidase in susceptible and resistant diamond back moth (*Plutella xylostella*). *Applied and Environmental Microbiology*, 63, 1024-1027.

Maclntosh, S. C., Stone, T.B., Jokerst, R.S., Fuchs, R.L. (1991) Binding of *Bacillus thuringiensis* proteins to a laboratory-selected line of *Heliothis virescens*. *Proceedings of National Academy of Sciences USA*, 88, 8930-8933.

Malik, K., Mahmood, T., Riazuddin, S. (2001) The receptor for *Bacillus thuringiensis* Cry1Ac delta-endotoxin in the brush border membrane of the lepidopteran *Helicoverpa armigera* is aminopeptidase N. *Journal of Biological Sciences*, 8, 782-784.

Mané-Padrós, D., Cruz, J., Vilaplana, L., Pascual, N., Bellés, X., Martín, D. (2008) The nuclear hormone receptor BgE75 links molting and developmental progression in the direct-developing insect *Blattella germanica*. *Developmental Biology*, 315, 147-160.

Manohar, D., Gullipalli, D., Dutta-Gupta, A. (2010) Ecdysteroid-mediated expression of hexamerin (arylphorin) in the rice moth, *Corcyra cephalonica*. *Journal of Insect Physiology*, 56, 1224-1231.

Masler, E.P., Kovalera, E.S. (1997) Aminopeptidase-like activity in hemolymph plasma from larvae of the gypsy moth, *Lymantria dispar* (Lepidoptera Lymantriidae). *Comparative Biochemistry and Physiology*, 11613, 11-18.

Masson, L., Erlandson, M., Puzstai-Carey, M., Brousseau, R., Juarez-Perez, V., Frutos, R. (1998) A holistic approach for determining the entomopathogenic potential of *Bacillus thuringiensis* strains. *Applied and Environmental Microbiology*, 64, 4782-4788.

Masson, L., Lu, Y.J., Mazza, A., Brousseau, R., Adang, M.J. (1995) The Cry1Ac receptor purified from *Manduca sexta* displays multiple specificities. *Journal of Biological Chemistry*, 270, 20309-20315.

Maya-Monteiro, C.M., Daffre, S., Logullo, C., Lara, F.A., Alves, E.W., Capurro, M.L., Zingali, R., Almeida, I.C., Oliveira, P.L. (2000) HeLp, a heme lipoprotein from the hemolymph of the cattle tick, *Boophilus Microplus*. *Journal of Biological Chemistry*, 275, 36584-36589.

McGaughey, W.H. (1985) Insect resistance to the biological insecticide *Bacillus thuringiensis. Science*, 229, 193-195.

McGaughey, W.H., Gould, F., Gelernter, W. (1998) Bt resistance management. *Nature Biotechnology*, 16, 144-146.

McNall, R.J., Adang, M.J. (2003) Identification of novel *Bacillus thuringiensis* Cry1Ac binding proteins in *Manduca sexta* midgut through proteomic analysis. *Insect Biochemistry and Molecular Biology*, 33, 999-1010.

Mizuki, E., Ohba, M., Akao, T., Yamashita, S., Saitoh, H., Park, Y.S. (1999) Unique activity associated with non-insecticidal *Bacillus thuringiensis* parasporal inclusions: *in vitro* cell-killing action on human cancer cells. *Journal of Applied Microbiology*, 86, 477-486.

Mizuki, E., Park, Y.S., Saitoh, H., Yanashita, S., Akao, T., Higuchi, K., Ohba, M. (2000) Parasporin, a human leukemic cell-recognizing parasporal protein of *Bacillus thuringiensis*. *Clinical and Diagnostic Laboratory Immunology*, 7, 625-634.

Moscardi, F. (1999) Assessment of the application of baculoviruses for control of Lepidoptera. *Annual Reviews of Entomology*, 44, 257-287.

Nagamatsu, Y., Koike, T., Sasaki, K., Yoshimoto, A., Furukawa, Y., (1999) The cadherin-like protein is essential to specificity determination and cytotoxic action of the *Bacillus thuringiensis* insecticidal Cry1Aa toxin. *FEBS Letters*, 460, 385-390.

Nakanishi, K., Yaoi, K., Nagino, Y., Hara, H., KitamiAtsumi, S., Miura, N., Sato, R. (2002) Aminopeptidase N isoforms from the midgut of *Bombyx mori* and *Plutella xylostella*- their classification and the factors that determine their binding specificity to *Bacillus thuringiensis* Cry1A toxin. *FEBS Letters*, 9, 215-220.

Nakanishi, K., Yaoi, K., Shimada, N., Kadotani, T., Sato, R. (1999) *Bacillus thuringiensis* insecticidal Cry1Aa toxin binds to a highly conserved region of aminopeptidase N in the host insect leading to its evolutionary success. *Biochimica et Biophysica Acta*, 1432, 57-63.

Narayan, K., Jayaraj, S. (1974) Mode of action of *Bacillus thuringiensis berliner* in citrus leaf caterpillar, *Papilio demoleus*. *Indian Journal of experimental biology*, 12, 89-91.

Nayeem, A., Sitkoff, D., Krystek, S.Jr. (2006) A comparative study of available software for high-accuracy homology modeling: from sequence alignments to structural models. *Protein Science*, 15, 808-824.

Nijhout, F.H. (1994) Insect hormones. Princeton: Princeton University Press.

Nishiura, J.T., Burgos, C., Aya, S., Goryacheva, Y., Lo, W. (2007) Modulation of larval nutrition effects midgut neutral lipid storage and temporal pattern of transcription factor expression during mosquito metamorphosis. *Journal of Insect Physiology*, 53, 47-58.

Oppert, B., Kramer, K.J., Johnson, D.E. (1994) Altered protoxin activation by midgut enzymes from a *Bacillus thuringiensis* resistant strain of *Plodia interpuctella*. *Biochemical and Biophysical Research Communication*, 198, 940-947.

Pazos, S.A., Salamanca, J.A. (2008) Minireview and hypothesis: Homology modeling of *Spodoptera litura* (Lepidoptera: Noctuidae) Aminopeptidase N receptor. *Revista Academia Colombiana Ciencias*, 32, 139-144.

Pennington, J.E., Wells, M.A. (2002) Triacylglycerol-rich lipophorins are found in the dipteran infraorder *Culicomorpha*, not just in mosquitoes. *Journal of Insect Sciences*, 2-15.

Peyronnet, O., Vachon, V., Brousseau, R., Baines, D., Schwartz, J., Laprade, R. (1997) Effect of *Bacillus thuringiensis* toxins on the membrane potential of lepidopteran insect midgut cells. *Applied and Environmental Microbiology*, 63, 1679-1684.

Phillips, J.C., Braun, R., Wang, W., Gumbart, J., Tajkhorshid, E., Villa, E., Chipot, C., Skeel, R.D., Kale, L., Schulten, K. (2005) Scalable molecular dynamics with NAMD. *Journal of Computational Chemistry*, 26, 1781-1802.

Pigott, C.R., Ellar, D.J. (2007) Role of receptors in *Bacillus thuringiensis* crystal toxin activity. *Microbiology and Molecular Biology Reviews*, 71, 255-281.

Pigott, C.R., Ellar, D.J. (2007) Role of receptors in *Bacillus thuringiensis* crystal toxin activity. *Microbiology and Molecular Biology Reviews*, 71, 255-281.

Price, G.M. (1973) Protein and nucleic acid metabolism in fat body tissue. *Biological Reviews of the Cambridge Philosophical Society*, 48, 333-375.

Profile-3D user guide, Accelrys, Inc., San Diego, USA, (1999)

Rajagopal, R., Agrawal, N., Selvapandiyan, A., Sivakumar, S., Ahmad, S., Bhatnagar, R.K. (2003) Recombinantly expressed isoenzymic aminopeptidases from *Helicoverpa armigera* (American cotton bollworm) midgut display differential interaction with closely related *Bacillus thuringiensis* insecticidal proteins. *Biochemical Journal*, 370, 971-978.

Rajagopal, R., Sivakumar, S., Agrawal, N., Malhotra, P., Bhatnagar, R.K. (2002) Silencing of midgut aminopeptidase N of *Spodoptera litura* by double-stranded RNA establishes its role as *Bacillus thuringiensis* toxin receptor. *Journal of Biological Biochemistry*, 277, 46849-46851.

Reed, B.J., Chandler, D.S., Sandeman, R.M. (1999) Aminopeptidases as potential targets for the control of the Australian sheep blowfly, *Lucilia cuprina*. *International Journal of Parasitology*, 29, 839-850.

Riddiford, L.M. (1981) Hormonal control of epidermal cell development. *Integrative and Comparative Biology*. 21, 751-762.

Riddiford, L.M. (1993) Hormones and *Drosophila* development. In: Bate, M., Martinez Arias, A. editors. The development of *Drosophila melanogaster*. Cold Spring Harbor: Cold Spring Harbor Laboratory Press, 899-939.

Riddiford, L.M. (1994) Cellular and molecular actions of juvenile hormone-General considerations and premetamorphic actions. *Advances in Insect Physiology*, 24, 213-274.

Riddiford, L.M. (1996) Juvenile hormone: The status of its “Status Quo” action. *Archives of Insect Biochemistry and Physiology*, 32, 271-286.

Riddiford, L.M. (2008) Juvenile hormone action: a 2007 perspective. *Journal of Insect Physiology*, 54, 895-901.

Riddiford, L.M., Cherbas, P.T., Truman, J.W. (2001) Ecdysone receptors and their biological actions. *Vitamins and Hormones*, 60, 1-73.

Rimoldi, O.J., Córsico, B., González, M.S., Brenner, R.R. (1996) Detection and quantification of a very high density lipoprotein in different tissues of *Triatoma infestans* during the last nymphal and adult stages. *Insect Biochemistry and Molecular Biology*, 26, 705-713.

Romeis, J., Meissle, M., Bigler, F. (2006) Transgenic crops expressing *Bacillus thuringiensis* toxins and biological control. *Nature Biotechnology*, 24, 63-71.

Roush, R.T., Tabashnik, B.E. (1990) Pesticide resistance in arthropods. Chapman and Hall, New York, N.Y.

Sakurai, S., Kaya, M., Satake, S. (1998) Hemolymph ecdysteroid titer and ecdysteroid-dependent developmental events in the last-larval stadium of the silkworm, *Bombyx mori*: role of low ecdysteroid titer in larval-pupal metamorphosis and a reappraisal of the head critical period. *Journal of Insect Physiology*, 44, 867-881.

Sangadala, S., Walters, F., English, L.H., Adang, M.J. (1994) A mixture of *Manduca sexta* aminopeptidase and alkaline phosphatase enhances *Bacillus thuringiensis* insecticidal Cry1A(c) toxin binding and $^{86}Rb^{1}$-K^{+} leakage *in vitro*. *Journal of Biological Chemistry*, 269, 10088-10092.

Schnepf, E., Crickmore, N., Van Rie, J., Lereclus, D., Baum, J.R., Feitelson, J., Zeigler, D., Dean, D.H. (1998) *Bacillus thuringiensis* and its pesticidal crystal proteins. *Microbiology and Molecular Biology Reviews*, 62, 705-806.

Schwartz, L.M. (1992) Insect muscle as a model for programmed cell death. *Journal of Neurobiology*, 23, 1312-1326.

Shelton, A.M., Roberson, J.L., Tang, J.D., Perez, C., Eigenbrode, S.D., Preisler, H.K., Wilsey, W.T., Cooley, R.J. (1993) Resistance of diamondback moth (Lepidoptera: Plutellidae) to *Bacillus thuringiensis* subspecies in the field. *Journal of Economic Entomology*, 86, 697-705.

Shelton, A.M., Zhao, J.Z., Roush, R.T. (2002) Economic, ecological, food safety and social consequences of the deployment Bt transgenic plants. *Annual Reviews on Entomology*, 47, 847-881.

Shinkawa, A., Yaoi, K., Kadotani, T., Imamura, M., Koizumi, N., Iwahana, H., Sato, R. (1999) Binding of phylogenetically distant *Bacillus thuringiensis* Cry toxins to a *Bombyx mori* aminopeptidase N suggests importance of Cry toxin's conserved structures in receptor binding. *Current Microbiology*, 39, 14-20.

Simpson, R.M., Newcomb, R.D., Gatehouse, H.S., Crowhurst, R.N., Chagne, D., Gatehouse, L.N., Markwick, N.P., Beuning, L.L., Murray, C., Marshall S.D., Yauk, Y.K., Nain, B., Wang, Y.Y., Gleave,

A.P., Christeller, J.T. (2007) Expressed sequence tags from the midgut of *Epiphyas postvittana* (Walker) (Lepidoptera: Tortricidae). *Insect Molecular Biology*, 16, 675-690.

Simpson, R.M., Poulton, J., Markwick, N.P. (2008) Expression levels of aminopeptidase-N genes in the lightbrown apple moth, *Epiphyas postvittana*. *Insect Science*, 15, 505-512.

Singh, A., Sivaprasad, C.V.S. (2009) Functional interpretation of APN receptor from *Manduca sexta* using a molecular model. *Bioinformation*.

Sivakumar, S., Rajagopal, R., Venkatesh, G.R., Srivastava, A., Bhatnagar, R.K. (2007) Knockdown of aminopeptidase-N from *Helicoverpa armigera* larvae and in transfected Sf21cells by RNA interference reveals its functional interaction with *Bacillus thuringiensis* insecticidal protein Cry1Ac. *Journal of Biological Chemistry*, 282, 7312-7319.

Siviter, R.J., Taylor, C.A., Cottam, D.M., Denton, A., Dan, M.P., Milner, M.J., Dhirras, A.D., Isaac, R.E. (2002) Ance, a *Drosophila* angiotensin-converting enzyme homologue, is expressed in imaginal cells during metamorphosis and is regulated by the steroid, 20-hydroxyecdysone. *Biochemical Journal*, 367, 187-193.

Soberón, M., Gill, S.S., Bravo, A. (2009) Signalling versus punching hole: How do *Bacillus thuringiensis* toxins kill insect midgut cells. *Cellular and Molecular Life Sciences*, 66, 1337-1349.

Srivastava, D.P., Yu, E.J., Kennedy, K., Chatwin, H., Reale, V., Hamon, M., Smith, T., Evans, P.D. (2005) Rapid, non-genomic responses to ecdysteroids and catecholamines mediated by a novel *Drosophila* G-protein-coupled receptor. *Journal of Neurosciences*, 25, 6145-6155.

Sumithra, P., Britto, C.P., Krishnan, M. (2009) Modes of cell death in the pupal perivisceral fat body tissue of the silkworm, *Bombyx mori*. *Cell Tissue Research*, 339, 349-358.

Sun, X., Song, Q. (2006) PKC-mediated USP phosphorylation is required for 20E-induced gene expression in the silk glands of *Drosophila melanogaster*. *Archives of Insect Biochemistry and Physiology*, 62, 116-127.

Tabashnik, B.E., Cushing, N.L., Finson, N., Johnson, M.W. (1990) Field development of resistance to *Bacillus thuringiensis* in diamondback moth (Lepidoptera: Plutellidae). *Journal of Economic Entomology*, 83, 1671-1676.

Tabashnik, B.E., Fabrick, J.A., Henderson, S., Biggs, R.W., Yafuso, C.M., Nyboer, M.E. (2005) DNA screening reveals pink bollworm resistance to Bt cotton remains rare after decade of exposure. *Journal of Economic Entomology*, 99, 1525-1530.

Tang, B., Wang, S., Zhang, F. (2010) Two storage hexamerins from the beet armyworm *Spodoptera exigua*: Cloning, characterization and the effect of gene silencing on survival. *BMC Molecular Biology*, 11, 65.

Taylor, A. (1993) Aminopeptidases: structure and function. *The FASEB Journal*, 7, 290-298.

Telfer, W.H., Kunkel, J.G. (1991) The function and evolution of insect storage hexamers. *Annual Reviews of Entomology*, 36, 205-228.

Terashima, J., Yasuhara, N., Iwami, M., Sakurai, S. (2000) Programmed cell death triggered by insect steroid hormone, 20-hydroxyecdysone, in the anterior silk gland of the silk worm, *Bombyx mori*. *Developmental Genes and Evolution*, 210, 545-558.

Terenius, O., Papanicolaou, A., Garbutt, J.S., Eleftherianos, I., Huvenne, H., Kanginakudru, S., Albrechtsen, M., An, C., Aymeric, J., Barthel, A., Bebas, P., Bitra, K., Bravo, A., Chevalier, F., Collinge, D.P., Crava, C.M., de Maargd, R.A., Duvic, B., Erlandson, M., Faye, I., Felfoldi, G., Fujiwara, H., Futahashi, R., Gandhe, A.S., Gatehouse, H.S., Gatehouse, L.N., Giebultowicz, J.M., Gomez, I., Grimmelikhuijzen, C.J.P., Groot, A.T., Hauser, F., Heckel, D.G., Hegedus, D.D., Hrycaj, S., Huang, L., Hull, J.J., Iatrou, K., Iga, M., Kanost, M.R., Kotwica, J., Li, C., Li, J., Liu, J., Lundmark, M., Matsumoto, S., Meyering-Vos, M., Millichap, P.J., Monteiro, A., Mrinal, N., Niimi, T., Norwara, D., Ohnishi, A., Oostra, V., Ozaki, K., Papakonstantinou, M., Popadic, A., Rajam, M.V., Saenko, S., Simpson, R.M., Soberon, M., Strand, M.R., Tomita, S., Toprak, U., Wang, P., Wee, C.W., Whyard, S., Zhang, W., Nagaraju, J., ffrench-Constant, R.H., Herrero, S., Gordon, K., Swevers, L., Smagghe, G. (2010) RNA interference in Lepidoptera: An overview of successful and unsuccessful studies and implications for experimental design. *Journal of Insect Physiology*, 57, 231-245.

Terra, W.R., Ferreira, C. (1994) Insect digestive enzymes: properties compartmentalization and function. *Comparative Biochemistry and Physiology*, 109, 1-62.

Thomas, W.E., Ellar, D.J. (1983) *Bacillus thuringiensis* var *israelensis* crystal delta-endotoxin: effects on insect and mammalian cells *in vitro* and *in vivo*. *Journal of Cell Science*, 60, 181-197.

Thummel, C.S. (2001) Steroid triggered death by autophagy. *BioEssays*, 23, 677-682.

Tian, H., Peng, H., Yao, Q., Chen, H., Xie, Q., Tang, B., Zhang, W. (2009) Developmental control of a lepidopteran pest *Spodoptera exigua* by ingestion of bacteria expressing dsRNA of a non-midgut gene. *PLoS ONE*, 4, e6225.

Tian, L., Guo, E., Wang, S., Liu, S., Jiang, R.J., Cao, Y., Ling, E. (2010) Developmental regulation of glycolysis by 20-hydroxyecdysone and juvenile hormone in fat body tissues of the silkworm, *Bombyx mori*. *Journal of Molecular Cell Biology*, 2, 255-263

Tojo, S., Yoshiga, T. (1994) Purification and characterization of three storage proteins in the common cutworm, *Spodoptera litura*. *Insect Biochemistry and Molecular biology*, 24, 729-738.

Towbin, H., Staehelin, T., Gordon, J. (1979) Electrophoretic transfer of proteins from polyacrylamide gels to nitrocellulose sheets; procedure and some applications. *Proceedings of National Academy of Sciences USA*, 76, 4350-4354.

Tripathi, R., Singh, N.P. (2002) Biochemical alterations in the haemolymph of *Bacillus thuringiensis var kurstaki* (B.t.k) infected larvae of *Spodoptera litura*. *Asian Journal of Experimental Science*, 16, 35-39.

Truman, J.W., Riddiford, L.M. (2007) The morphostatic actions of juvenile hormone. *Insect Biochemistry and Molecular Biology*, 37, 761-770.

Turner, C.T., Davy, M.W., MacDiarmid, R.M., Plummer, K.M., Birch, N.P., Newcomb, R.D. (2006) RNA interference in the light brown apple moth, *Epiphyas postvittana* induced by double-stranded RNA feeding. *Insect Molecular Biology*, 15, 383-391.

Vadlamudi, R., Weber, E., Ji, I., Bulla, J. (1995) Cloning and expression of a receptor for an insecticidal toxin of *Bacillus thuringiensis*. *Journal of Biological Chemistry*, 270, 5490-5494.

Vadlamudi, R.K., Ji, T.H., Bulla, Jr., L.A. (1993) A specific binding protein from *Manduca sexta* for the insecticidal toxin of *Bacillus thuringiensis* subs. *berliner*. *Journal of Biological Chemistry*, 268, 5390-5494.

Valaitis, A.P. (2011) Localization of *Bacillus thuringiensis* Cry1A toxin-binding molecules in gypsy moth larval gut sections using fluorescence microscopy. *Journal of Invertebrate Pathology*, In press.

Valaitis, A.P., Jenkins, J.L., Lee, M.K., Dean, D.H., Garner, K.J. (2001) Isolation and partial characterization of Gypsy moth BTR-270 an anionic brush border membrane glycoconjugate that binds *Bacillus thuringiensis* Cry1A toxins with high affinity. *Archives of Insect Biochemistry and Physiology*, 46, 186-200.

Valaitis, A.P., Lee, M.K., Rajamohan, F., Dean, D.H. (1995) Brush border membrane aminopeptidase-N in the midgut of the gypsy moth serves as the receptor for the Cry1Ac delta-endotoxin of *Bacillus thuringiensis*. *Insect Biochemistry and Molecular Biology*, 25, 1143-1151.

Van Rie, J. (2000) *Bacillus thuringiensis* and its use in transgenic insect control technologies. *International Journal of Medical Microbiology*, 290, 463-469.

Van Rie, J., McGaughey, W.H., Johnson, D.E., Barnett, D.B., Van Mellaert, H. (1990) Mechanism of insect resistance to the microbial insecticide *Bacillus thuringiensis*. *Science*, 247, 72-74.

Verkuil, E.V.P. (1979) Hormone mediated induction of acid phosphatase activity in the fat body of *Calliphora erythrocephala* prior to metamorphosis. *Journal of Insect Physiology*, 25, 965-973.

Verkuil, E.V.P., Van Ronger, E., de Priester, W. (1979) Normal and experimentally induced lysosomal activity in fat body cell of *Calliphora erythrocephala* meigen. *Cell and Tissue Research*, 203, 443-445.

Verkuil. E.V.P. (1980) The induction of lysosomal enzyme activity in the fat body of *Calliphora erythrocephala*: changes in the internal environment. *Journal of Insect Physiology*, 26, 91-101.

Vimala-Devi, P.S., Balakrishnan, K., Ravinder, T., Prasad, Y.G. (2001) Identification of potent strains of *Bacillus thuringiensis* for the management of the castor semilooper *Achaea janata* (Linn.) and optimization of production. *Entomon*, 26, 98-103.

Vlahovic, P., Stefanovic, V. (1998) Kidney ectopeptidases: structure, function and clinical significance. *Pathologie Biologie*, 46, 779-786.

Von Gaudecker, B., Schmale, E.M. (1974) Substrate-histochemical investigations and ultrahistochemical demonstrations of acid phosphatase in larval and prepupal salivary glands of *Drosophila melanogaster*. *Cell Tissue Research*, 155, 75-89.

Wang, P., Zhang, X., Zhang, J. (2005) Molecular characterization of four midgut aminopeptidase N isozymes from the cabbage looper, *Trichoplusia ni*. *Insect Biochemistry and Molecular Biology*, 35, 611-620.

Wheeler, D.E., Nijhout, H.F. (2003) A perspective for understanding the modes of juvenile hormone action as a lipid signaling system. *BioEssays*, 25, 994-1001.

White, K.P., Rifkin, S.A., Hurban, P., Hogness, D.S. (1999) Microarray array of *Drosophila* development during metamorphosis. *Science*, 286, 2179-2184.

Whyard, S., Singh, A.D., Wong, S. (2009) Ingested double-stranded RNAs can act as species-specific insecticides. *Insect Biochemistry and Molecular Biology*, 39, 824-832.

Wolfersberger, M. G. (1990) The toxicity of two *Bacillus thuringiensis* delta endotoxins to gypsy moth larvae is inversely related to the affinity of binding sites on midgut brush border membranes for the toxins. *Experientia*, 46, 475-477.

Wolfersberger, M., Luthy, P., Maurer, A., Parenti, P., Sacchi, V.F., Giordana, B., Hanozet, G.M. (1987) Preparation of brush border membrane vesicles (BBMV) from larval lepidopteran midgut. *Comparative Biochemistry and Physiology*, 86, 301-308.

Wu, Y., Parthasarathy, R., Bai, H., Palli, S.R. (2006) Mechansims of midgut remodeling: Juvenile hormone analog methoprene blocks midgut metamorphosis by modulating ecdysone action. *Mechanisms of Development*, 123, 530-547.

Wyatt, G.R. (1975) Regulation of protein and carbohydrate metabolism in the fat body. *Verhandlungen der Deutschen Zoologischen Gesellschaft*, 1974, 209-226.

Xie, R., Zhuang, M., Ross, L.S., Gómez, I., Oltean, D.I., Bravo, A., Soberón, M., Gill, S.S. (2005) Single amino acid mutation in the cadherin receptor from *Heliothis virescens* affect its toxin binding ability to Cry1A toxins. *Journal of Biochemistry*, 280, 8416-8425.

Yao, T.P., Forman, B.M., Jiang, Z., Cherbas, L., Chen, J.D., McKeown, M., Cherbas, P., Evans, R.M. (1993) Functional ecdysone receptor is the product of EcR and Ultraspiracle genes. *Nature*, 366, 476-479.

Yao, T.P., Segraves, W.A., Oro, A.E., McKeown, M., Evans, R.M. (1992) *Drosophila* ultraspiracle modulates ecdysone receptor function via heterodimer formation. *Cell*, 71, 63-72.

Yaoi, K., Kadotani, T., Kuwana, H., Shinkawa, A., Takahashi, T., Iwahana, H., Sato, R. (1997) Aminopeptidase N from *Bombyx mori* as a candidate for the receptor of *Bacillus thuringiensis* Cry1Aa toxin. *European Journal of Biochemistry*, 246, 652-657.

Yaoi, K., Nakanishi, K., Kadotani, T., Imamura, M., Koizumi, N., Iwahana, H., Sato, R. (1999) *Bacillus thuringiensis* Cry1Aa toxin-binding region of *Bombyx mori* aminopeptidase N. *FEBS Letters*, 463, 221-224.

Yaoi, K., Nakanishi, K., Kadotani, T., Imamura, M., Koizumi, N., Iwahana, H., Sato, R. (1999) cDNA cloning and expression of *Bacillus thuringiensis* Cry1Aa toxin binding 120 kDa aminopeptidase N from *Bombyx mori*. *Biochimica et Biophysica Acta*, 1444, 131-137.

Yu, H., Chen, H., Zhang, Y., Wu, K., Liang, G., Liu, Z., Guo, Y. (2010) Gene cloning and expression of aminopeptidase N and cadherin from midgut of the rice stem borer, *Chilo suppressalis*. *Insect Science*, 17, 393-399.

Zhang, S., Cheng, H., Gao, Y., Wang, G., Liang, G., Wu, K. (2009) Mutation of an aminopeptidase N gene is associated with *Helicoverpa armigera* resistance to *Bacillus thuringiensis* Cry1Ac. *Insect Biochemistry and Molecular Biology*, 39, 421-429.

Zhang, X., Candas, M., Griko, N.B.,Taissing, R., Bulla, L.A.Jr. (2006) A mechanism of cell death involving an adenylyl cyclase/PKA signaling pathway is induced by the Cry1Ab toxin of *Bacillus thuringiensis*. *Proceedings of National Academy of Sciences USA*, 103, 9897-9902.

Zhu, Y.C., Karmer, K.J., Oppert, B., Dowdy, A.K. (2000) cDNAs of aminopeptidase-like protein genes from *Plodia interpunctella* strains with different susceptibilities to *Bacillus thuringiensis* toxins. *Insect Biochemistry and Molecular Biology*, 30, 2115-224.

Zhuang, M., Gill, S.S. (2003) Mode of action of *Bacillus thuringiensis* toxins, 213-234. *In* G. Voss and G. Ramos (ed.), *Chemistry of crop protection*. Wiley VCH, Weinheim, Germany.